

Argonne National Laboratory

REACTOR DEVELOPMENT PROGRAM

PROGRESS REPORT

November 1964

RETURN TO REFERENCE FILE
TECHNICAL PUBLICATIONS
DEPARTMENT

LEGAL NOTICE

This report was prepared as an account of Government sponsored work. Neither the United States, nor the Commission, nor any person acting on behalf of the Commission:

A. Makes any warranty or representation, expressed or implied, with respect to the accuracy, completeness, or usefulness of the information contained in this report, or that the use of any information, apparatus, method, or process disclosed in this report may not infringe privately owned rights; or

B. Assumes any liabilities with respect to the use of, or for damages resulting from the use of any information, apparatus, method, or process disclosed in this report.

As used in the above, "person acting on behalf of the Commission" includes any employee or contractor of the Commission, or employee of such contractor, to the extent that such employee or contractor of the Commission, or employee of such contractor prepares, disseminates, or provides access to, any information pursuant to his employment or contract with the Commission, or his employment with such contractor.

ARGONNE NATIONAL LABORATORY
9700 South Cass Avenue
Argonne, Illinois 60440

REACTOR DEVELOPMENT PROGRAM
PROGRESS REPORT

November 1964

Albert V. Crewe, Laboratory Director
Stephen Lawroski, Associate Laboratory Director

<u>Division</u>	<u>Director</u>
Chemical Engineering	R. C. Vogel
Idaho	M. Novick
Metallurgy	F. G. Foote
Reactor Engineering	L. J. Koch
Reactor Physics	R. Avery
Remote Control	R. C. Goertz

Report Coordinated by
R. M. Adams and A. Glassner

Issued December 21, 1964

Operated by The University of Chicago
under
Contract W-31-109-eng-38
with the
U. S. Atomic Energy Commission

FOREWORD

The Reactor Development Program Progress Report, issued monthly, is intended to be a means of reporting those items of significant technical progress which have occurred in both the specific reactor projects and the general engineering research and development programs. The report is organized in a way which, it is hoped, gives the clearest, most logical over-all view of progress. The budget classification is followed only in broad outline, and no attempt is made to report separately on each sub-activity number. Further, since the intent is to report only items of significant progress, not all activities are reported each month. In order to issue this report as soon as possible after the end of the month editorial work must necessarily be limited. Also, since this is an informal progress report, the results and data presented should be understood to be preliminary and subject to change unless otherwise stated.

The issuance of these reports is not intended to constitute publication in any sense of the word. Final results either will be submitted for publication in regular professional journals or will be published in the form of ANL topical reports.

The last six reports issued
in this series are:

May 1964	ANL-6904
June 1964	ANL-6912
July 1964	ANL-6923
August 1964	ANL-6936
September 1964	ANL-6944
October 1964	ANL-6965

TABLE OF CONTENTS

	<u>Page</u>
I. Boiling Water Reactors	1
A. Experimental Boiling Water Reactor (EBWR)	1
1. Postirradiation Examination of EBWR Spike Element S-1	1
II. Liquid-metal-cooled Reactors	2
A. General Fast Reactor Physics	2
1. ZPR-III	2
2. ZPR-VI	4
3. ZPR-IX	8
B. Fast Reactor Systems and Concepts	11
1. 1000-MWe Metal-fueled Fast Breeder Reactor Study	11
2. Comparison of Electricity-generating Units	17
C. General Fast Reactor Fuel Development	19
1. Metallic Fuels	19
2. Carbide Fuel Elements	19
3. Development of Jacket Materials	20
4. Irradiation of Uranium-Plutonium-Fizzium Alloys	22
5. Corrosion Inhibition in Sodium	22
D. General Fast Reactor Fuel Reprocessing Development	23
1. Skull Reclamation Process	23
2. Materials and Equipment Evaluation	23
3. Advanced Processes	24
4. Consolidation of Fission Product Wastes in Alloys	25
5. Decladding Studies for TV-20 Cladding	25
6. Eddy Current Induction Probe	26
7. Removal of Nitrogen from Argon	26
E. Sodium Coolant Chemistry	27
1. Cover-gas Impurities	27
2. Analysis for Oxygen	27

TABLE OF CONTENTS

	<u>Page</u>
F. EBR-II	28
1. Sticking of Control Rod and Oscillator Drive Mechanisms	28
2. Maintenance	30
3. Fuel Cycle Facility	31
G. FARET	34
1. Engineering	34
2. Cell Components	35
3. Core Instrumentation	35
4. Fuel Slip-fit Experiment	38
5. Fuel Assembly Sodium Flow Test Loop	41
III. General Reactor Technology	42
A. Experimental Reactor and Nuclear Physics	42
1. Elastic Scattering of Fast Neutrons	42
2. Gamma Rays Emitted Following Inelastic Scattering	44
3. (d,n) Stripping Reactions	44
4. Instrumentation	45
B. Theoretical Reactor Physics	45
1. Resonance Interference	45
2. Calculation of Cross Sections	46
3. Analysis of Fuel Requirements for Ceramic-fueled Breeder Reactors	46
4. Calculation of Physical Properties of Reactor Materials at High Temperatures	47
C. High-temperature Materials Development	49
1. Ceramics	49
2. Thorium-base Fuels	55
3. Corrosion by Liquid Metals	56
D. Other Reactor Fuels and Materials Development	57
1. Zirconium Alloys for Superheated Steam	57
2. Corrosion of Iron and Nickel Alloys in Superheated Steam	57
3. Nondestructive Testing	57

TABLE OF CONTENTS

	<u>Page</u>
E. Remote Control Engineering Development	61
1. Electric Master-Slave Manipulator Mark E4	61
2. Servo Studies	61
3. Special Motors for Master-Slave Manipulators	61
4. Viewing Systems	62
F. Heat Engineering	62
1. Two-phase Flow Studies	62
2. Boiling Liquid Metal Technology	63
3. General Heat Transfer	65
4. ANL-AMU Program	66
G. Chemical Separations	67
1. Fluidization and Volatility Separation Processes	67
2. General Chemistry and Chemical Engineering	70
3. Chemical-Metallurgical Process Studies	71
4. Calorimetry	72
H. Plutonium Recycle Program	73
1. Physics Calculations	73
IV. Advanced Systems Research and Development	74
A. Argonne Advanced Research Reactor (AARR)	74
1. Fuel and Core Design	74
2. Heat Transfer	74
3. Critical Experiment	75
B. Magnetohydrodynamics (MHD)	79
1. MHD Power Generation - Jet Pump Studies	79
C. Regenerative Emf Cells	79
1. Bimetallic Cells	79

TABLE OF CONTENTS

	<u>Page</u>
D. Thermionic Conversion	80
1. Comparison of Dc and Rf Power Output	80
2. Rf-voltage Pulses	81
V. Nuclear Safety	82
A. Thermal Reactor Safety Studies	82
1. Metal-Water Reactions	82
2. Metal Oxidation-Ignition Studies	86
B. Fast Reactor Safety Studies	86
1. Transient Tests with Uranium Sulfide	86
2. Analysis of Coolant Expulsion from Heated Channels	90
3. Sodium Expulsion Studies	91
C. TREAT	91
1. Large TREAT Loop	91
VI. Publications	93

I. BOILING WATER REACTORS

A. Experimental Boiling Water Reactor (EBWR)

1. Postirradiation Examination of EBWR Spike Element S-1

The first portion of the examination of EBWR spike element S-1 after an estimated burnup of 4.5 a/o of the uranium atoms has been completed. The fuel assembly was composed of forty-nine fuel rods of Zircaloy-2 tubing containing pellets of 9.24 w/o CaO, 8.93 w/o UO_2 , and 81.83 w/o ZrO_2 in a 7 by 7 array. The fuel rods were supported in the assembly by stainless steel end fittings and a Zircaloy-2 center spacer.

Visual examination of the fuel assembly indicated that none of the components had suffered any deleterious effects. The fuel rods and end fittings were covered with a thin layer of powdery grey oxide which was generally nonadherent. Bowing of the individual fuel rods could not be detected, and no fretting corrosion was observed at either end fitting or the center spacer.

The four corner rods were removed from the fuel rod assembly and examined in detail. The diameters of the rods, determined at 25-mm intervals and at three 120° angular orientations before and after puncturing for fission gas, were within 0.02-0.05 mm of the original specified diameter. Each rod was measured for bowing and none found. The area of maximum gamma activity was between 86 to 96 cm from the top of each rod. Fission gas measurements indicated that a large amount of gas was contained in each rod, the amount increasing with gamma activity. The results of this measurement have not yet been coordinated with fuel burnup to obtain release rates.

The second phase of the postirradiation analysis, now under way, includes a detailed examination of the fretting corrosion of the rod surface at the center spacer interface, fuel burnup analyses, and metallography.

II. LIQUID-METAL-COOLED REACTORS

A. General Fast Reactor Physics

1. ZPR-III

Assembly 45A is being used to investigate the Doppler effect in simulated fast power breeder reactors.

The Assembly 45 test zone contained an intentionally softened neutron spectrum to enhance the Doppler effect (see Progress Report for July, 1964, ANL-6923, p. 14). The composition of the central zone of Assembly 45A more nearly represents a projected fast power breeder reactor. It simulates a large, sodium-cooled, plutonium monocarbide core with a uranium-to-plutonium ratio of 7 to 1. The driver is the same composition as Assembly 45, but contains a modified buffer and a full density depleted uranium radial blanket. The Assembly 45 radial reflector, used to help soften the driver spectrum, has been deleted. The compositions of the various zones of Assembly 45A are listed in Table I.

Table I. Composition of Assembly 45A, atoms/cm³ x 10⁻²⁴

Isotope	Central Zone	Low-density Axial Blanket	Buffer	Driver	High-density Blanket
Pu ²³⁹	0.001065	-	-	-	-
Pu ²⁴⁰	0.000051	-	-	-	-
Pu ²⁴¹	0.000005	-	-	-	-
U ²³⁵	0.000015	0.000020	0.000010	0.00448	0.000079
U ²³⁴	-	-	-	0.000046	-
U ²³⁶	-	-	-	0.000019	-
U ²³⁸	0.00723	0.00968	0.00482	0.000256	0.03998
Na	0.01058	0.01072	0.00844	-	-
C	0.00833	0.00833	-	0.0416	-
Ni	-	-	-	0.0186	-
SS (304)	0.0106	0.00953	0.0386	0.00775	0.00624

The zone locations are shown in cross section in Figure 1. The control safety rods and channels that the Doppler elements may occupy are also shown.

Assembly 45A went critical with 56.18 kg of plutonium and 0.75 kg of U²³⁵ in the central zone (the same as with Assembly 45). The driver mass was increased to 315 kg of U²³⁵, compared to 245 kg U²³⁵ in the previous assembly. Because of the spontaneous fission of Pu²⁴⁰ in the central zone, the reactor was found to be approximately 0.5 lh subcritical at a power level of 15 W.

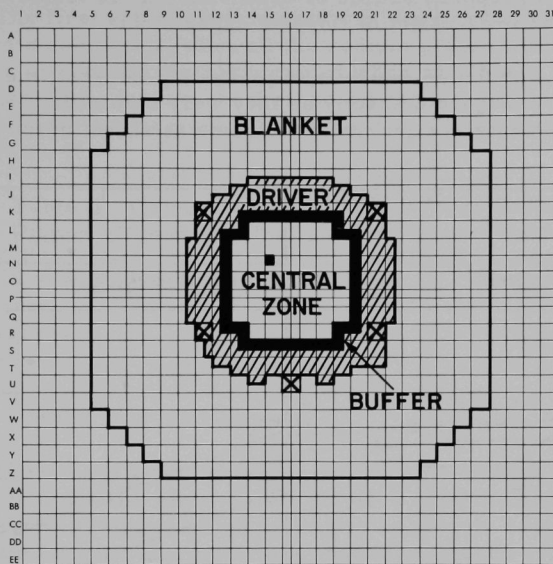


Figure 1. Zone Locations in Assembly 45A of ZPR-III

A measurement of the U^{238} Doppler reactivity effect in Assembly 45A showed that the effect was reduced by very nearly a factor of two from that observed in Assembly 45.

Measurements of the Doppler effect of Pu^{239} have been started. The uncorrected reactivity effect measured for Pu^{239} in Assembly 45 was very small and negative. Assembly 45A also showed a small negative Pu^{239} Doppler coefficient.

A test was performed to determine the importance of expansion effects upon the reactivity signal measured for the plutonium sample. The present design of Doppler equipment consists of two Doppler elements along a single axial channel. This arrangement was chosen so that, when the elements expand upon heating, one element expands toward the core center into an increasing flux, while the other expands away from the center into a decreasing flux. A large part of non-Doppler expansion effects should thus cancel out. If only one of the two elements is heated, this first-order correction would disappear and expansion effects would be greatly magnified.

When only that element which moves outward on expansion was heated, the additional expansion effect for this element was about 15% of the two-element total reactivity signal. Thus, the compensated net expansion correction to the plutonium Doppler measurement must be well under 15% of the signal seen.

A second proposed source of expansion will be tested before the completion of the present set of Doppler experiments.

Since the plutonium value is of particular interest, the experimental data are shown in Figure 2 exactly as they were obtained. The results for all the measurements are generally the same as shown in the figure.

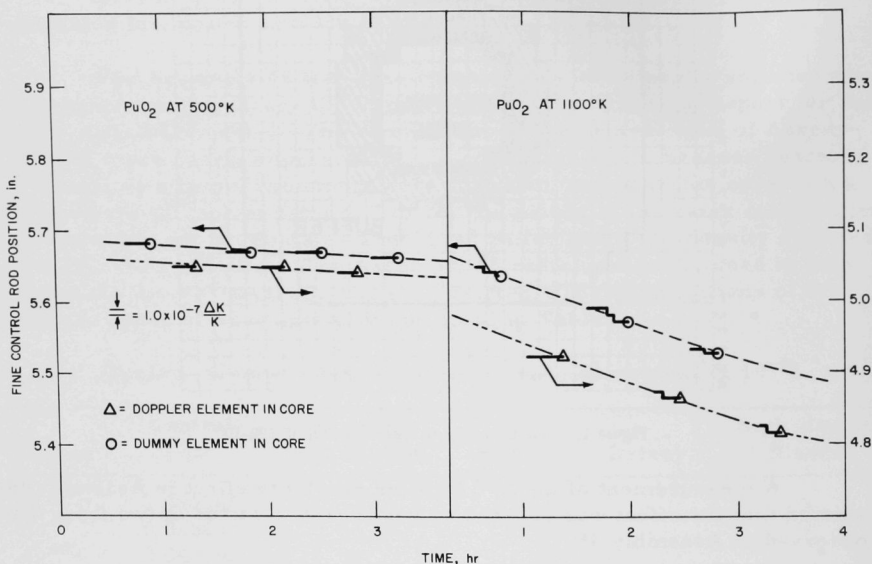


Figure 2. Doppler Reactivity Measurements for Plutonium-239 in Assembly 45A of ZPR-III

2. ZPR-VI

a. Sodium Void Coefficients. A series of measurements were made in Assembly No. 3 of ZPR-VI to determine the effects of various parametric changes on the sodium void coefficient. The experiments were performed in a (~27-cm diameter) region which contained 21 central drawers in each half of the reactor. The experimental region included the entire core length of 50 cm.

The core is approximately cylindrical, with a length-to-diameter (L/D) ratio of about one-third. The core materials are in the form of rectangular plates of various thicknesses (1/16 in., 1/8 in., and 1/4 in.) which are loaded into drawers. Placing these drawers into the reactor matrix square tubes forms continuous planes of the various materials extending in the radial and axial directions.

The first set of experiments was designed to compare the apparent sodium void coefficient, when all the sodium planes within the experimental region are voided, to that obtained when only every other sodium-filled can is voided to form a checker-board pattern. The sodium-filled cans used in these experiments were all 2 in. or 3 in. long. The results are summarized in Table II.

Table II. Comparison of Reactivity with Sodium Planes Aligned and Unaligned in Reactor Halves

Configuration	Ih/kg
Void Planes Discontinuous	$-3.22 \pm 0.11^*$
Void Planes Continuous	-3.45 ± 0.06

* 451 Ih \equiv 1% reactivity.

In the next set of experiments, the thicknesses of the sodium columns within a drawer were varied. In each case the remaining core materials were rearranged to approximate, as closely as practicable, a homogeneous mixture. The materials contained in each drawer are listed in Table III.

Table III. Material Schedule of Each Test Drawer

Material	Symbol	Thickness, in.	Number of Columns
Enriched Uranium	E	1/16	2
Depleted Uranium	D	1/8	4
Carbon	C	1/8	3
Sodium	Na	1/4	4
Void	V	1/4	-

The arrangement of these components within each drawer, as viewed from the front, is shown in Table IV for each thickness of sodium. The movable half-drawer loadings were mirror images of the stationary half-drawer loadings. For this experiment the test zone extended only 15 cm axially outward from the core center into each half of the reactor. (The total axial length of the region was 30 cm.) The experiment was performed by removing all of the sodium in the drawer and replacing it with voids to obtain the effect of sodium on reactivity.

Table IV. Reactivity Measurement When Sodium in Both Reactor Halves Is Aligned

Pattern	Sodium Thickness, in.	Material Arrangement		Ih/kg
		Stationary Half	Movable Half	
1-A	1/4	NaCEDNaDCDNaCEDNa	NaDECNaDCDNaDECNa	-1.24 ± 0.07
2-A	1/2	DCEDNaNaCDECDNaNa	NaNaDCEDCNaNaDECD	-1.52 ± 0.07
3-A	1	NaNaNaNaDCEDCDECD	DCEDCDECDNaNaNaNa	-1.96 ± 0.09
		Stationary and movable halves are the same		
4-A	2	NaNaNaNaNaNaNaNaDCEDCDECDDECDCECD*		-2.64 ± 0.07

*Iterated over two drawers.

In the above experiments the sodium columns in the stationary half were aligned with the sodium columns in the movable half, as were the other materials in the drawers. Thus, continuous columns of the same materials extended axially through the core.

The second part of these experiments with sodium columns of different thickness involved measurements in which the sodium columns in the stationary half of the reactor were not aligned with those in the movable half. Other parameters were the same as those in the previous experiment, in which the sodium columns in both halves of the reactor were aligned. The results are shown in Table V.

Table V. Reactivity Measurements When Sodium in Both Reactor Halves Is Not Aligned

Pattern	Sodium Thickness, in.	Material Arrangement		Ih/kg
		Stationary Half	Movable Half	
1-A	1/4	-	-	-
2-A	1/2	-	-	-
3-A	1	See Table IV and Text	See Table IV and Text	-2.12 ± 0.09
4-A	2	See Table IV and Text	See Table IV and Text	-2.98 ± 0.07

The results shown in Tables IV and V are difficult to interpret because of the rearrangement of other drawer materials which was necessary to obtain the various thicknesses of sodium.

The next sets of measurements were designed to aid in this interpretation. The drawers were loaded as indicated in Table VI, and selected regions of various thicknesses were voided from the one-inch-wide sodium columns. The measured data are also tabulated in Table VI.

Table VI. Reactivity Measurements Made When Selected Regions Are Voided Next to the Sodium Columns

Material Arrangement		Notes	Ih/kg
Stationary Half	Movable Half		
DCDECNaNaNaNaDECD	DCEDNaNaNaNaCEDCD	Reference Loading	-
DCDECV*NaNaVDECD	DCEDVNaNaVCEDCD	1/4-in. Voids Aligned	-1.94 ± 0.09
DCDECVNaVNaDECD	DCEDVNaVNaCEDCD	1/4-in. Voids Not Aligned	-1.89 ± 0.09
DCDECNaVVNaDECD	DCEDNaVVNaCEDCD	1/2-in. Voids Aligned	-2.00 ± 0.09
DCDECVVNaNaDECD	DCEDVVNaNaCEDCD	1/2-in. Voids Not Aligned	-1.90 ± 0.09
DCDECVVVVDECD	DCEDVVVVCEDCD	1-in. Void Aligned	-1.85 ± 0.09

*In this and the subsequent table, voids are indicated by "V" to show which sodium columns were removed for the experiment. The columns listed as sodium were not voided during these experiments.

The above void configurations resulted in the same sodium void coefficient (within the experimental uncertainties), which is the same as found for the 1-in. void experiment in Table IV. The latter is perhaps not too surprising since the loading patterns are quite similar.

From these measurements one is tempted to infer that the material arrangement within a drawer and not the thickness of the voided region is the important parameter. Thus, the last set of measurements was designed to investigate the sodium void coefficient when the sodium was selectively voided near certain other drawer materials. The measurements were made with the experimental region extended axially both 30 cm and 50 cm. Only the 50-cm data are presented here since the associated uncertainties are lower and since the same characteristics are exhibited in the 30-cm data. Again, the material columns are continuous through both halves of the reactor, i.e., they are not staggered. The loading patterns utilized and the resulting data are presented in Table VII. The results are being analyzed.

Table VII. Reactivity Measurements Made with Voids Placed Adjacent to Selected Materials

Material Arrangement		Notes	Ih/kg
Stationary Half	Movable Half		
DVCEVDVCECDV	VDCEVDCVCECD	Normal Drawer Loading Voided	-3.48 ± 0.06
DVCECVCDNaDEDNa	NaDEDNaDCVCECD	Voided by C	-4.06 ± 0.06
DNaECNaCDVDEDV	VDEDVDCNaECNaD	Voided by D	-3.10 ± 0.06
DVCECVCDVDEDV	VDEDVDCVCECD	Voided by C and D	-3.59 ± 0.06
VCEDVDCVCECDV	VDECVDVCECDV	Fuel between C and D	-3.66 ± 0.06

3. ZPR-IX

a. Hydrogen Worth. From the outset of the ZPR-IX program it has been recognized that the influence of hydrogen on core reactivity would be quite difficult to predict theoretically because of the relationship between hydrogen concentration and core composition. The measurements and corresponding analyses which have been performed to date confirm this.

The experiments, confined to determining the dependence of central hydrogen worth on concentration, have shown that the magnitude and even the sign of central hydrogen worths are very sensitive to small changes in core composition. Thus, for ZPR-IX Assembly No. 4 which had 60 v/o tungsten in the core, a positive central hydrogen worth of +3.35 lh/g was measured. For ZPR-IX Assembly No. 4B, which differed from Assembly 4 only by having 3.7% of the core volume replaced by rhenium (see Progress Report for October, 1964, ANL-6965, p. 4), the central hydrogen worth was -2.9 lh/g of hydrogen.

This sensitivity of the hydrogen worth is reflected in the theoretical calculations. Several available codes (such as MAIM-6 and DSN) were used to predict the reactivity effect of uniformly distributed hydrogen in the core and the reflector. The ANL-224 and ANL-201 cross-section libraries were used in the calculations. The results showed a large dependence on the method and the cross sections used. Differences for identical starting conditions in some cases varied by a factor of 3 in hydrogen worth.

An experimental program to measure the uniformly distributed hydrogen worth has been planned. The central worth measurements are complicated by unavoidable concentration dependence. Uniformly distributed worth can be measured more consistently for low hydrogen concentrations. Interpretation of these results is therefore more straightforward than from highly concentrated, centrally located material.

b. Assembly No. 5. Previous reports have presented the experimental data obtained from a series of assemblies: uranium; uranium-tungsten; tungsten; and tungsten-rhenium diluted; U^{235} -fueled; and aluminum reflected. Analysis of these data has in a large measure been relative to similar measurements made on systems diluted and reflected only with uranium. Such parameters as critical mass and central reactivity coefficients have not been markedly sensitive to neutrons with energies below about 100 keV because of the hardness of the spectra characterizing these systems. In order to gain more information regarding the dependence of critical mass and central worths on resonance absorption and scattering of tungsten, an aluminum-reflected core with a large volume fraction of graphite was assembled in the ZPR-IX facility. This assembly (No. 5) has the softest spectrum of any of the ZPR-IX assemblies studied to date and provides a good test of the available cross section sets for the resonance energy region.

Composition and experimentally determined properties of Assembly No. 5 are listed in Table VIII.

Table VIII. Composition and Properties of ZPR-IX Assembly No. 5

<u>Reflector:</u> Aluminum			
<u>Typical Drawer Loading:</u>			
Fuel, 4 col. 1/16 x 2 x 11 in.,	1.153 kg U ²³⁵		
	0.1125 kg U ²³⁸		
Diluent, 7 col. 1/8 x 2 x 11 in.,	0.5097 kg C		
	5.626 kg W		
<u>Critical Mass, Uncorrected:</u> 365.01 kg U ²³⁵			
Excess Reactivity	112.9 Ih		
Length, including air and aluminum central gap		56.22 cm	
Radius, equivalent		31.54 cm	
<u>Central Fuel Worth:</u>			
	198.03 Ih/drawer		
	129.08 Ih/kg U ²³⁵		
<u>Edge Fuel Worth:</u>			
	59.13 Ih/drawer		
	19.77 Ih/kg U ²³⁵		
<u>Critical Composition, Corrected for Excess Reactivity:</u>			
Volume	199.2 liters		
U ²³⁵	358.27 kg	0.00461 x 10 ²⁴ atoms/cm ³	
U ²³⁸	26.27 kg	0.000334 "	" "
W	1297.27 kg	0.0213 "	" "
C	117.54 kg	0.0296 "	" "
Al	60.295 kg	0.00675 "	" "
Fe	4.191 kg	0.000227 "	" "

A series of measurements of central reactivity worth were made with the same samples as previously reported on the preceding assemblies. These data are summarized in Table IX.

Table IX. Measurements of Central Reactivity Worth

Sample	Weight, g	Measured Worth	
		Ih	Ih/kg
U ²³⁵	135.04	+26.61	+197.1
U ²³⁸	507.0	-4.16	-8.2
U ²³³	110.33	+40.08	+363.0
W	1052	-17.14	-16.3
Re	1267.6	-83.10	-65.6
B ¹⁰	29.29	-97.24	-3330
C	103	-2.12	-20.6
W oxide	51.699	-0.8775	-17
Al	166.9	+0.05	+0.3
Al ₂ O ₃	237.9	+0.99	+4.2
Au	1186	-37.47	-31.6

In an effort to determine the relative reactivity of a bare core to a reflected core, all the radial reflector material in about a 15° angular zone from the core axis was removed from one octant of the reactor. This produced a reactivity loss of 89 lh. For voiding about a 30° angular zone, the loss was 158 lh. Extrapolation over the whole core from these two measurements yields an estimated radial reflector worth of $11\% \Delta k/k$.

Other studies related to the radial reflector worth included measurements with a $1/2$ -in. air-and-graphite layer over 18.8% of the core surface at the core reflector interface in the stationary half. Results are given in Table X.

Table X. Edge Worths of Reflector

	Worth of Sample, lh	Extrapolated around Entire Core, lh
$1/4$ -in. layer of aluminum, reference	0	
$1/4$ -in. air (removal of 1188.4 g Al)	-5.2	-55.5
$1/2$ -in. air (removal of 2376.8 g Al)	-11.4	-118.5
$1/2$ -in. graphite, 1326.7 g	+7.2	+76.8

Of interest to the control problem is the worth of a B^{10} ring surrounding the core at various radial positions in the reflector. For these measurements, a ring of boron enriched in B^{10} was placed at different radial positions through a 43° pie section (about one-eighth of the radial reflector in $1/2$ of the reactor). Results are given in Table XI.

Table XI. Boron Worth in Reflector

Run No.	Ring Radius, cm		Thickness, cm	Weight of B^{10} , g	Reactivity, lh
	Inner	Outer			
1	36.22	36.54	0.318	97.6	-20.9
2	36.22	36.86	0.636	195	-42.05
3	41.75	42.07	0.318	98.0	-11.65
4	36.66	36.73	0.638	195	-24.14
5	45.87	46.83	0.638	195	-14.14
6	45.87	46.83	0.638	234	-18.05
7	51.72	52.35	0.638	273	-17.02
8	57.25	57.88	0.638	315	Not reported
9	62.78	63.41	0.638	352	
10	73.84	74.47	0.638	390	

B. Fast Reactor Systems and Concepts

1. 1000-MWe Metal-fueled Fast Breeder Reactor Study

a. Design. A reference concept of a metal-fueled fast reactor is being examined to delineate its thermal, neutronic, and economic performance for the production of electricity at competitive cost according to private utility practice consistent with a breeding ratio of 1.4 to 1.6. General data for the concept are presented in Table XII.

Table XII
General Data for Metal-fueled Fast Reactor

1. Reactor Geometry		7. Axial Blanket	
Core Module Height	3 ft	Uranium Density, Final	15 gm/cm ³
Core Module Equipment Diameter	3.5 ft	Design Maximum Burnup	1.2 a/o
Core Module Volume	840 liters	Weight of Uranium in Reactor	17.2 metric tons
Number of Modules	6 in a ring		
Diameter of Ring at Blanket Edge	19 ft		
2. Fuel Data for Core Modules		8. Beryllium Blanket	
Fissile Concentration of Fuel:		Height of Zone	51 in.
Initial	15 w/o	Zone Thickness	2.1 in.
Final	13.4 w/o	Composition (v/o)	
Internal Breeding Ratio	0.65	Beryllium	83
		Stainless Steel	12
		Sodium	5
3. Fuel Data for the Reactor		9. Inner Radial Blanket	
Total Breeding Ratio	1.5	Thickness	2.4 in.
Plutonium Fissions/Total Fission	0.80	Cladding Outside Diameter	0.21 in.
Net Plutonium Produced	0.45 gm/MWD	Expanded Uranium Density	15 gm/cm ³
4. Power		Design Maximum Burnup	2 a/o
Total Reactor Power	2520 MWt	Weight of Uranium in Reactor	8.5 metric tons
Fraction Produced in Core	0.87		
Core Average Power Density	434 kW/liter		
Core Specific Power	740 kW/kg		
5. Fuel Element		10. Outer Radial Blanket	
Composition (v/o)		Cladding, Outside Diameter	0.58 in.
Cladding of V-20 w/o Ti	30	Expanded Uranium Density	15 gm/cm ³
Expanded Fuel	70	Design Maximum Burnup	1.8 a/o
		Weight of Uranium in Reactor	73.3 metric tons
6. Core Composition and Loading			
Composition (v/o)			
Sodium	40		
Stainless Steel Structure	9		
Control Regions	6		
Fuel Element	45		
Initial Core Loading U + Pu	18.4 metric tons		

A metal-fueled model which allows swelling is used to postulate high burnup. Swelling restraint is provided by the cladding tube. Most of the swelling is attributed to the fission product gases which gradually build up pressure until a limiting stress condition is reached which depends on the volumetric allowance for swelling and the properties of the cladding. According to this model, the burnup can proceed to an arbitrary limit. In practice, the limit is set by the heavy-atom density required for suitable neutronic performance.

An average burnup of 5.5 percent of the uranium and plutonium is provided for by restraint of the fission product gases by 17-mil-thick vanadium-20 w/o titanium cladding. At a linear heat rate of 6.5 kW/ft (13 kW/ft maximum), the fuel centerline hot spot temperature is about 1500°F. A mixed exit sodium temperature of 1000°F is consistent with an average sodium velocity of 20 ft/sec and maximum cladding temperature of about 1100°F. At this temperature, the expected creep rate is low enough to permit end-of-burnup hoop stress of about 25,000 psi for the burnup rate of 5.5 percent in 1.5 years.

The above performance data are based on a fuel alloy with a diameter of 0.150-in. centered in a sodium-bonded clad tube of 0.21-in. outside diameter. As burnup proceeds, the fuel expands to a diameter of 0.176 in., displacing the sodium bond to a region above the upper axial blanket. The axial expansion is limited to 5 percent. The average density of the uranium-plutonium alloy upon expansion is 12 gm/cc. This is the minimum density of the fuel which occurs at about 1% burnup and does not change thereafter. The resulting reactivity change over a six-month period can easily be compensated for and still allow shutdown margin of about 5% $\Delta k/k$ within the 6 v/o allocation for control.

The fuel element arrangement allows 40 percent of the core cross section for coolant flow. The temperature rise of the sodium is 280°F for core height of 3 ft.

The thermal and structural design is based on an acceptable combination of reactivity effects for the materials employed. The overall effect at 40% removal of sodium is roughly -0.3% $\Delta k/k$. Some negative due to axial expansion of the fuel is expected.

The operating temperature levels discussed above are based on a fuel with the solidus temperature typical of a 5% fissium, 18% plutonium mixture in uranium. The solidus temperature is reduced roughly 10°C for each percent of fissium and plutonium in the mixture to give first melting at about 900°C (1630°F). The design is feasible for a fuel with recycle fission products, but there is a significant penalty in temperature level because of their presence.

Since there does not seem to be any inherent reason for using fissium in a design based on any model of metal fuel behavior at high burnup, it is not being considered in the economic or nuclear performance of the current reference design. The thermal performance predicted is not to be re-evaluated until experimental results are available on the characteristics of tertiary systems of titanium or zirconium in U-Pu. Preliminary information on these systems indicates that fuel densities of 12 to 13 gm/cc of U-Pu are possible at a solidus temperature near the melting point of uranium, 1130°C (2060°F).

If the thermal conductivity and other properties of the tertiary systems are favorable, improvement in thermal performance as follows may be obtained:

- (i) a larger temperature difference for a greater Doppler effect on reactivity before any fuel melting occurs;
- (ii) a higher linear power rating than 6 kW/ft to allow a larger pin size at fixed specific power;
- (iii) a higher mixed exit sodium temperature;
- (iv) higher burnup than 5.5 percent at 12 to 13 gm/cc.

b. Physics. Initial studies were based on the use of uranium-plutonium-4.5 w/o fissium fuel alloy with heavier plutonium isotopes appropriate to a pyrometallurgical reprocessing scheme in which excess plutonium is removed from the blankets. Additional studies with a uranium-plutonium fuel alloy containing titanium or zirconium showed such fuels to have significant overall neutronic advantages compared with the fissium fuel.

Multigroup diffusion-theory calculations have been used to determine static characteristics, including sodium void and Doppler coefficients, breeding parameters, and power distributions. The effect of the introduction of zones of metallic beryllium in the blanket to enhance the Doppler coefficient have been studied.

Some analyses in spherical geometry for an 840-liter module with a zero flux outer boundary condition are summarized in Table XIII. The calculated total breeding ratios are somewhat pessimistic when module coupling is truly accounted for.

Table XIII
Idealized Calculations

Problem Number:	46	47 ^a	48	49	50	52	53	54	55
Fuel Diluent	Fs	Fs	Fs	None ^b	Ti	Fs	Fs	Ti	None ^c
N ²³⁵ /N ²³⁸ Pu	5.7	5.4	5.5	6.0	6.0	5.5	5.6	5.8	6.2
Presence of Beryllium	Yes	No	No	Yes	Yes	No	Yes	No	No
Blanket Thickness (cm)	23	33	23	23	23	46	46	23	23
Core Sodium Void Coefficient (% $\Delta k/k$) ^d	-0.27	-	-0.29	-	-0.44	-	-	-0.53	-0.39
Doppler Coefficient (% $\Delta k/k$) ^e	-0.32	-	-0.12	-	-0.47	-	-	-0.18	-0.17
CCR ^f	0.65	0.61	0.62	0.71	0.71	0.62	0.65	0.66	0.72
TBR ^g	1.37	1.39	1.56	1.45	1.44	1.68	1.43	1.62	1.65

^aAxial Blanket - All other problems with radial blanket and dimensions.

^bLow-density U-Pu.

^cHigh (theoretical) density U-Pu.

^dFor 40% sodium loss in core.

^eFor 750-1500°K.

^fCore Conversion Ratio.

^gTotal Breeding Ratio; all blankets surrounded by steel reflector.

The neutronic penalty through use of an economic blanket may be seen by comparing Problem No. 52 with No. 48 and No. 53 with No. 46.

Dynamic analyses have been initiated to set realistic safety criteria under reactor operating conditions. In addition, a variety of pertinent calculations in cylindrical geometry have been performed to obtain more detailed neutronic understanding of the reactor design, including module coupling coefficients, long-term reactivity behavior, and requirements for reactor control.

c. Fuel Cycle. The fuel cycle used with this study is the EBR-II system, using injection casting for fuel fabrication, and pyrometallurgy for reprocessing both core and blanket. The initial studies were related to the fissionium alloys; more recent exploratory work considered U-Pu systems containing titanium or zirconium.

The overall fuel-fabrication operation was broken down into its component parts as shown in Figure 3. From this a FORTRAN Computer program was formulated, made up of about two hundred variables which influence fabrication costs and add flexibility to the system of calculation, to estimate fabrication costs versus throughput fuel-pin diameter and fuel-pin length. Two types of core fuel pins are considered: "segregated" and "integrated." In the former, the core and axial blanket sections are in separate jackets; in the latter, both are in the same jacket.

The chemical separation procedure for fissionium fuel is presented in Figure 4. The process employs molten metals and salts to recover and partially decontaminate uranium and plutonium by a sequence of selective oxidation and reduction reactions. The pyrometallurgical processing does not provide complete separation of fission products.

The core and blanket fuel assemblies are removed from the reactor and transferred to a sodium-cooled tank, where they are retained for 15 days. During the period of cooling the rate of heat generation from the decay of fission products diminishes sufficiently to afford a substantial reduction in the cooling requirements in subsequent process steps. The influent streams in pyrometallurgical processing are not subject to radiation damage; therefore, an extended period of cooling is not required.

After cooling, the fuel assemblies are steam cleaned to remove residual sodium and then disassembled; the excess structural metal is removed and discarded. The cladding is mechanically stripped from the fuel elements.

The core and blanket fuels are processed separately, and only the core fuel is treated to remove some of the nonvolatile fission products. The blanket nonvolatile fission products appear either in the uranium or in the plutonium product, which is recycled to the core fuel to replenish its fissile content.

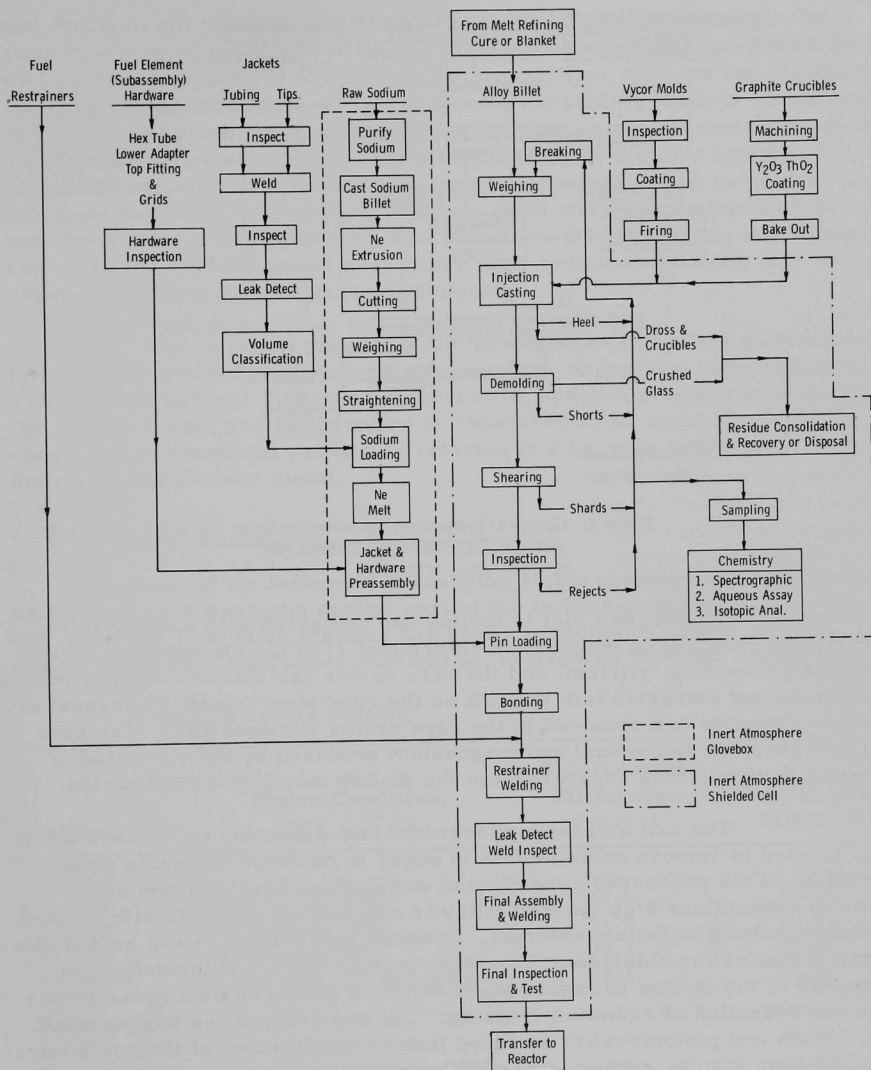


Figure 3. Fabrication of Metal Fuel

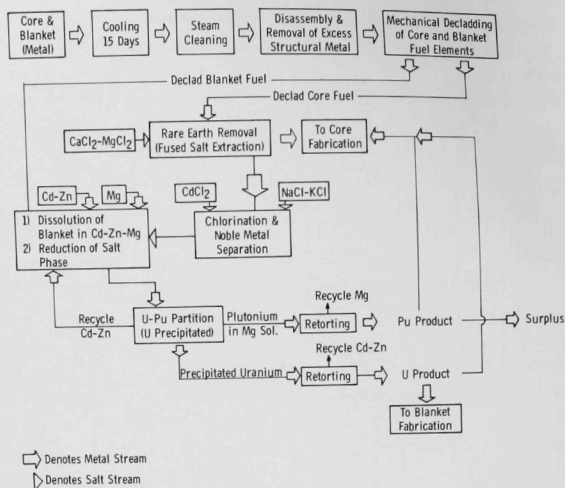


Figure 4. Chemical Separations Procedure for Pyrometallurgical Processing of Metal Fuel (U-Pu-Fs Core; U Blanket)

Declad core fuel is melted and contacted with a fused salt extractant containing magnesium chloride at 1150°C . Strontium, barium, rubidium, cesium, yttrium, and the rare earths are oxidized by magnesium chloride and extracted into the salt as the chlorides. About 99 percent of these elements are removed in the rare earths removal step. The rare gases (krypton and xenon) and magnesium produced by the reduction of magnesium chloride separate from the molten metal by volatilization.

The salt stream is discarded, and a fraction of the core alloy is treated to remove noble metals in order to maintain the noble metal content of the processed core alloy at any desired level. In the noble metal separations step the core alloy is chlorinated at 650°C with a fused salt containing cadmium chloride. Uranium and plutonium are held in the salt phase as the chlorides. The noble metals are not chlorinated and appear in the molten cadmium phase which is produced as a consequence of the reduction of cadmium chloride. The cadmium phase is discarded. Uranium and plutonium are stripped from the salt phase of the noble metal separation step by reduction at 600°C with magnesium in cadmium-zinc solution.

The declad blanket fuel is dissolved in an 89.4 w/o cadmium-10.6 w/o zinc solution at 650°C . This metal stream is combined with the portion of the core that was stripped of noble metals as a solution of UCl_3

and PuCl_3 in molten salt. Sufficient magnesium is added to reduce the actinides from chlorides to metal and bring the magnesium content of the molten metal solution to about 10 w/o. To partition uranium and plutonium, the magnesium concentration is increased by distilling most of the cadmium and some zinc from the mixture. When the magnesium concentration of the solution is increased to 50 w/o, uranium precipitates as the metal and plutonium remains in solution. The uranium product, which is used to fabricate blanket fuel elements, contains about one part of plutonium per one-thousand parts of uranium. The plutonium product, which is used to replenish the fissile content of the core fuel, contains about one part of uranium per one-hundred parts of plutonium.

The uranium product of the partition step consists of precipitated uranium metal and about 10 w/o residual magnesium superreactant. The uranium product stream is retorted in a beryllia crucible to volatilize the solvent metal, and the uranium is recovered as an ingot of metal. The concentrated plutonium product is retorted in a beryllia crucible to remove the remaining solvent metal.

2. Comparison of Electricity-generating Units

A study of the influence of changing steam pressure and temperature on thermal efficiency and capital cost of the turbine-generator plant for 500 MWe and 1000 MWe stations has been completed by United Engineers and Constructors, Inc., under subcontract to Argonne National Laboratory.

The results are as follows:

Designation	Steam Condition, Psig - °F/°F	Net Thermal Efficiency, Percent	Capital Cost, \$/Net kW
500 MWe			
500 A	3500-1000/1000	42.6	52.06
500 B	2400-1000/1000	41.8	50.99
500 C	1800- 900/900	39.7	52.17
500 D	1000- Dry and Saturated	33.2	66.26
1000 MWe			
1000 A	3500-1000/1000	42.9	46.26
1000 B	2400-1000/1000	42.1	44.98
1000 C	1800- 900/900	39.8	48.37
1000 D	1000- Dry and Saturated	33.5	60.62

One of the major reasons for the study was to have comparative, consistent, and documented information about the electricity-generating portion of a central station power plant. Having this information, one may draw some preliminary conclusions. First, the 2400-1000/1000 steam condition results in the lowest capital cost in both sizes and is only 2% less

efficient than the 3500 psig case. Second, the 1800, 2400, and 3500 psig steam cycles exhibit significant improvement in cost and thermal performance over a steam cycle representative of present water-cooled nuclear reactors. Third, the selection of an 1800-900/900 steam cycle for fast reactors does not appreciably penalize the electricity-generation part of the plant; the reduced temperature requirements in such a plant over a plant having a 2400-1000/1000 cycle may alleviate critical materials problems in certain reactor designs; or the 1800 psig cycle may allow greater temperature differences to be used in heat exchange equipment for a given reactor top temperature over the 2400-1000/1000 or 3500-1000/1000 steam cycle.

Broadly, the scope of the cost estimate was to include all materials, labor, and equipment costs from the inlet steam line to the turbine-generator building through the high-voltage transformer. In addition, the indirect costs items were included (with specific exceptions) and the costs were reported under the Federal Power Commission system of accounts.

The information prepared for the cost estimate and thermal efficiency is in sufficient detail to be of use in the evaluation of various sodium-cooled fast reactor concepts. The above work is part of an overall effort on fast power reactors. It is planned in the next phase of the work to examine the sodium-heated steam-generator plant in similar fashion. Plant layout and building arrangement will be consistent with the study of the turbine-generator plant. Matching steam conditions and flow rates will be employed. It is planned to examine the operation of once-through boilers to establish that satisfactory control of the overall plant can be achieved. Temperature profiles of secondary sodium and water-steam versus energy fraction transferred will be selected for optimization studies to ascertain boiler size and piping arrangement. All significant plant features will be incorporated in the study for cost analysis.

C. General Fast Reactor Fuel Development

1. Metallic Fuels

Uranium-plutonium-base alloys are being investigated for use as fertile-fissile fuel materials in fast breeder reactors. Alloying additions appear necessary to improve the stability of these alloys in a fast reactor environment and to improve the compatibility with jacketing materials.

a. Improved Uranium-Plutonium-base Fuels. U-Pu-Ti and the U-Pu-Zr alloys offer promise as fuel materials that will withstand higher burnup and/or higher operating temperatures. The melting temperature was selected as a criterion for screening the alloys, since a higher melting temperature should lead to improved swelling resistance. The greater range before melting should also permit a higher operating temperature, and it should be a safety factor in the event of an excursion.

As part of a screening study two series of alloys based on an atom ratio for uranium to plutonium of 4 to 1 were made with additions of the following elements: Sc, Ti, Y, Zr, Mo, Pd, and Th (either 30 a/o or 10 a/o of one of these elements in each respective alloy). The solidus temperatures were determined by heat-treating the alloys in vacuum, quenching them in NaK, and then examining them metallographically. Thermal-expansion coefficients of the as-cast alloys were also determined, and metallographic studies were made.

Only the 30 a/o Ti and 30 a/o Zr alloys had solidus temperatures over 1100°C, so it is planned to concentrate further studies on these two alloy systems.

2. Carbide Fuel Elements

a. Interaction of U-Pu Mixed Carbides with Potential Refractory Metal Cladding

For fast breeder reactors solid-solution uranium-plutonium monocarbide fuels have the advantage over solid metallic fuels of being usable at higher temperatures and over oxide fuels of having superior thermal conductivity.

Interest in (U,Pu)C as a fast reactor fuel in the temperature range from 650 to 1100°C, in particular, has occasioned the initiation of a systematic study to determine the extent and mode of interaction with potential cladding materials. A study of this interaction is necessary for two reasons: (1) extensive interaction can make possible a rupture of the fuel element cladding, thereby allowing a release of fuel into the coolant, and (2) interactions that are less extensive but appreciable can

adversely affect such pertinent properties of the cladding as mechanical strength and thermal conductivity. The materials to be studied include iron- and nickel-base alloys and a number of refractory metals.

An evaluation of pertinent literature information associated with the compatibility of cladding materials with (U, Pu)C is in progress. Preliminary annealings of four (U, Pu)C/cladding diffusion couples at 800 and 1100°C indicate that the experimental techniques employed are sound.

3. Development of Jacket Materials

a. Vanadium Alloys.

(i) Fabrication of V-Ti-base Ternary Alloys. A series of V-Ti alloys with varying additions of Cr, Mo, Ta, and Nb have been prepared. Of the nine alloy compositions in the series, six have been reduced to 0.08-cm (0.031-in.) sheet by hot and cold rolling:

V-15 w/o Ti-5 w/o Cr	V-20 w/o Ti-2 w/o Mo
V-15 w/o Ti-7.5 w/o Cr	V-20 w/o Ti-2 w/o Nb
V-20 w/o Ti-5 w/o Cr	V-20 w/o Ti-2 w/o Ta

Samples for tensile and corrosion testing are being cut from the rolled sheet stock.

The alloys V-30 w/o Ti-5 w/o Cr and V-30 w/o Ti-10 w/o Cr have been rolled to a thickness of 0.16 cm (0.062 in.) and will be further rolled to 0.08-cm (0.031-in.) sheet stock for test specimens.

The other alloy, V-5 w/o Ti-15 w/o Cr, has been hot rolled, but attempts to cold roll this alloy have been unsuccessful. The material is now being heat-treated after which hot and cold rolling will again be attempted.

(ii) Properties of V-20 w/o Ti Alloy. The heat content of the V-20 w/o Ti alloy was measured between about -80 and 1150°C. These data are needed to aid in reactor kinetics calculations. The change in heat content between 25 and 200°C was 20.9 cal/g; that between 25 and 1000°C, 126 cal/g. Mean values of specific heat were calculated over the same intervals to be 0.119 and 0.131 cal/g-°C, respectively. Smithells¹ gives values for vanadium of 0.121 and 0.139 cal/g-°C for these same temperature intervals.

Tube-burst tests have been initiated to study the relationship between tangential (hoop) stress and time to rupture for a biaxially

¹Smithells, C. J., Metals Reference Book, 2nd Ed., Vol. II, Butterworth, London (1955), p. 602.

stressed tubular geometry. Test specimens have an over-all length of 10.2 cm and a gauge length of 7.6 cm located between re-enforced collars at each end. Stress is applied by an internal helium gas pressure.

A tube-burst specimen of seamless Type 304 stainless steel tested at 550°C under a tangential stress of 23.2 kg-mm^{-2} ruptured in 324 hr. The total true radial strain at rupture was 12%, as determined by diameter measurements made at given time intervals. This value of true radial strain before rupture appears to represent the maximum strain sustained by the specimens of the type described for rupture times in excess of 25 hr.

(iii) Corrosion. A series of V-20 w/o Ti samples, shaped like the tensile specimens, lost 6.30 mg/cm^2 while under load and exposed to flowing (0.15 cm/sec) sodium for 168 hr at 650°C. Since plugging-meter analyses of the sodium before and after exposure of the loaded specimens indicate an oxygen concentration of probably less than 10 ppm, the high weight losses cannot therefore be attributed to the effect of a high oxygen content of the sodium.

The present group of specimens show evidence of intergranular attack. This is the first time that such attack has been observed on exposure of V-20 w/o Ti alloy to low-oxygen sodium.

The effect, if any, of the loading on the corrosion behavior is not known, since all the samples were under stress. The next group of samples will, therefore, include an unloaded control so that the effect of stress can be evaluated.

V-20 w/o Ti samples exposed for 99 hr at 650°C in static sodium containing 50 ppm of oxygen, have lost 0.88 mg/cm^2 . This is in direct contrast with earlier experimental runs, in which the samples gained weight (see, for example, Progress Report for October 1964, ANL-6965, p. 9).

The irreproducibility of this behavior might be due to changes in environmental conditions and to differences in materials. Our experimental techniques must therefore be re-examined, and re-refined if necessary, so that reproducible environmental conditions will be assured.

(iv) Corrosion of Other Vanadium Alloys in Oxygen-contaminated Sodium. A number of arc-melted binary vanadium-alloy buttons were exposed to sodium for 4 to 6 days at 650°C. Weight losses after defilming (see Progress Report for August 1964, ANL-6936, pp. 25-6) indicate that titanium, molybdenum, and chromium were the most effective in preventing weight losses. However, the oxygen

penetration was very deep in the molybdenum binary and moderately deep in the chromium binary. The titanium binaries (V-10 w/o Ti and V-20 w/o Ti) had the smallest oxygen penetration of all those tested, and the yttrium and the nickel binaries also had relatively shallow oxygen penetration. All of the binaries had less oxygen penetration than occurred for pure vanadium.

More precise data than here reported require better homogeneity in the alloys and much better control of the oxygen access to the specimens. In this connection a diaphragm pump is being modified for use in slowly recirculating the sodium in a test facility now under construction.

4. Irradiation of Uranium-Plutonium-Fizzium Alloys

Metallographic examinations are being conducted of highly irradiated U-20 w/o Pu-10 w/o Fz fuel pins jacketed in Nb-1 w/o Zr tubing (see Progress Reports for July 1964, ANL-6923, p. 25, and September 1964, ANL-6944, p. 27, for results of other postirradiation section). One set of specimens had been jacketed with tubing having a 0.23-mm wall thickness; the other had tube walls of 0.38-mm thickness.

Metallographic sectioning was in a transverse plane and in selected areas that had representative jacket failure. The jacket was also examined in areas that did not show superficial defects.

All jacket material was characterized by incipient cracking that originated at the inner surface of the tubing. These cracks appeared at random places and propagated anywhere from 10 to 100% of the jacket wall thickness. Fractures in jacketing appeared to be of a brittle nature.

Jacketing that had been irradiated at maximum temperatures of 635°C showed a fuel-jacket reaction layer on the inner surface of the jacket tubing. The thickness of the layer varied from 0.03 to 0.18 mm and was directly related to the maximum temperatures of the jacket. In some instances the fuel-jacket interaction made it difficult to determine a line of separation between both materials.

5. Corrosion Inhibition in Sodium

A preliminary test of the corrosion behavior of available zirconium-base alloys has been made in a calcium-gettered sodium environment at 650°C. Samples of unalloyed extruded zirconium, of hot-rolled Zr-3 w/o Ni-0.5 w/o Fe, and of as-cast Zr-1 w/o Cu-1 w/o Fe were wet-ground, etched, and exposed to sodium saturated with calcium for six days in a stainless steel autoclave at 650°C. After exposure, the samples were washed with water and examined.

Metallographic examination of sample cross sections showed a reaction layer a few microns thick on portions of the unalloyed zirconium and on quaternary samples, but no similar layer on the nickel-bearing material. Weight changes were gains of about 1 mg/cm^2 . Microhardness traverses inward from the metal surface of each sample (Knoop, 15-g load) indicated no point of hardness above 310 and no evidence of embrittlement to within 5μ of the surface, although the point scatter was appreciable.

D. General Fast Reactor Fuel Reprocessing Development

1. Skull Reclamation Process

A problem of flux foaming which had been encountered in several runs was eliminated in two recent runs by pretreatment of the flux (47.5 m/o CaCl_2 , 47.5 m/o MgCl_2 , and 5 m/o CaF_2) with magnesium to remove any water present in the flux. The prevention of foaming by this pretreatment bears out the contention that foaming had been caused by the reaction of magnesium and residual water of hydration to produce hydrogen. An additional precaution taken in these runs was to degas the mixed oxides at 800°C for 6 hr under vacuum prior to use.

2. Materials and Equipment Evaluation

The effect of the argon-5% nitrogen atmosphere of the Argon Cell of the EBR-II Fuel Cycle Facility on structural materials of the equipment is being investigated. Brunhouse² reports that pure nitrogen reacts with Inconel 600 and Hastelloy X alloys at a temperature of 950°C . It is believed that a complex nitride phase forms, causing serious embrittlement of the alloy. Consequently, a program has been initiated to study the effect of argon-5% nitrogen on Inconel-600, Inconel-800, Hastelloy C, Hastelloy X, Type 304 stainless steel, Type 316 stainless steel, tungsten, and molybdenum-30% tungsten alloy. These materials may see service in the Argon Cell.

Tests of the eight materials at 900°C for 450 hr have been completed. Inconel and Hastelloy suffered a loss of ductility but were still usable. The 300 series stainless steels, which are used in the Argon Cell, were not significantly affected.

These tests will continue until 2000-hr exposure has been obtained. It is doubtful that nitridation will present a serious problem in the EBR-II cell because of the limited use of high nickel alloys at temperatures above 650°C . Should a problem develop, however, protection methods such as oxide scaling or diffusion-bonded coating of these alloys will be used.

²Brunhouse, J. S., Corrosion and Compatibility of Nickel-based Alloys with High-purity Nitrogen, paper presented at the 13th Annual AEC Corrosion Symposium, Argonne, Illinois, May 1964.

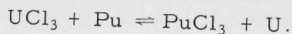
3. Advanced Processes

a. Chloride Flux-Melt Refining of Uranium-Plutonium-Fissium Fuels. A halide slagging process is being studied (see Progress Reports for March 1964, ANL-6880, p. 28, and May, 1964, ANL-6904, p. 38) in which rare earth and other highly electropositive fission products are selectively oxidized and extracted from molten fuel alloy into an overlying molten salt phase. A high-density beryllia crucible has been used to contain the salt and metal phases. Potential advantages of this process, as compared with the melt refining process to be used for recovery of the first EBR-II core, are higher product yields, a lower operating temperature, and a shorter processing time. Plant-scale application of this process is presently made difficult by the unavailability of suitable large beryllia crucibles. The technology for fabricating large beryllia crucibles is currently under development by commercial suppliers.

The separation of cerium (considered a typical rare earth element) from plutonium is being investigated. In the most recent run, twice the amount of CaO theoretically required to react with the cerium in the charge, assuming no reaction of cerium with impurities, was added as oxidant to a 75 m/o BaCl_2 -25 m/o CaCl_2 salt mixture. The metal charge was 81 w/o U-10 w/o Pu-9 w/o fissium to which was added about 0.7 w/o cerium. The weight ratio of flux to metal was 2:7. After liquation at 1150°C for 1 hr under argon in an isopressed, high-density, high-purity BeO crucible, the crucible contents were cooled to 860°C, which caused the alloy to solidify, and the flux was poured off. Subsequently, the metal was melted by heating to 1300°C and was poured into a separate vessel.

Analyses of samples of the two phases indicated very satisfactory separation of cerium from plutonium - removal of 92% of the cerium from the ingot with a transfer of only 0.004% of the plutonium to the flux, giving a separation factor, $(\text{Ce in flux/Ce in metal})/(\text{Pu in flux/Pu in metal})$ of 7100. Cerium removal and plutonium retention were satisfactorily high. The amount of plutonium extracted into the salt was smaller than in previous runs (see Progress Report for March 1964, ANL-6880, p. 28) in which a stoichiometric or an excess quantity of MgCl_2 was used.

b. Halide Slagging Studies. Plans are underway to investigate halide slagging as a method for the extraction of plutonium from blankets discharged from power breeder reactors. The blanket material would be melted, and the plutonium extracted into a flux consisting of calcium chloride and uranium trichloride oxidant. An attempt is being made to obtain reliable equilibrium constants for the reaction



Equilibrium constants will be determined at 1150-1250°C, using 0.2-4.5 w/o plutonium. Apparatus for the equilibration studies has been completed and is being tested, and pure CaCl_2 and UCl_3 are being prepared.

c. Ion Exchange in Fused Salts. An investigation of the feasibility of separating ions in molten salts in ion exchange columns is in progress. Four runs have been made to measure the distribution of Ba^{+2} (spiked with ^{133}Ba) between molten mixtures of KBr and AlBr_3 , and potassium hexatitanate (Tipersul). The mole ratio of KBr to AlBr_3 in the salt solution was varied in order to determine the influence of varying polarity of the solvent on ion-exchange behavior. The salt solutions were approximately 0.01 M in Ba^{+2} (added as BaBr_2).

In runs at 140°C and 190°C with a mole ratio of KBr to AlBr_3 in the solvent of less than unity, Ba^{+2} was not removed from the salt solution by potassium hexatitanate. In a run at 220°C with an equimolar KBr-AlBr_3 solvent, however, the Ba^{+2} favored the hexatitanate; the distribution coefficient (specific activity of solid-specific activity of melt) was about 1700. When the reverse experiment was performed (the Ba^{+2} initially on the solid), a distribution coefficient of approximately 3600 was obtained. These results indicate that ion-exchange media might be used to remove certain fission products from recycled process salts.

4. Consolidation of Fission Product Wastes in Alloys

Extraction of rare earth fission products from molten chlorides by aluminum-magnesium alloy is being studied as a possible method of purifying salt for recycle to plutonium-rare earth separation steps and as a means of consolidating most of the fission products in a small volume of metal for storage. Experiments have been performed in which distribution coefficients of lanthanum between 30 m/o NaCl -20 m/o KCl -50 m/o MgCl_2 and aluminum alloys containing 13, 20, or 30 w/o magnesium were determined in the temperature range from 550 to 900°C. The solubility of lanthanum in these alloys also was determined. The distribution coefficient values (concentration in salt/concentration in metal) fell between 3×10^{-3} and 1×10^{-1} ; the values increased with rising temperature. The solubility of lanthanum in the magnesium-aluminum alloys increased with temperature up to about 700°C and appeared to become retrograde above this temperature. The solubilities of rare earths in aluminum-magnesium alloys reached values of several percent. These solubility values, in conjunction with the favorable distribution coefficients, should permit the preparation of a highly concentrated waste alloy.

5. Decladding Studies for TV-20 Cladding

Uranium-plutonium-fissium alloy clad with vanadium-20 w/o titanium alloy (TV-20) appears to be a promising fast reactor fuel material. Several methods for the chemical separation of fuel alloy from TV-20

cladding are being investigated, one of them being the removal of TV-20 cladding from metallic fuels by hydriding the fuel. A uranium-fissium alloy pin sealed in TV-20 tubing was exposed to hydrogen at 2 atm pressure for 3 hr at 250°C. The hydrogen apparently diffused through the cladding and hydrided the fuel, since the TV-20 split open. Further hydriding then occurred. This procedure, followed by dehydriding, dissolution of the fuel in liquid metal, and filtration, maybe a promising method for separating the fuel from the cladding without prior chopping of clad fuel pins.

6. Eddy Current Induction Probe

The eddy current induction probe for liquid metal-level measurement has been calibrated with bismuth as the liquid metal. Values of signal output versus depth for bismuth were compared with those for cadmium at the same settings (i.e., 50-kc input frequency, 7-V input voltage, 35 mV of bucking voltage). The change of output signal with change of melt depth was less for bismuth than for cadmium, as was expected since bismuth has a higher electrical resistivity than cadmium. Development of this probe is nearly complete. The probe has been developed for use in Argonne pyrometallurgical processes, but can be applied to other remote measurement of liquid metal level.

7. Removal of Nitrogen from Argon

The removal of nitrogen from argon by gettering the nitrogen on hot (~900°C) titanium sponge is under study because of a possible future need to remove nitrogen from the argon atmosphere in the Argon Cell of the EBR-II Fuel Cycle Facility. Two sets of experimental equipment have been constructed and operated: (i) equipment for a study of the kinetics of nitrogen removal from argon on hot titanium sponge (see Progress Report for July 1964, ANL-6923, p. 31) and (ii) a pilot plant for obtaining overall process performance data and information on component reliability (see Progress Report for April 1964, ANL-6885, p. 23).

Preliminary kinetic data have been obtained on the rate of reaction at 900°C of titanium metal sponge with argon containing 5000, 1000, and 300 ppm nitrogen. The circulation rate was such that only a very small fraction of nitrogen in the gas stream reacted with titanium in a single pass through the beds. The nitrogen concentration of the gas was returned to its initial concentration before each pass. For the three gas mixtures, the conversions after 50 hr were about 50, 45, and 37%, respectively. The reactions were rapid for 40 to 50 hr, and then decreased to low rates. The data indicate that the reactions probably follow a modified parabolic or exponential rate law, with the ultimate nitrogen content of the sponge dependent upon the partial pressure of nitrogen in the gas phase.

The pilot plant was operated continuously for 575 hr at 900°C with argon containing 100 ppm nitrogen circulating at 10 cfm. After this, the pilot plant was shutdown and the titanium bed sampled. Analytical results

for the samples indicate a conversion of about 30% of the titanium to the mononitride, the assumed product of the reaction.

E. Sodium Coolant Chemistry

1. Cover-gas Impurities

Studies have continued of the reaction of various possible contaminant gases with liquid sodium, which is used as a coolant in nuclear reactors. Experiments are underway to ascertain whether the reaction $2\text{H}_2 + \text{C}$ (in sodium) $\rightarrow \text{CH}_4$ can be used to decarbonize sodium. The initial results do not indicate a significant amount of methane produced when sodium is sparged with a He-1% H_2 mixture at 300°C.

2. Analysis for Oxygen

A study of some of the factors affecting plugging-valve operation revealed that the method of providing driving force to the sodium in the plugging meter loop is important. Current experiments are directed toward:

- (i) the use of flow control valve in the main loop between the sodium inlet and exit of the plugging valve loop;
- (ii) the use of an electromagnetic pump with ac operation;
- (iii) the use of an electromagnetic pump with dc operation.

F. EBR-II

1. Sticking of Control Rod and Oscillator Drive Mechanisms

Early in the month, the bulk sodium temperature in the primary tank was lowered from 700 to 580°F and then to 375°F to permit work on the control rod and oscillator components. After the primary system had been cooled to 375°F, the secondary sodium was dumped to the storage tank, and the secondary piping and steam systems were cooled to ambient temperature.

When the primary tank had cooled to 580°F, the sticking No. 7 control rod shaft (see Progress Report for October 1964, ANL-6965, pp. 19-21) was removed. Inspection showed that small steel balls, about 1/8 in. in diameter, had caused the binding in the reactor vessel cover (see Figures 5-8). Control drive shaft No. 9 was also removed, and a similar binding situation was found. The balls apparently came from one or both of the linear ball bushings that failed in the oscillator drive shaft. Presumably, the ball bearings were dislodged from the oscillator shaft and came to rest in the 0.030-in. diametral clearance between the control rod drive shaft labyrinths and the Stellite sleeves in the reactor vessel cover. Chemical analysis of the balls showed they are carbon steel. Special ball-retriever tools were used during removal of the malfunctioning oscillator drive shaft assembly in an effort to catch the small steel balls that might otherwise drop on top of the subassemblies in the reactor grid.

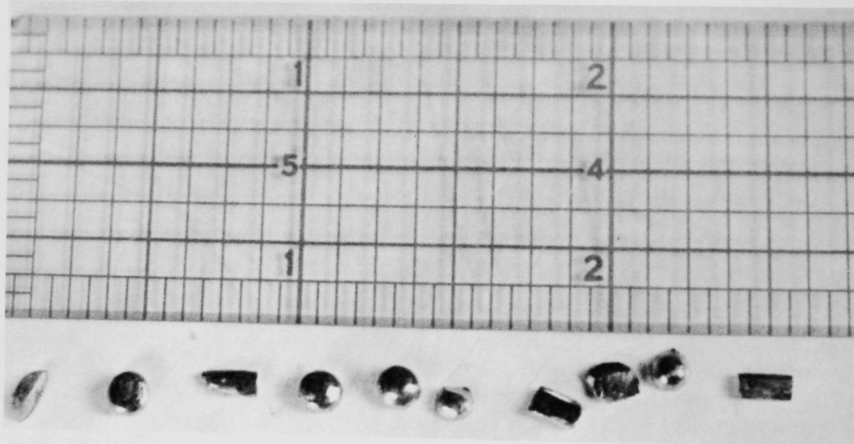


Figure 5. Debris Taken from Labyrinth Area of No. 7 Control Rod Down Shaft

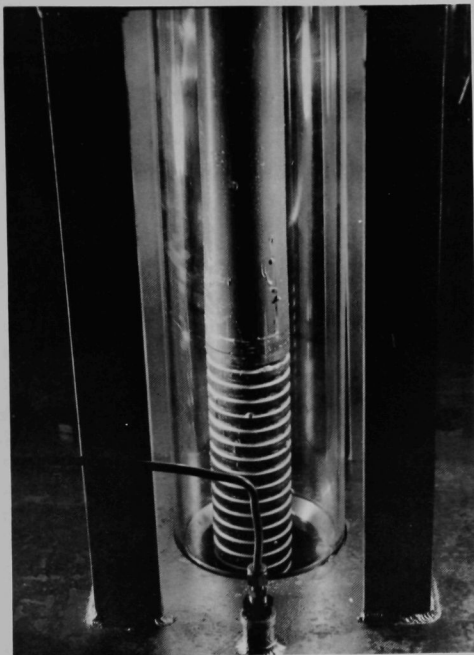
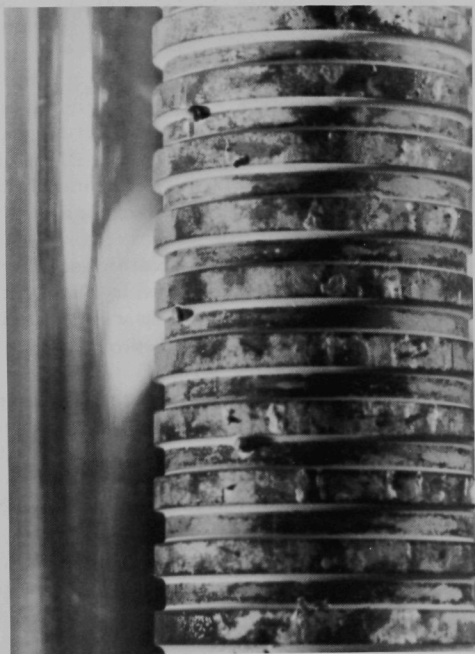


Figure 6

Labyrinth Area of No. 7 Control Rod
Drive Shaft Showing Scoring from
Steel Balls. Shaft Diameter - 2.5 in.

Figure 7

Control Rod Drive Shaft
Labyrinth No. 9 Show-
ing Steel Balls



When the oscillator drive mechanism was disconnected from the oscillator rod, the rod was stuck in the oscillator thimble. This will complicate removal of the oscillator rod.

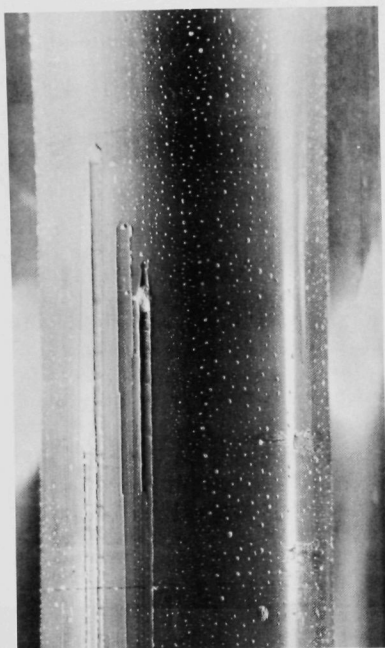


Figure 8. Control Rod Drive Shaft No. 9 Showing Scored Area Just above Labyrinth

2. Maintenance

The main fuel gripper jaws were actuated in a test and appear to work satisfactorily.

The plugging temperature of the secondary sodium was maintained between 250°F and 300°F by intermittent use of the cold trap. When the system was dumped on November 20, the plugging temperature was 260°F. The entire system was cooled to ambient temperature with the exception of the storage tank which was maintained at 350°F. During the month, the composition of the blanket gas remained practically constant at 10 ppm hydrogen and 800 ppm nitrogen.

The composition of the primary system cover gas remained fairly constant at less than 10 ppm hydrogen and 1.3% nitrogen.

Because of difficulties caused by leaks in the vacuum system for the surge tank on the primary purification system, the latter was shut down during this month. The leak was traced to the seat of the syphon break valve in the vacuum system, and a new valve has been ordered.

The Dowtherm-water heat exchanger for the secondary purification system was disassembled to clean the water side. Some silt and other debris were found. It was reinstalled with flanged joints so that future cleaning will be simplified.

Faulty performance of the large, automatic steam bypass valve, which tended to open fully after the stem position reached half-open and seemed to stick in the fully open position, has been corrected. A switch was installed on the steam graphic panel to permit operators to close the 1,250-psig steam bypass block valve between the headers and the main condenser. This enables an operator to stop the bypass steam flow in case of bypass valve malfunction or bellows failure without leaving the control room.

Stellite trim for the small bypass steam valve was received and installed upon the manufacturer's recommendation. This valve had performed unsatisfactorily during the power demonstration run.

A remote operator was installed to permit operation of the main steam line block valve from the operating deck level of the Sodium Boiler Plant.

3. Fuel Cycle Facility

a. Argon Cell. An argon-atmosphere enclosure system is being installed in the Chemical Engineering Division at Argonne, Illinois, in order to test the effect of a dry argon environment on the operation of equipment to be used in the EBR-II Argon Cell (see Progress Report for July 1964, ANL-6923, p. 35). One glovebox and an argon-purification system, similar to that in the EBR-II Argon Cell, were previously installed and placed in operation. Construction of a large inert atmosphere enclosure, 24 ft long by 12 ft wide by 14 ft high, which will be a part of the enclosure system is nearing completion. It will be equipped with glove ports and a large roof hatch (12 ft long by $7\frac{1}{2}$ ft wide) for handling large pieces of equipment. A cooling system has been provided for controlling the temperature within the enclosure. All windows have been installed. The major portion of the service piping and electrical work has been completed. After the installation of supporting equipment is completed, leak-testing of the enclosure will be performed. Following the leak tests and repair of any leaks, installation will start of plant-scale prototype equipment for demonstrating the skull reclamation and blanket processes. Initially, the inert atmosphere enclosure will be used for the testing of a prototype (M-2) skull oxide reclamation furnace whose fabrication is underway (see ANL-6923, p. 35). Fabrication of a panel board for control of the M-2 furnace is in progress.

As part of the routine maintenance program, one of the Argon Cell electromechanical manipulator carriages, which had been in service in the contaminated cell for two months, was removed for inspection and exchanged for an Air Cell carriage. Although the gamma-activity level was only a few mr/hr, surface contamination greater than 10^6 dis/(min) (dm^2) was found. This was readily reduced by a factor of several hundred by vacuuming and wiping with damp cloths. Hoist cables and asbestos-insulated wiring were not readily decontaminated. The hoist drive unit was removed for clutch modification and replaced, and the exchange of carriages was completed.

b. Fuel Recovery and Fabrication. Sampling of the Fibrefrax fume trap from the first melt refining of irradiated fuel indicated that a major fraction of the I^{131} content of the charge was retained by the trap. Analysis of a sample of oxidized skull remaining after this melt refining operation showed no partition of molybdenum during oxidation, and pickup of about 3 g of zirconia from the crucible.

Work has continued on the reclamation of approximately 2,500 fuel elements obtained by destruction of special assemblies that had been prepared for dry and wet critical operations. Of the more than 2,000 elements of demonstrated acceptability (by rebonding and bond testing) and the 350 elements remotely fabricated, 1,673 have been made into reactor assemblies (12 control, 2 safety, and 9 core-type).

The straightness-checking part of the final test machine has required some adjustment. The assembly machine, with which some early difficulty had been encountered in welding, now produces good welds reliably.

c. Fuel Surveillance. A vessel to be used for removal of sodium from decanned fuel elements segregated for measurement is being installed in the Air Cell. A prototype unit to be used for determination of gas pressure and for sampling the gas in these fuel elements has been fabricated and is being tested.

The jacketed, metallic fuel pins in the capsules that were inspected are enclosed in a vanadium-barrier thimble and bonded to this barrier with sodium; the barrier thimble is in turn sodium bonded to the outer jacket of stainless steel tubing. Thus a double annulus of sodium is formed, divided by the vanadium-barrier thimble. The quality of the bond is important in both annuli.

A little success was obtained in inspection of the inner annulus by means of an ultrasonic method. The barrier was cut from rolled material, formed into a cylinder, and spot welded along the overlapping edges. This line of alternately welded and unwelded areas in addition to the relatively rough shape of the thin material forming the barrier thimble caused so much interference and scatter to the ultrasonic beam that it was not possible to clearly distinguish echoes from voids in the inner annulus.

It is possible to detect nonbonds by radiography, if careful masking to prevent undercutting and contrast enhancement by reprinting are employed. If either the fuel pin or thimble is slightly off center, either annulus may become too narrow for the nonbonds to be visible. Unfortunately, it is often the narrow annuli that are the most difficult to bond satisfactorily. Nevertheless, radiography provides the only method available to inspect any part of the inner annulus of these capsules, and it is being used to inspect those areas of the inner annulus that are visible on the radiographs.

The outer sodium annulus can be inspected by eddy-current methods. A test facility has been constructed to test these capsules and those which will follow. Since even the most careful quenching procedure will not always eliminate all shrinkage voids, this facility is designed to test the capsules at a temperature high enough to melt the sodium. A

double-pulse eddy-current test system is used to search for nonbonds at 60° intervals around the circumference and along the entire length. With this equipment it is possible to insure that the capsules have at least the bond quality in the outer annulus possessed by the sodium bond in the EBR-II blanket rods themselves.

The bonds on the first 19 capsules are now being evaluated.

d. Skull Reclamation Process. The retorting step of the skull reclamation process is being demonstrated in engineering-scale runs (see Progress Report for September 1964, ANL-6944, p. 43). The demonstrations are being conducted in a modified melt refining furnace which is installed in the argon-atmosphere glovebox described in Section 3a. In the retorting step, magnesium-zinc is distilled from the material resulting from the uranium dissolution step, after which the residual uranium is melted. Two additional retorting runs have been completed; a BeO crucible was used for the recovery of uranium from two charges (~6 kg each) having a nominal composition of Zn-12 w/o Mg-10 w/o U. (The BeO crucible used in these runs had been previously used in three earlier runs.) The Zn-Mg was distilled from the uranium at a low pressure (30 to 40 Torr) and the residual uranium melted at a final crucible temperature of 1250°C. In the two runs, 99.5% of the volatilized Mg-Zn vapor was collected in a graphite distillate collector and the remaining 1/2% was found on the Fiberfrax insulators.

G. FARET1. Engineering

The principal activities for the current reporting period continued to be concerned with Title II engineering at the Laboratory and at the Architect-Engineer offices. Based on current estimates, submittal of the final design package, Package IX, is expected by the middle of January, rather than December 1, as previously scheduled. Subsequent work on Package IX and certain special design problems should result in completion of Title II by the end of March.

The status of the rest of the design packages of the Title II design is as follows:

Package I - Site Preparation - complete.

Package II - Reactor Vessel - complete. The procurement package has been compiled and delivered to prospective bidders. Proposals have been requested by November 30, 1964.

Package III - Liquid Metal Heat Exchangers - The draft has been returned to the Architect with Laboratory comments.

Package IV - Liquid Metal Pumps - The draft has been returned to the Architect with Laboratory comments.

Package V - Control and Instrumentation - The draft is being reviewed at the Laboratory.

Package VI - Special Piping Materials and Valves - Laboratory's review of the draft is completed and ready for transmittal back to the Architect.

Package VII - Special Early Procurement Items - The draft is being reviewed by the Laboratory.

Package VIII - Specialty Steel - This package has been deleted. Some of the major areas of work receiving the most attention are the following:

1. The structure and shielding in the cavity and in the immediate vicinity exterior to the reactor vessel. This includes the neutron shield, radial energy absorber, shield-cooling system, and instrumentation thimble arrangement.

2. The cell liner and structural design, particularly with regard to missile energy considerations, containment, and leak testing.

3. The fuel-transfer system in the south end of the cell, comprised of the fuel-transfer port and cover, and all equipment connected with the fuel-transfer tunnel.

4. Cell, cavity, and vault liner with penetration details.

Plans for the procurement of the sodium heat exchangers and pumps for FARET have been revised. These major components involving procurement costs of approximately \$1,000,000 were originally scheduled to be purchased by the Laboratory. However, certain advantages inherent to their procurement by United Engineers and Constructors, Inc., have been recognized. The major advantage of this revised arrangement will be to allow more effective coordination of these procurements with Package V - Instrumentation. Major instrumentation is involved in Packages III - Heat Exchangers, IV - Pumps, and V - Instrumentation. Single procurement by UE&C will permit better coordination.

2. Cell Components

a. Cell Shielding Windows. The test fixture for the shielding window glass has been finished and shipped to Building 308 where the hydrostatic test will be conducted. The four glass slabs (29 in. x 44 in. x $8\frac{1}{2}$ in.) to be used in the test program are already on hand.

Technical specifications for the shielding-window bid package are being written.

3. Core Instrumentation

a. Flowmeters. Three types of instruments are currently being considered to measure the coolant flow rates through the FARET fuel assemblies (see Progress Report for June 1964, ANL-6912, p. 54):

(i) Turbine-type Flowmeter. The turbine flowmeter (see Figure 9a) is designed to be completely contained within a FARET fuel assembly. The meter is installed between the inlet nose piece and bottom reflector section.

A typical turbine-type flowmeter consists of the body, a turbine with a small four-pole magnet cast into it, and a coil mounted on the body adjacent to the turbine. When the liquid flows through the meter body, the turbine rotates at a speed determined by the speed of the fluid passing the rotor blade and the blade angle. As the magnets rotate, an

ac voltage is induced in the coil. The frequency of this voltage is equal to twice the speed of the turbine. This ac voltage can be converted to a direct current proportional to input frequency and hence speed.

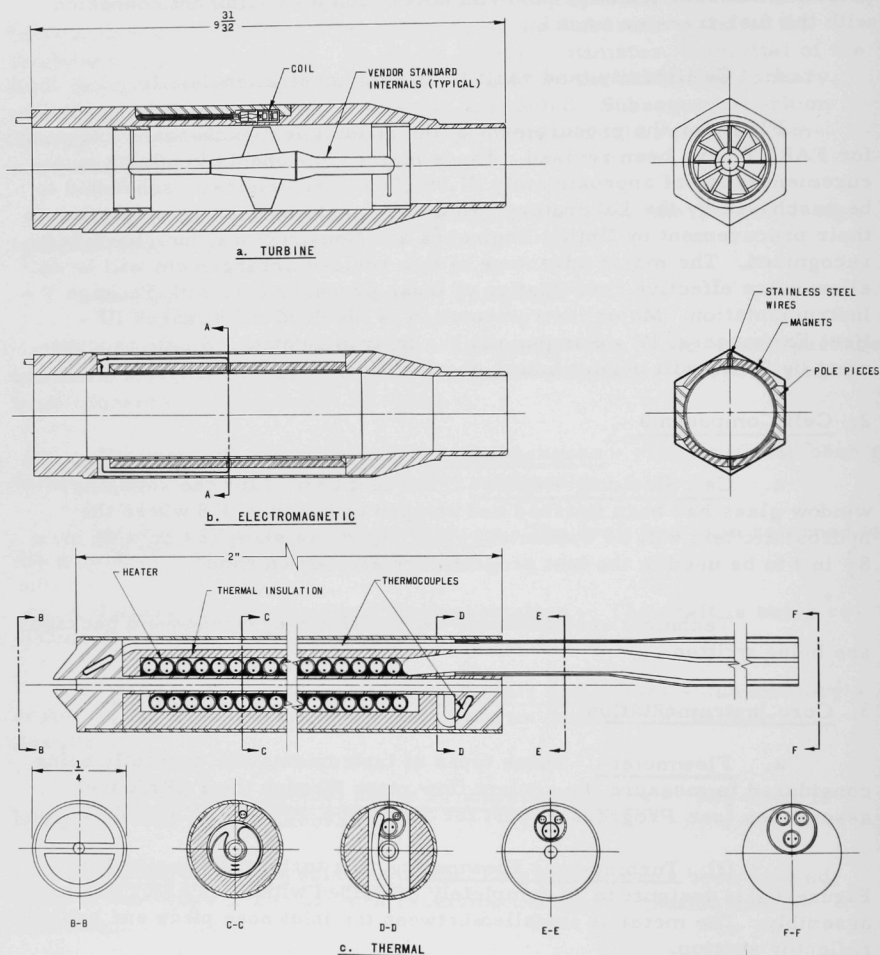


Figure 9. In-core Flowmeters

The body and all other parts exposed to the sodium with the exception of the bearings are constructed of 304 stainless steel. The

guide bearing journals will be made of molybdenum and the turbine shafts of Hastelloy C, materials selected on the basis of performance in high-temperature sodium.³ Alnico VB magnets were selected because they retain approximately 80% of their magnetization at 650°C.⁴ A special miniature high-temperature coil has also been designed. The coil assembly is only 0.25 in. high by 0.5 in. in diameter.

A turbine flowmeter is currently being modified for sodium service. The existing bearings and shafts are being changed to the above materials. The coil is also being fabricated. The turbine flowmeter will then be tested in a sodium loop.

The use of the turbine flowmeter to measure coolant flow rates will depend upon the acceptable performance of the bearings, the coil, and the magnets operating in sodium at the FARET design temperature of 650°C.

(ii) Electromagnetic (EM) Flowmeter. The EM flowmeter (see Figure 9b) is also designed to be completely contained within the FARET fuel assembly. Since the external dimensions are identical with those of the turbine-type flowmeter, the two are interchangeable; either can be used to measure the coolant flow rate without the need for fuel assembly redesign.

The EM flowmeter consists of the body, magnets, pole pieces, and electrodes. The body is made of 304 stainless steel and the magnets of Alnico VB alloy. The pole pieces are tentatively selected as soft iron, and the electrodes are stainless steel wire to reduce extraneous emfs which can be generated by dissimilar metals. For the configuration shown, a magnetic flux of about 42 G was calculated. With this flux an output voltage of about 0.6 mV/ft/sec will result. A prototype flowmeter is now being fabricated and will be tested in a sodium loop. Other configurations are being investigated to improve the meter sensitivity.

The stability of the magnets in the high-temperature nuclear radiation environment of FARET will determine the suitability of the EM flowmeter to measure the coolant flow rates.

(iii) Thermal Flowmeter. A so-called "thermal" flowmeter (see Figure 9c) has been designed. This flowmeter will be placed in the outlet piece of the fuel assembly. A small amount of sodium is passed through the cylindrical hole in the center of the meter and the sodium temperature is increased by the power supplied to the heater element.

³Sarnecki, S. E., Materials for Mechanisms Operating in 1200°C Sodium, NAA-SR-Memo-9340 (Dec 1963).

⁴Underhill, E. M., Permanent Magnet Handbook, Crucible Steel Company, Pittsburgh, Pa. (1957), pp. 1-5.

Two thermocouples are used to measure the temperature rise. At a constant heater power, the temperature rise is a function of the sodium flow rate. The flowmeter will be manufactured by an outside vendor.

The present design calls for a heater power of about 150 W. Chromel/alumel thermocouples will be used to measure the temperature rise. A layer of thermal insulation is placed around the heater element to decrease the heat loss to the surrounding sodium.

The exact position of the sensor in the flow stream and the dimensional variations during manufacture will influence the flow-temperature characteristic. An initial calibration will be performed in a water loop to determine whether the flowmeter sensitivity will be sufficient for use in the FARET fuel assembly. If acceptable, the flowmeter will receive a final performance test and calibration in a sodium system.

b. Electrical Connectors. Screening tests at room temperatures and in an air atmosphere to evaluate the probable performance of various commercial all-metal seals are about to be completed.

Preparations have been made to extend the work on a selected number of the pre-tested models under environmental conditions of sodium and temperature. For this purpose a compact test rig for testing the instrumented fuel-assembly connector has been completed (see Figure 10). It provides vertical motion necessary to engage the connector plug (see Progress Report for September 1964, ANL-6944, p. 47) firmly to the fuel element. Levers, operating through a pair of bellows, on two extensions attached to the locking sleeve, furnish the rotary motion which provides the necessary clamping or sealing force and locks the connector body to the fuel element. The rig will permit testing the integrity of a seal at temperatures in either an argon or liquid sodium environment. It will also permit breaking and remaking the seal to check its resealing characteristics without opening or removing any of the components from the test pot. The testing program is expected to cover the evaluation of at least two different connector designs and possibly three or four different sealing elements.

4. Fuel Slip-fit Experiment

The FARET Slip-fit Experiment is a fuel irradiation test experiment being performed in CP-5. The experiment consists of a pressure tube immersed in the CP-5 D₂O. Inside the pressure tube is a heat-transducer and a fuel capsule (see Figure 11).

The heat transducer consists of five thermocouples divided into two pairs and a single thermocouple. One pair is located at the bottom plane of the fuel and the second pair 2 in. below the first. The single

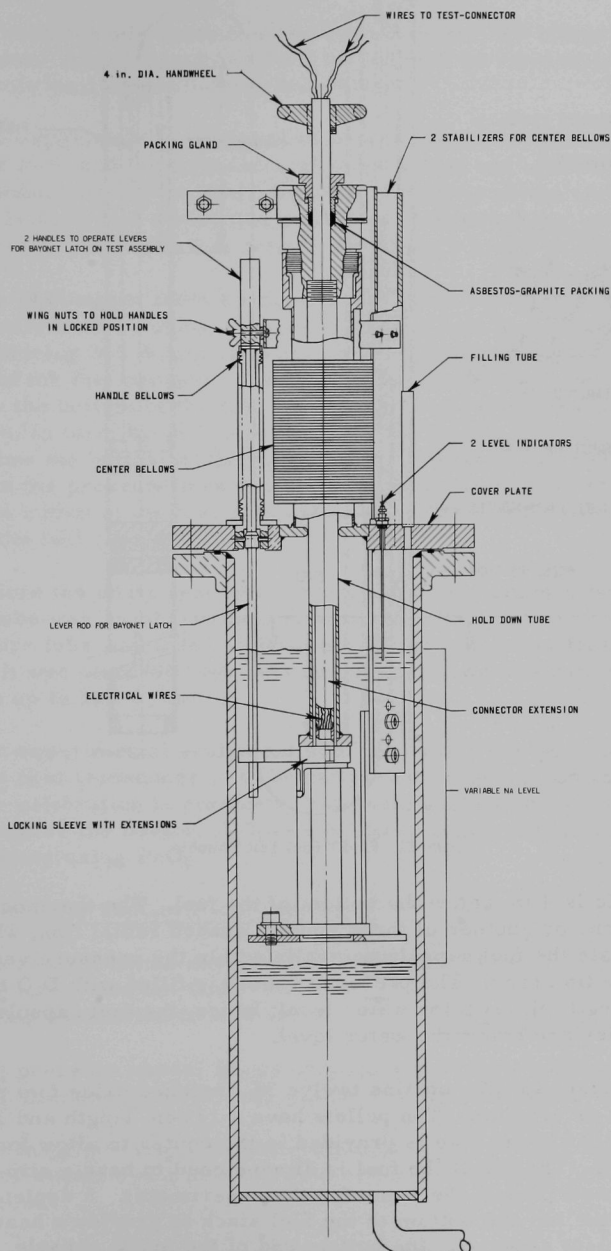


Figure 10. Connector Test Assembly

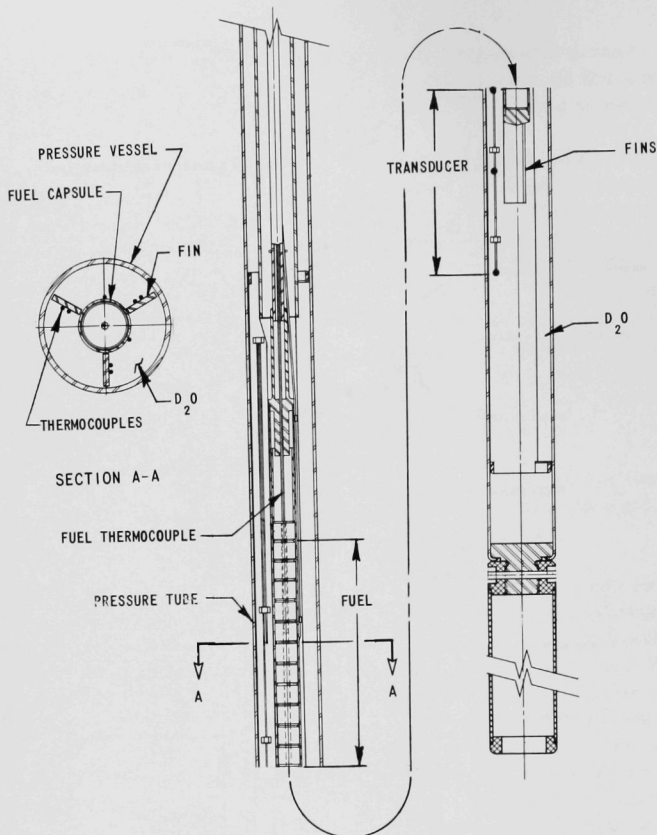


Figure 11. FARET Fuel Test Thimble

thermocouple is 4 in. below the bottom of the fuel. The thermocouples are attached to one or another of three equally spaced radial fins, which also serve to locate the fuel capsule centrally within the pressure vessel at the center of the fin array. The pressure vessel is filled with D_2O to a height corresponding to the reactor water level; hence, the fuel capsule and thermocouples are below the water level.

The fuel capsule contains twelve 3% enriched oxide fuel pellets of plutonium or uranium. The pellets have a 1/2-in. length and 1/2-in. diameter. A 0.070-in. hole is provided in the center to allow for a thermocouple. The OD of the fuel is dimensioned to have a slip-fit with the capsule wall (hence, the name for the experiment). A depleted pellet of UO_2 is at the top and bottom of the fuel stack to provide a heat transfer buffer to protect especially the bottom end of the metal capsule. The thermocouple terminating at the midplane of the fuel measures the central fuel temperature.

A thermocouple measures the experimental D_2O temperature at the fuel midplane. Also located at this level are two thermocouples imbedded in the capsule wall for wall-temperature data.

The experiment is designed to determine the temperature drop through the fuel, and the influences of irradiations and other effects on the thermal conductivity of the fuel. The enrichment of plutonium or U^{235} in the UO_2 pellet is such that a heat flux of 300 W/cm is obtained, which corresponds to the expected flux in the test zone of the zoned FARET core.

The heat output from the fuel is measured by the heat transducer which has been calibrated by using a heater in place of the fuel. The heater is capable of producing 300 W/cm and very closely simulates the physical dimensions of the fuel capsule. The two thermocouple pairs at the bottom and 2 in. below the bottom of the fuel are hooked in parallel. These thermocouples are, in turn, hooked in series with the bottom thermocouple, which is 4 in. below the bottom of the fuel. The D_2O temperature in the downward direction in the pressure tube decreases with distance away from the fuel. The voltage output of the thermocouple arrangement is a function of the heat flux from the fuel capsule.

Before the equipment was put into CP-5, a mockup was made. The pressure tube was immersed in a water bath held at reactor temperature. The pressure tube was filled with water and the heat transducer and heater inserted. It was found that the heat output could be predicted to within ± 1.5 W/cm up to 300 W/cm.

The experimental equipment with the heater has been installed in CP-5. The heat transducer is to be calibrated in the operating reactor. As soon as the calibration is complete, a capsule containing 3% enriched UO_2 fuel will replace the heater. UO_2 is used first to gain operating experience and data before using PuO_2 .

5. Fuel Assembly Sodium Flow Test Loop

The rework on the dump and expansion tanks has been completed by the manufacturer, and the tanks have been installed in the loop. The heaters are now being assembled to both units.

The pressure vessel is now in process of final welding and radiographing at the manufacturer, and will be delivered about November 30.

The installation of thermal insulation on the vessels and piping has been delayed because of a delay in delivery of anchor pins for support of the insulation.

The interim pump case is in final stages of rework.

III. GENERAL REACTOR TECHNOLOGY

A. Applied Nuclear Physics

1. Elastic Scattering of Fast Neutrons

Time-of-flight techniques have been employed to study fast-neutron scattering from Al, Be, Na, Re, As, Te, and Mn. The incident neutron energies ranged from 0.5 to 1.2 MeV with resolutions of about 20 keV. The results are being processed and added to those previously determined for these and a number of other elements. A general tabulation of the elastic scattering cross sections measured in this group has been issued as an EANDC document US-62. The same information is available in a computer compatible format for direct incorporation in reactor calculations.

A representative set of results for U, Ta, Zr, and Fe are compared in Figure 12 with those (YOM) given in a familiar reference.⁵ Here $\bar{\mu} = \cos \theta$ is given as a function of neutron energy. The results for uranium and tantalum are in reasonable agreement with the reference values. The experimental points for zirconium indicate some energy-dependent structure. This effect is grossly more pronounced in the case of iron. This is evident not only from Figure 12 but also from Figure 13, which gives the measured energy-dependent differential elastic scattering cross section of iron measured with a resolution of about 20 keV. As the experimental resolution is improved to about 1 keV, the resonance behavior becomes even more prominent, as indicated by the measured total neutron cross section of iron shown in Figure 14.

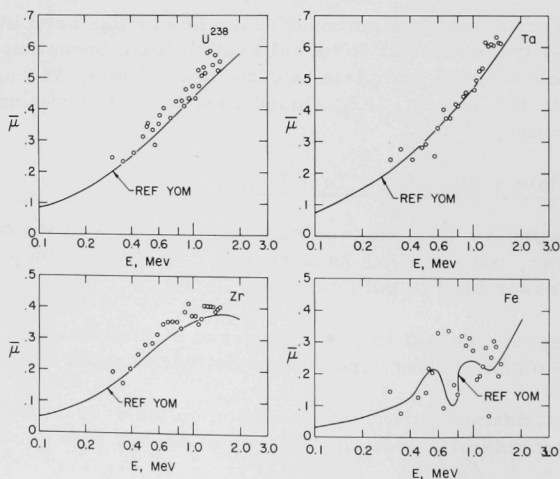


Figure 12. A Comparison of Measured Values of $\bar{\mu} = \overline{\cos \theta}$ for U, Ta, Zr, and Fe with those of YOM

⁵Yiftah, S., Okrent, D., and Moldauer, P. A., "Fast Reactor Cross Sections," (Pergamon Press, New York, 1959) Vol. 4.

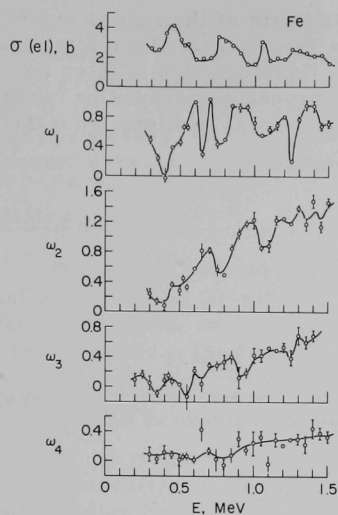


Figure 13
Differential Elastic Scattering Cross Section
of Iron Expressed in the Form

$$\frac{d\sigma}{d\Omega} = \frac{\sigma}{4\pi} \left[1 + \sum_{i=1}^5 \omega_i P_i \right]$$

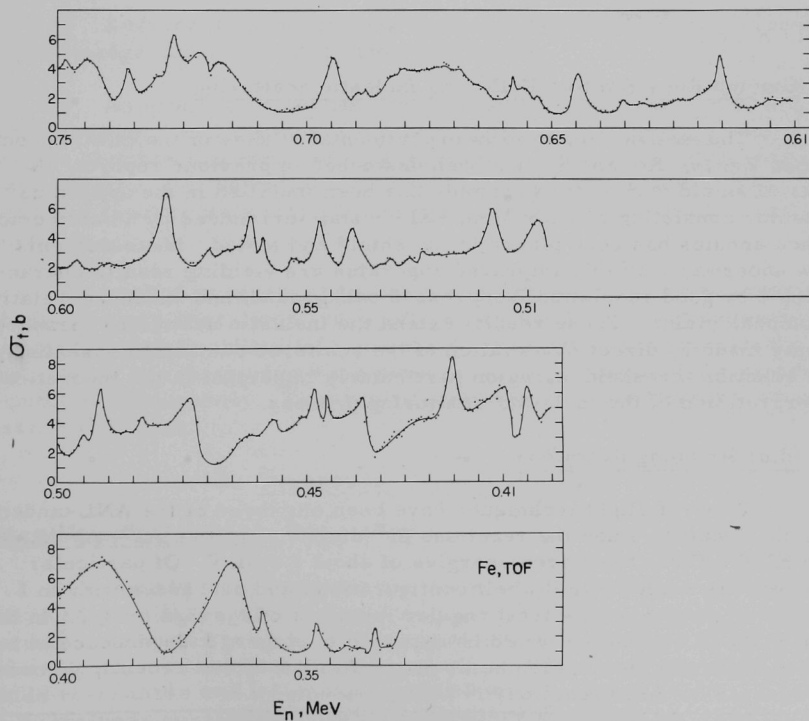


Figure 14. Total Neutron Cross Section of Iron (resolution of ~ 1 keV)

In some instances, the resonance structure of the lighter nuclei can be interpreted in detail. An example is the analysis of the total cross section of magnesium, shown in Figure 15. However, this is often not practicable, and it is always important that proper cognizance be taken of resonance effects in the derivation of group cross sections from the microscopic data.

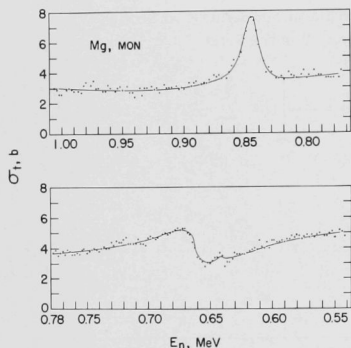


Figure 15

Total Neutron Cross Section of Magnesium Showing Fit to Resonance. Parameters are indicated.

2. Gamma Rays Emitted Following Inelastic Scattering

The method employed in experimental studies of the $(n, n'\gamma)$ process in Nb, Zr, Ho, Re, and Fe has been described in previous reports. A special shield collimator assembly has been installed in the apparatus. A detector consisting of a 3 x 3-in. NaI crystal surrounded by an anticoincidence annulus has been placed in the shield and tested. Measurements now underway with this improved apparatus are yielding results characterized by good resolution, suppressed background, and enhanced relative photopeak yields. These results extend the inelastic scattering measurements made by direct observation of the scattered neutron to essentially the reaction threshold, a region particularly important in the theoretical interpretation of the inelastic-scattering process.

3. (d,n) Stripping Reactions

Time-of-flight techniques have been employed at the ANL tandem Van de Graaff to study the reactions $\text{Si}^{28}(\text{d}, \text{n})\text{P}^{29}$, $\text{Mg}^{24}(\text{d}, \text{n})\text{Al}^{25}$, $\text{Al}^{27}(\text{d}, \text{n})\text{Si}^{28}$, and $\text{K}^{39}(\text{d}, \text{n})\text{Ca}^{40}$ at deuteron energies of about 7.0 MeV. Of particular interest are nuclei with d-shell configurations and processes with an ℓ change of 2 and possible total angular momenta of $J = 5/2$ or $3/2$. In these cases, the (d,n) process would be expected to show a J dependence at reaction angles in the forward hemisphere similar to that recently demonstrated for the (d,p) reaction.⁶

⁶Lee, L., and Schiffer, J., Phys. Rev. 136, B10 (1964).

Measurements completed and now being processed do indicate such a J dependence in the (d,n) reaction where $\Delta l = 2$. A case in point is the neutron groups resulting from proton capture to the 1.38- and 1.93-MeV states in P^{29} . It is hoped that further measurements will define this effect in (d,n) processes, thereby providing the nuclear spectroscopist with an improved technique for the study of nuclear structure.

4. Instrumentation

For nearly two years an on-line computer system has been operational in the Van de Graaff accelerator laboratory. It has been employed in data acquisition, on-line data processing, and feedback accelerator-control functions. The benefits have been such as to fully warrant expansion of the technique and the system. To this end, the following actions have been taken:

a) A magnetic drum storage unit has been received. Necessary interface circuitry is now under construction including provisions for live display of data and analytical functions.

b) Additional equipment has been ordered sufficient to increase the fast storage capacity to 24K (from 8K) words.

c) An order for a second computer has been placed. With this unit the "system" will consist of two computers coupled to each other through a common memory unit. Laboratory operation, including that of the accelerator, will be under executive control of one computer unit. The second will function as a satellite carrying out all data acquisition and processing.

The applied program of this group is well suited to these automated procedures since operations are repetitive enough to warrant automation, yet varied enough to utilize fully the stored program capabilities of the computer. These are the fundamental reasons for the success of the on-line computer in this activity. They are not necessarily characteristic of other research activities.

B. Theoretical Reactor Physics

1. Resonance Interference

A formulation to determine the resonance absorption of neutrons in a rod in an infinite, regular lattice has been derived and is being used to construct a computer program. The formulation, involving a narrow resonance approximation in the moderator, is capable of treating absorption by wide resonances and by closely spaced fissile nuclides more accurately than do methods currently in use that are based on the use of a flat-flux approximation.

The method divides an energy range of interest into many narrow intervals, or groups, of equal lethargy widths. The width of a group is much less than the maximum lethargy gain per collision with uranium; therefore, a neutron will be scattered to a group of lower energy after each scattering collision. From the spatial distribution of the neutron source for a group and from the cross sections of the materials in the rod and the moderator, the absorption in the rod and the flux distribution in the rod and the moderator are obtained in the form of a polynomial in terms of radius. The source distribution for a given group is obtained from the flux distribution and scattering cross sections in those groups from which neutrons can be scattered into the given group.

2. Calculation of Cross Sections

Cross section set No. 224, a 26-group set intended for use in investigating fast-thermal systems, is being extended to regions of lower energy. Until recently, the cross sections of the materials in set No. 224 were evaluated only for the first 22 groups (down to neutron energies of 29 eV).

MC² and ELMOE codes were used to calculate values for these 22 groups. The cross sections for the thermal or 26th group (≥ 0.683 eV) were obtained from the TEMPEST code. The values for groups 23, 24, and 25 are being calculated by the GAM I code. Some moderators, H, D, and Be, were included in set No. 224; values of the moderator cross sections were calculated for all groups by means of the GAM I and TEMPEST codes.

The GAM code has been used to calculate the cross sections for groups 23 through 25, for all materials in set No. 224, and for all cross sections above thermal for the moderators. The feasibility of using GAM to produce all cross sections above thermal for all materials was investigated. (Calculation with the GAM code uses less machine time, which is an advantage.) The feasibility of use of GAM for calculating all cross sections depends upon its accuracy in predicting the elastic scattering and transport cross sections. The cross sections for sodium obtained by use of both the GAM and ELMOE codes were compared. The agreement between the values for the two codes was good except in the 2-keV resonance region. The use of the GAM code for this application is continuing.

3. Analysis of Fuel Requirements for Ceramic-fueled Breeder Reactors

Several existing conceptual designs for large fast breeder reactors were analyzed from the standpoint of conserving fissionable material. The amount of plutonium which would have to be supplied from other sources to enable a breeding system of the given type to meet a postulated, rapidly growing demand for power was computed. Since the system eventually becomes self-supporting with respect to plutonium, the outside supply required

to reach equilibrium is finite. Table XIV lists the results of such calculations for four recent designs of ceramic-fueled breeders, each producing 1000 MWe, together with fuel-cycle costs estimated by the designers using the current AEC use charge of $4\frac{3}{4}\%$.

Table XIV. Comparison of a Breeder Design with
Respect to Fuel Requirements

Item	Fuel Form			
	No. 1 Carbide	No. 2 Carbide	No. 3 Oxide	No. 4 Oxide
Required outside supply, metric tons plutonium	146	1710	1270	2900
Fuel-cycle cost, mills/kWh	0.43	0.42	0.57	0.70
Doubling time, yr	6.3	11.2	12.2	17.3
Surplus plutonium, kg/yr	275	400	240	245
Inventory, kg/MWe	1.73	4.48	2.92	4.24

The two carbide-fueled designs have the same fuel-cycle costs but differ by more than a factor of ten in the plutonium required. However, higher fixed charges on plutonium inventory, to be expected with the advent of private ownership of fuel, will provide some economic incentive toward conservation.

4. Calculation of Physical Properties of Reactor Materials at High Temperatures

The thermodynamic and transport properties of metal vapors can be calculated from the interatomic potential energy as a function of the internuclear separation distance, using well-known formulae. However, since the metals have free valence electrons, repulsive as well as attractive states exist. Suitable averaging procedures have been developed for calculating the properties of atoms interacting along multiple potential-energy curves, and these are being tested against the available experimental data.

Computer programs have been written to obtain the attractive potential curves from spectroscopic data, and these potentials are being put into a reduced form by scaling the energy in accordance with the depth of the potential well, and the internuclear separation distance at the potential

minimum. The reduced form of the true potential curve is being compared with shapes of various empirical potential curves to fit potential parameters for extrapolation to points beyond the range of the calculated potentials.

This method simplifies the computations of properties since tabulations of virial coefficients and transport integrals exist for some empirical potentials. The alkali metals scale well with the Rydberg potential, as expected. Further comparisons are in progress between the ground-state potentials for uranium and plutonium as calculated by a Thomas-Fermi-Dirac statistical model and the Rydberg potential.

An empirical relation for the behavior of the density of liquid and vapor near the critical point has been substantiated by comparisons with such diverse fluids as liquid helium and mercury. Theoretical support of this empiricism has been found in the predictions of the Ising model of a lattice gas. Calculations of thermodynamic properties from this relation will be made and tested against experimental data.

C. High-temperature Materials Development

1. Ceramics

a. Reaction of Uranium Carbide with Water. The oxidation reaction of compositions in the system UC-US with water is being investigated by differential thermal analysis (DTA). Only UC, US, and UC-60 w/o US, which is the composition of the limit of solubility of UC in US, are under investigation.

Sintered specimens of UC, UC-60 w/o US, and US were crushed under alcohol and the powders sieved to -100 +325 M (U. S. Standard Sieve) after evaporation of the alcohol. The powders, mixed with an equal weight of Al_2O_3 , were heated in flowing, water-saturated argon at $5^\circ\text{C}/\text{min}$ to 1000°C in the DTA apparatus.

All three compositions produced DTA plots containing three distinct exothermic peaks. Each was broad and was terminated on the upper side by the beginning of the next peak. The first exotherm for UC reached a maximum at 315°C , for UC-60 w/o US at 405°C , and for US at 400°C . Each of the exotherms began approximately 100°C below the peak temperature. The second exotherm for UC peaked at 500°C , for UC-60 w/o US at 500°C , and for US also at 500°C . The third exotherm was at 775 , 730 , and 675°C for UC, UC-60 w/o US, and US, respectively. The first peak for UC occurs approximately 35°C lower than the lower of the two exothermic peaks for UC oxidized in air, whereas the US and UC-60 w/o US produced initial peaks in water at approximately the same temperature as their single peaks in air. X-ray analyses are being done to determine the reactions for each of the exothermic effects.

b. Sintering Characteristics and Properties of PuS and PuP. The sintering characteristics and properties of plutonium monosulfide and plutonium monophosphide are being investigated as part of a broad program to evaluate potential fast reactor fuels. The compounds were prepared by reaction of partially decomposed plutonium hydride with hydrogen sulfide or phosphine. The resulting sulfide or phosphide powder was then homogenized for 4 hr under vacuum at 1600 and at 1500°C , respectively.

Chemical analysis showed that high-purity PuS containing about 0.01 w/o oxygen and 0.01 w/o nitrogen could be made by the above procedure. No analyses of the PuP powder are available. The lattice constant of PuS in equilibrium with Pu_2S_3 is $5.5409 \pm 0.0001 \text{ \AA}$, whereas pure PuS has a lattice constant of $5.5383 \pm 0.0001 \text{ \AA}$. Further work is needed before any conclusion can be drawn regarding the compositional limits of the PuS phase. The lattice constants of Pu_2S_3 in equilibrium with PuS are $8.4182 \pm 0.0001 \text{ \AA}$ and $8.4193 \pm 0.0001 \text{ \AA}$. A change in the

lattice constant of PuP from 5.6562 to 5.664 Å indicates that the PuP phase field may exist over a range of composition. Microstructures of sintered PuS pellets show a small amount of Pu₂S₃ phase at the PuS grain boundaries.

The changes in density and in percent weight loss of PuS and PuP pellets as a function of sintering temperature were investigated. Plutonium monosulfide pellets heated in vacuum attained a geometric density of about 94% of theoretical at an optimum sintering temperature of 1600°C. The weight loss at this temperature was 1.2% of the original weight, including 0.5 w/o of binder loss. At temperatures above 1600°C the density decreased slightly, the change being accompanied by a rapid increase in the rate of vaporization. In one atmosphere of argon, the weight loss was reduced and geometric densities of 92% theoretical were attained on pellets sintered at 1700°C. Plutonium monophosphide pellets sintered under vacuum attained a maximum geometric density of 88% of theoretical when held at 1600°C for 2 hr. The weight loss at this temperature was appreciable, being 2.1%. Sintering above 1600°C produced a rapid increase in the rate of vaporization, whereas the density decreased slightly.

Melting points of PuS and PuP were measured in a tungsten-filament furnace. Plutonium monosulfide melted at 2330°C under a pressure of 1 atm. The rate of vaporization of PuP heated above 2400°C under a pressure of 1 atm was so great that the sight glass fogged and the melting point could not be measured. A sample heated under 2 atm melted at a power setting on the furnace that corresponded to a temperature of about 2900°C. This value is quite high for a plutonium compound. Further work is needed to determine a more exact melting point. The best estimate for the melting point of PuP is that it lies between 2540°C, the melting point of UP, and 3000°C, the melting point of ThP.

The average value for the room-temperature electrical resistivity of PuS was 2450 ± 150 micro-ohm-cm. This value is considerably greater than the range of 112 to 359 micro-ohm-cm reported for US.

The average linear thermal expansion coefficient of PuS over the range from 18 to 960°C was $18.54 \times 10^{-6}/^{\circ}\text{C}$. This high rate of expansion was unexpected, since the coefficient for US is $11.6 \times 10^{-6}/^{\circ}\text{C}$ for the same temperature range.

c. The Preparation of Uranium Monosulfide. Several attempts to synthesize US electrolytically were made with commercial Na₂S and UCl₄ as starting materials and a NaCl-KCl salt bath (see Progress Report for September 1964, ANL-6944, p. 59). The cathode and anode consisted, respectively, of a rotating molybdenum paddle and a graphite crucible. In the runs that appeared to be successful, the application of an emf of 5.0 V resulted in a rapid rise in back-emf to 3.2-3.4 V. The back-emf then remained constant until the completion of the reaction was indicated

by a rapid rise in current and corresponding drop in back-emf. Despite both drying with anhydrous HCl and electrolytic predrying of the melt, the products obtained appeared to be mainly UOS and UO_2 . The hygroscopic commercial Na_2S was a likely source of the oxygen contamination. Therefore, sulfides less hygroscopic than Na_2S were used.

The use of lead and calcium sulfides resulted in rapid destruction of the molybdenum cathodes, probably because of the formation of low-melting alloys. With a graphite cathode, lead and sulfur were visually identified as the main products in the case of lead sulfide. However, results with calcium sulfide and a graphite cathode were similar to those reported for sodium sulfide except for a lower back-emf of 2.6 V. The product from this run is presently being evaluated.

The use of sulfides containing metals capable of reducing uranium, such as sodium and calcium, apparently leads to a reaction between sulfur and uranium. Similar results have been reported for the electrolytic preparation of various metal phosphides.⁷

More experiments are planned with CaS as the sulfide source to enable a decision concerning the practicability of synthesizing US by the electrolytic method now being employed.

d. Properties of (Th, U) Phosphides. The relative stability of UP and the fact that ThP exhibits a melting point of about 3000°C has aroused interest in the use of actinide phosphides as fuel and breeding materials in reactors at very high temperatures. Before the phosphides of uranium and thorium can be evaluated for reactor use, much information on the characteristics of UP, ThP, and their solid solutions must be obtained.

The high-temperature stability, stoichiometry, and fabricating characteristics are being investigated. ThP and UP have been shown by X-ray diffraction to exhibit complete mutual solubility across the entire compositional range. Lattice constants lie on a fairly smooth curve that exhibits a slight positive deviation from linearity. In addition, sintered densities and weight losses in vacuum at 2200°C are higher toward the UP end of the binary system, despite the lower surface area. These results, based on later work, supersede those reported in the September monthly report (ANL-6944, p. 60).

Melting temperatures of three intermediate compositions (see Table XV) fell on a smooth curve.

⁷Chene, M., The Production of Metallic Phosphides in Fused Electrolytes, Ann. Chim. (Paris) 15, 187-285 (1941).

Table XV. Melting Temperatures in the Binary System ThP-UP

Composition	Melting Temp in Helium (°C)
ThP	2900
75 w/o ThP-25 w/o UP	2860
50 w/o ThP-50 w/o UP	2825
25 w/o ThP-75 w/o UP	2725
UP	2600

A series of UP pellets were prepared and fired for one hour in vacuum at temperatures from 1600 to 2200°C. Some of the UP powder was pelletized without any further treatment, and some was ball milled for 5 hr. Results given in Table XVI show the improvement produced by ball milling on sintered density, which was marked for pellets fired at the lower temperatures. The main effect seemed to be an increase of the activity of the powders. There was little improvement in sintered density by firing over 2000°C, since further densification was offset by weight losses, which increase rapidly above this temperature. Weight losses for UP at 2200°C were about four times greater than those at 2000°C.

Table XVI. Sintered Density* as a Function of Firing Temperature and Treatment

	1600°C	1700°C	1800°C	2000°C	2200°C
Untreated	86.8	90.3	93.0	95.6	96.1
Ball Milled	93.7	95.6	95.9	96.6	96.7

*Percent of theoretical density.

e. **Mechanical Properties of Uranium Compounds.** Fracture tests have been made with specimens of UO_2 at about 1000°C and 1250°C with the variations in load rate reported in Table XVII. Tests at 1250°C initially proved difficult to control because of the small plastic deformation occurring at this temperature and the inability to detect the moment of contact between stressing tools and specimens. A dial gauge bearing on the cross-head of the machine proved effective in assessing the required movement and also allowed some measure of strain to be made. Reproducibility of the curves obtained by this means was remarkably good, and values of 1800 to 1950 kb were obtained for Young's modulus, well within the figures reported in the literature.

Table XVII. Fracture Test Data for UO_2

Batch Number of Samples	Density		Modulus of Rupture		Mean Load Rate, g/sec	Temp, °C
	Mean Value, gm/cc	Standard Deviation σ	Mean Value σ , kg/cm ²	Standard Deviation, kg/cm ²		
4	10.55	0.003	1239	92.0	63.4	1015
5	10.47	0.027	1097	61.9	575.3	1025
5	10.51	0.016	1044	81.7	1114.4	1020
4	10.60	0.01	1759	98.2	27.2	1250
2	10.62	0.005	1624	53.0	194.8	1255
2	9.60	0.2	1154	62.8	199.5	1250
4	10.52	0.01	377	10.8	362.4	1250

The results indicate a significant rise in modulus with rise in temperature (see Progress Report for October 1964, ANL-6965, pp. 58-9) for similar rates of loading and similar density. The difference in values obtained at 1020°C and 1250°C is greater than that from room temperature to 1020°C for low and medium rates of stressing. The low figures for high rates of stressing at 1250°C were obtained before the introduction of the dial gauge and will be rechecked. Lower density has a similar effect on modulus at 1250°C as at lower temperatures.

Density changes in fractured specimens have been recorded in all cases tested. There appears to be little correlation with load rate at both 1000 and 1250°C, which might suggest the change is mainly due to increase in volume of the pores. Microscopic examination of one specimen broken at room temperature provided an example of cracks joining up pores in the grain boundary. These cracks travel partly transgranularly and confirm the model proposed by Hasselmann.⁸

f. Anelasticity of Some Uranium Compounds. The Young's modulus for four bars of UO_2 was determined. Two of the bars were brought to the final dimensions by lapping; the other two were as sintered. Bars 1 and 2 were prepared by pressing the UO_2 powder plus binder in a steel die at 140 kg/cm² and repressing them isostatically at 3850 kg/cm². The specimens were sintered in hydrogen at 1700°C for 4.5 hr. The O/U ratio was 2.005. They were finished by automatic lapping with silicon carbide papers 80C, 120C, 180C, 240A, 400A, and 600A. Water was used as a coolant. Bars 3 and 4 were prepared by prepressing the powder and binder isostatically at 3850 kg/cm², granulating, forming in a steel die at 420 kg/cm², and repressing isostatically 3850 kg/cm². They were sintered in hydrogen at about 1700°C for 4.5 hr. The O/U ratio has not yet been determined. It should be pointed out that this sintering was done in a different furnace than for bars 1 and 2, and this could have introduced some changes.

⁸Hasselmann, D. P. H., Relation Between Effects of Porosity on Strength and Young's Modulus of Polycrystalline Materials, J. Am. Ceram. Soc., 46(11) 564 (1963).

The Young's modulus was determined by the resonance technique introduced by Förster.⁹ The flexural resonance frequencies were excited by two methods. In the first one the specimen was supported on foam rubber and driven by placing the needle of a record cutting head (Astatic X-26) against the bar. The vibrations were detected by the needle of a phonograph cartridge (Astatic L-12). The second method consisted in suspending the specimen by two platinum wires, 0.0254 cm in diameter and 41 cm long, placed 2 mm from the nodes of the sample. One wire was attached to the needle of the record cutting head and the other to the phonograph cartridge. The flexural resonance frequency of bar 1 was determined by both methods and the results were consistent.

In the case of bars 2, 3, and 4 it was not possible to excite consistently the flexural resonance frequency by the second method of excitation. The lack of response was attributed to the fact that the specimens were heavier. An attempt was made to reduce the dimensions of bar 2, but it was broken during the lapping operation.

Dimensions, density, and elastic modulus are shown in Table XVIII. The Poisson's ratio was assumed to be 0.3.¹⁰ It can be observed that the Young's modulus of the finished pieces was larger than that obtained from the unfinished specimens. Probable causes might be: (a) lack of precision in the parallelism and dimensions of bars 3 and 4, (b) dissimilar microstructures due to the different fabrication procedures, and (c) skin effect occasioned by the lapping of specimens 1 and 2. Further study will be made with one of the previously unfinished specimens lapped. The torsional resonance frequency was only excited for bars 3 and 4, and even in these cases the readings were not reproducible.

Table XVIII. Dimensions, Density, and Elastic Modulus of UO₂ at Room Temperature

Sample	After Sintering					After Lapping					E _f , kb (3)	E _g , kb (4)	G, kb (5)
	Width, cm (1)	Depth, cm (1)	Length, cm	Weight, gm	Density, gm/cc (2)	Width, cm	Depth, cm	Length, cm	Weight, gm	Density, gm/cc (2)			
1	0.712	0.711	6.459	34.1734	10.62	0.564	0.417	6.459	15.9332	10.53	2056	2070	794
2	0.741	0.738	6.350	34.5539	10.61	0.538	0.480	6.350	17.2532	10.54	2062	2062	794
3	0.819	0.465	7.351	29.0712	10.54	-	-	-	-	-	1813	1856	714
4	0.818	0.470	7.350	29.1831	10.49	-	-	-	-	-	1846	1851	705

(1) Average of 3 measurements.

(2) Density determined by the Archimedes' method.

(3) Young's Modulus calculated from the flatwise flexural vibration.

(4) Young's Modulus calculated from the edgewise flexural vibration.

(5) Shear modulus calculated from the expression: $\mu = (E/2G) - 1$, where μ is the Poisson's ratio and E the average of E_f and E_g.

⁹Förster, F., Z. Metalkunde, 29(4) 109-115 (1937).

¹⁰Lang, S. M., Properties of High Temperature Ceramic and Cermets, Elasticity and Density at Room Temperatures, U. S. Nat. Bur. Standards, Monograph 6 (March 1, 1960).

2. Thorium-base Fuels

a. Fabrication of Thorium-Uranium-Plutonium Alloys. Alloys with 60 w/o of thorium, 20 w/o of uranium, and 20 w/o of plutonium were successfully cast by the injection-casting process. Alloys with 70 w/o of thorium and more, however, had too high a liquidus temperature to be cast by the same method. The quartz and Vycor tubes used as mold materials softened at the required high casting temperature (1400°C or higher). In looking for a suitable mold material several grades of graphite were tried. Impervious graphite appeared to be a reasonable substitute. Still it soon became obvious that a great deal more development work would have to be done to be able to produce sound castings of high-temperature alloys in a controlled and reproducible manner.

Because of the need for preparing specimens for irradiation testing, a method was developed for fabricating ternary thorium-uranium-plutonium alloys by rolling and swaging. It was reasonable to try this approach since thorium is a face-centered cubic material that can be worked easily. The ternary alloys of concern are two-phase alloys consisting of α_{Th} and α_U , β_U or γ_U , depending upon temperature. The plutonium constituent is distributed between the thorium-base solid-solution phase and the uranium-base solid-solution phase. The second phase does not form a continuous network, but is present as uniformly distributed oblong or nearly spherical inclusions in the thorium-base matrix.

Fabrication by rolling and swaging was generally successful. Three high-purity alloys investigated were:

- (i) Th-30 w/o Pu;
- (ii) Th-20 w/o U-10 w/o Pu;
- (iii) Th-10 w/o U-10 w/o Pu.

Alloys (ii) and (iii) were chosen because earlier phase studies have shown that they contain no liquid phase at least up to 900°C. All three alloys could be cold rolled to 50% reduction.

When the same method was tried with alloys (ii) and (iii) made from commercial thorium, ingot uranium, and reactor-grade plutonium, the alloys, which were of lower purity, cracked in the first or second rolling passes. Metallographically these alloys showed considerable thorium dioxide contamination in the form of dendrites.

After several trials a process was developed by which arc-melted alloys of so-called commercial purity could be fabricated into irradiation pins. The process consists of

- (i) a 24-hr heat treatment at 850°C followed by water quenching to dissolve and keep in solution as much as possible of the impurity content of the alloys;
- (ii) hot rolling at 450°C for a total reduction of 50%;
- (iii) A repetition of the heat treatment described in (i);
- (iv) swaging at 450°C for a total reduction of 30 to 40%;
- (v) continuation of heat treatments and swaging until the desired size is obtained.

The entire process was monitored by hardness tests. The alloys of commercial purity had hardness values of 50 to 60 R_B for the heat-treated materials and 70 to 75 R_B for the worked materials. The high-purity alloys are softer. Their hardnesses are 18 to 35 R_B for the heat-treated alloys and about 60 R_B for the worked alloys.

3. Corrosion by Liquid Metals

a. Lithium Corrosion at Elevated Temperature

(i) Nitrogen Determination. The most common nonmetallic impurities in lithium are hydrogen, oxygen, nitrogen, and chlorine. Of these, oxygen and nitrogen are regarded as the major impurities causing corrosion. To study the nature of these influences on a refractory metal-lithium system, a suitable analytical procedure for determining the oxygen and nitrogen contents in lithium is of vital importance.

A reliable technique of analyzing lithium for oxygen has not yet been developed, although neutron activation reportedly shows some promise. Analyses of lithium for nitrogen can be made with reasonable accuracy by a method based on the hydrolysis of lithium nitride to form ammonia and lithium hydroxide.

An analytical apparatus for nitrogen determination has been assembled, and a protective sample-transfer container has been built. Preliminary runs with known samples show that the sensitivity of the analytical method is adequate for nitrogen in the 20 to 250 ppm range.

(ii) Corrosion Test. A high-purity arc-melted molybdenum capsule partly filled with lithium, to provide a lithium-molybdenum system for corrosion testing, was encapsulated in a quartz tube containing zirconium turnings as getter material. The assembly was tested in a resistance furnace under atmospheric conditions. After 100 hr of continuous exposure of the molybdenum to lithium at 1000°C, a sample of the lithium was taken in a helium glovebox. The nitrogen content of the lithium was determined to have increased to 60 ppm from an initial 30 ppm.

Since the molybdenum exhibited little or no metallographic evidence of corrosion, 60 ppm of nitrogen in lithium presumably has no short-term corrosive effect on molybdenum at 1000°C.

Tests with higher concentrations of impurities and at higher temperatures will be conducted as soon as the required instruments and high-temperature furnaces are available.

D. Other Reactor Fuels and Materials Development

1. Zirconium Alloys for Superheated Steam

Samples of Zr-3 w/o Ni-0.5 w/o Fe and Zr-1.1 w/o Cu-1.2 w/o Fe in hot-rolled condition have been corrosion tested in deoxygenated steam at 540°C and 42 kg/cm² gauge (600 psig) for a total of 316 days in a rerun of a previous test. The purpose of the rerun was to determine whether an increase in weight-gain rate seen after 220 days in the previous test had been associated with an overtemperature excursion that occurred or with an apparent general tendency toward increasing rates at extended times. The more recent data show that the excursion did contribute substantially to the increase; weight-gain rates are continuing to decrease slightly with time, being 3.4 mdd for the Zr-Ni-Fe alloy and 2.4 mdd for the Zr-Cu-Fe alloy for the most recent period. Although the surfaces bear the usual corrosion product without blemishes, the usual film edge cracks are present. The test is continuing.

Four samples, similar in composition to those discussed, had been formed from the as-cast material by the high-energy Magneform process and had then been corrosion tested in deoxygenated steam at 560°C and 42 kg/cm² gauge (600 psig) for 127.5 days. The corrosion behavior was not unusual for these materials, and the surface appearance equalled the best observed previously on hot-rolled samples after a corrosion test.

Since as-cast material from the same ingots as the Magneformed samples had developed blisters during corrosion tests under the same conditions, a limited amount of further study was made of surface blemishing. Since the high-energy process reduction had been up to 10%, material was prepared by 10% cold rolling and (separately) 10% hot rolling, and corrosion tested at 650°C to accelerate the test. Blemishes were seen on the cold-rolled samples but not on the hot-rolled. Blemishes are therefore apparently associated with physical defects in the as-cast structure that may be reduced by hot rolling or by high energy forming but not by cold rolling.

2. Corrosion of Iron and Nickel Alloys in Superheated Steam

This program is essentially completed and a terminal report is in preparation.

3. Nondestructive Testing

a. Determination of Elastic Moduli of High-temperature Materials by Ultrasonics. The object of this program is to measure the temperature dependence of the elastic moduli of materials that show promise in high-temperature reactor applications. To obtain these data a vacuum furnace has been constructed in which solid bar-shaped samples will be mounted.

Pulsed ultrasonic waves will be propagated along the length of these samples, and the transit times of pulses passing a heated, indexed region in each bar will be measured. The indexing is done by machining one end to a smaller diameter than the rest of the bar.

The velocity of sound in the indexed region can be calculated from the length of this region and the transit time in it. Both shear-wave velocities and longitudinal velocities are determined.

The furnace was taken apart and the heater rewound. The heater was modified so that more power could be put into the furnace. A TV-20 specimen that was heated and previously measured (see Progress Report for October 1964, ANL-6965, pp. 61-2) was remounted and the measurement run extended to 1150°C. Work is continuing on the reduction of data from these runs and on controlling the thermal gradient in the samples.

b. Ultrasonic Imaging. A two-element polystyrene ultrasonic lens¹¹ has been fabricated and studied in connection with the ultrasonic imaging system. The lens is much superior to those previously evaluated and, with a magnification of about 2X, does somewhat improve the resolution of the system.

c. Correlation of Heat Transfer and Bond Quality. The correlation between ultrasonic transmission capabilities of various types of mechanical bonds and their heat-transfer capabilities is being studied. To determine the thermal properties of the bonds the thermal pulse method for measuring diffusivity and conductivity developed by Parker et al.¹² is being utilized. The front surface of the specimens is uniformly irradiated by a very short pulse (of approximately 600- μ sec duration) of radiant energy supplied by a xenon flash tube. The temperature history of the back surface is continuously monitored by feeding the output of a thermocouple in contact with the back surface into a differential amplifying system and then into an oscilloscope.

Calculations of the thermal diffusivity α and conductivity K for the roll-bonded BORAX-V fuel plates have been completed. Values of α ranged from 0.0289 to 0.0248 cm²/sec, and values of K from 0.0329 to 0.0271 cal-cm/cm²-sec-°C.

Through-transmission ultrasonic tests at a number of frequencies on the BORAX-V specimens are now in progress.

¹¹ Suckling, E. E., and Ben-Zvi, S., Attempts to Predict the Performance of an Image-Forming Ultrasonic Microscope, IRE Trans. Ultrasonic Engineering, UE9, 56-59 (1962).

¹² Parker, W. J., Jenkins, R. J., Butler, C. P., and Abbott, G. L., Flash Method of Determining Thermal Diffusivity, Heat Capacity and Thermal Conductivity, J. Appl. Phys., 32, 1679 (1961).

d. Transducer and Technique Development. Current ultrasonic techniques for the inspection of small-diameter, thin-walled tubing utilize transducers with highly concentrated beams. This concentration can be achieved by using tubular or hemispherical forms of the piezoelectric crystal material or by attaching lenses to the front of crystals. More often than not, formed crystals with the desired characteristics are not readily obtainable.

With this in mind, developmental efforts for the design and fabrication of focused transducers have been concentrated on the use of a lens for accomplishing the focusing of ultrasonic beams. This month, two spherically focused, 5-Mc transducers were fabricated by attaching Araldite epoxy lenses to the front of conventional transducer units. Schlieren photographs taken of these focused units revealed that they need to be more sharply focused.

Work is now under way to improve the Schlieren system in both versatility and image quality. A rf-power amplifier is being constructed to function in conjunction with a sine-wave oscillator as the continuous wave source. Various grades of optical glass are being considered and investigated for replacing the regular glass sidewalls of the water tank.

A Lamb-wave transmission technique has been applied and evaluated for its feasibility as a method of inspecting plate-type fuel. In this test, separate send and receive transducers were utilized as in a conventional transmission technique. However, the transducers were positioned at a predetermined angle from normal incidence in order to generate the 1A Lamb-wave mode. As with the conventional technique, nonbonds or similar types of defects show up as a decrease in amplitude or complete loss of the first transmitted pulse.

The results of the Lamb-wave test were encouraging. However, such a technique seems applicable only when parameters such as dispersion and thickness changes are closely controlled in the manufacturing process. Otherwise, the generation of Lamb-wave energy will be lost, and testing will be impossible. Separate transmit and receive transducers positioned at the proper angle on one side of the fuel plate (pulse-echo) would eliminate the fuel dispersion factor but would necessitate two scans instead of one as in the transmission technique. However, this technique shows promise in detecting flaws other than nonbonds in fuel plates.

e. Development of a Neutron-image Intensification System. The first neutron-image intensifier tube has been received from the Rauland Corporation and placed in operation. The tube functions very much according to the predictions based on preliminary tests and according to previous film results with neutron scintillator materials. The threshold sensitivity

(the minimum neutron intensity needed to yield a signal from the image intensifier) appears to be even better than the predicted value of 10^5 thermal n/cm^2 -sec, determined by direct observation of the output phosphor of the tube. With a closed-circuit Vidicon television system to bring the image out of the radiation area, the threshold sensitivity appears to be somewhat in excess of 10^5 thermal n/cm^2 -sec (using $f/1.5$, 2.5-cm focal length optics).

The ability of the system to discriminate thickness changes in metals has not yet been thoroughly studied. However, preliminary results indicate that changes in thickness of the order of 8 to 10% can be detected in natural uranium 2 to 4 cm thick. This result is comparable with film neutron radiographic techniques employing scintillator screens.¹³

Initial speed-of-response measurements indicate that the complete imaging system (intensifier plus closed-circuit Vidicon system) will follow object motion velocities at least as fast as 1 m/min with no smear of the image. The resolution properties of the system presently appear to be limited by the necessary distance between the object and the input detecting screen in the intensifier, because of the geometry of the tube. Nevertheless, the system is capable of resolving 0.5- to 0.75-mm-diameter holes in neutron-absorbing material.

Further and more complete evaluation of the present intensifier is now in progress.

f. Development of Infrared Systems for Nondestructive Testing. Two stainless steel-jacketed samples containing Wood's metal to simulate a sodium bond were fabricated and inspected with the Infrascopes. One sample contained a heating coil so that it could be heated internally. The sample was heated to 160°C, and the surface temperature was recorded around the circumference at various points. Surface temperature differences of 2 to 3°C were observed over local areas around the circumference. The jacket was stripped from the sample and examined. The Wood's metal did not wet the stainless steel jacket, but the numerous voids were all 5 mm or less in diameter, except for a large void near the end.

The second sample was resistance heated from the ends, but the results were inconclusive. Stripping showed that the sample tube had not been completely filled, and the sample had been heated above the melting point in a horizontal position while testing. Therefore the side toward the radiometer was probably essentially empty.

A simulated duplex-tube sample with voids in the form of rings machined around the circumference of the inner tube was inspected with the

¹³ Berger, H., and Kraska, I. R., Neutron Radiographic Inspection of Heavy Metals and Hydrogenous Materials, Materials Evaluation, 22 305-310 (July 1964).

Infrascopes. The tube was heated by placing a tungsten filament source in the center. The dimensions of the voids were 3 mm wide x 0.25 mm deep, 3 mm wide x 0.75 mm deep, 6 mm wide x 0.25 mm deep, and 6 mm wide x 0.75 mm deep. The 3-mm-wide voids produced a surface temperature difference of 1°C at 190°C, and the 6-mm voids produced a 3°C difference. Since the depth had no measurable effect, the temperature difference was due to conductivity and was not affected by the heat capacity. The wall thickness of the inner tube was 3 mm, the outer tube wall was 0.5 mm, and the material was 304 stainless steel.

E. Remote Control Engineering Development

1. Electric Master-Slave Manipulator Mark E4

Work has continued on various aspects of this 50-lb capacity manipulator. Several layouts have been made of the shoulder joint and part of the upper slave arm. The major problems have been solved, and a detailed layout is being started. Articulated full-scale models were used to provide a three-dimensional checkout of the configuration layouts.

Considerable detail study has been carried out on linkages for driving the "Y" motion. The "Y" motion is, of course, associated with the shoulder-joint arrangement as well as with the elbow-joint and counterweighting system. The major problems associated with the "Y" motion drive have been solved.

The wiring of one of the two control consoles is about 25% complete.

2. Servo Studies

Studies are being made of ways of reducing the cost of the electronics for force-reflecting servo amplifiers. The servos are being investigated to reduce the complexity of the amplifier and reduce the number of wires needed for the slave arm. One arrangement that looks promising is the mixing of the tachometer and position signals. Then, by using a small feedback amplifier at the slave arm, these combined signals could be fed back to the servo amplifiers through one wire for each motion.

3. Special Motors for Master-Slave Manipulators

Further tests have been performed on the aluminum cup-rotor two-phase servo motor (see Progress Report for July 1964, ANL-6923, p. 62). The motor is designed to power a future slave arm which has a load capacity of about 100 lbs. The speed of the motor under no-load conditions was previously found to be less than expected. Several changes in the core inside the cup-rotor have been shown to reduce this no-load slip somewhat. The

best of these is a core with 18 slots skewed with respect to the stator teeth. For a temperature rise of 177°C in the cup-rotor, the motor delivers a stall torque of 29 lb-in., which is equivalent to a manipulator capacity of 115 lb.

4. Viewing Systems

In order to understand the role of various modifying elements in the glass structure and its contribution to radiation-induced coloration, the optical absorption of thallium in glass is being studied. It has been found that one of the ultraviolet absorption bands, due to single Tl^+ in glass (5.82 eV in fused silica and 5.75 eV in aluminoborate glass), fits the following empirical equation:

$$\lambda(\text{in eV}) = 0.306 r_+ - 1.789 r_- + 8.195,$$

where r_+ is the radii of the cations and r_- the radii of the anions nearest the Tl^+ . The equation was initially derived for alkali halide crystals and was then extended to glasses. The present studies have indicated that thallium present as Tl^+ is probably octahedrally coordinated. In both glasses, it has O^{2-} as nearest neighbors. As its next nearest neighbors, it has Si^{4+} in fused silica and B^{3+} in the aluminoborate glass of the particular composition studied.

F. Heat Engineering

1. Two-phase Flow Studies

a. Void Fraction - Pressure-drop Facility. This experimental facility is designed to investigate the two-phase flow characteristics of boiling sodium; in particular, it is desired to obtain experimental information pertinent to the vapor volume fraction and two-phase fractional losses in an adiabatic test section. The loop is constructed of Type 316 stainless steel and is limited to short-term operation at atmospheric pressure and about 1630°F.

The loop has been operating continuously for approximately 1500 hr at temperatures above 1000°F. During the first two weeks in November, intermittent boiling was obtained during several slowly increasing temperature transients at the boiler exit. At the low power density in the homogeneous boiler (up to 56 kW/ℓ) and low inlet velocity (~1 ft/sec), the boiling was quite unstable, and the boiling period was highly variable, ranging from a few seconds to 5 min over a temperature range from 1330 to 1410°F. The loop pressure ranged from 2.5 to 3.9 psia and was highly variable in an irregular manner within this range. Although the initial data are sparse and not thoroughly evaluated at this time, it appears that the superheat requirements for volumetric resistance heating of sodium are of the order of 20-40°F, much less than the initial 200-400°F requirements reported by experimenters utilizing surface boiling.

The boiler section and the instrumentation are now being prepared for operation at increased power density, flow rate, and subcooling; these increases are in the direction of increased stability and should produce a stable boiling regime as the system pressure is increased to the 10-15 psia range.

The gamma attenuation and electromagnetic void detectors appear to yield satisfactory results, although the use of the latter will require a higher-response-recording circuit for the accuracy needed at higher void fractions; this modification is easily accomplished and will be available at the time two-phase pressure-loss data are obtained in the adiabatic test section.

2. Boiling Liquid Metal Technology

a. Niobium-1% Zirconium Loop. This facility is designed to investigate the heat-transfer and two-phase flow characteristics of boiling sodium to a temperature of 2100°F at a pressure of approximately 8 atm. Among the variables to be investigated are boiling heat flux and temperature difference up to the critical heat flux occurrence, boiling, and adiabatic two-phase pressure drop, vapor volume fraction, boiling stability, and possibly flow patterns.

The Nb-1% Zr loop will be fabricated at the Pratt and Whitney-CANEL facility. A procurement directive has been issued by COO-AEC to CANEL-AEC along with the final specifications and drawings. CANEL staff are now in the process of determining the construction procedure and schedule.

The purchase order for the electromagnetic-induction sodium pump has been approved and sent to the vendor. As soon as the Nb-1% Zr pump tube is completed, it will be shipped to CANEL for welding into the high-temperature loop.

Instrumentation design for measurement of various parameters throughout the loop is continuing. Specifications have been written, and price and delivery requisitions have been sent out for 30 niobium-sheathed W5 Re W26 thermocouples with extension leads for the radiation-heater section. Price and delivery are also being obtained for the 30 stainless steel-sheathed chromel-alumel couples for the loop and condenser sections. A preliminary layout of the instrumentation and control circuitry has been made. An inventory of the "on hand" recorders revealed additional recording equipment will be necessary.

Specifications have been written and price and delivery requisitions have been sent out for four differential and four absolute pressure

transducers. It is expected that the prices of these transducers, if available, will be quite high. Pressure transducers of the type desired have been fabricated at this Laboratory. A design for transducers of the proper ranges is under way as a backup effort.

It has been proposed that an electromagnetic flowmeter be used for the determination of void fraction in this loop.¹⁴ In such a method a correction factor must be applied to account for the change in conductivity of the two-phase field. An investigation for a theoretical and an empirical¹⁵ correction factor is in progress; preliminary results indicate that this correction is appreciable at high void fraction, due to considerable departure from the linear theory.

The vacuum-chamber vendor has abandoned efforts to repair the defective bell jar cooling water lines and will completely rebuild this portion of the vessel. The lower portion of the chamber and the vacuum pumping system has been received. Installation of this equipment and the walkway has begun. The hardware necessary for the electrical connection of the equipment has been ordered and arrangements have been made for this work.

Specifications for relatively small, portable liquid nitrogen containers have been completed. Plans for the alternatives of a large mobile tank and a nitrogen condenser have been eliminated on the basis of excessive cost.

b. Heater Experiments

(i) Thermal Radiation Heater Experiment. The thermal-radiation-heated boiler section and a thermal radiation preheat section for the Nb-1% Zr loop have been designed. Fabrication drawings for both the boiler section and preheater have been completed. Information gained from the thermal radiation heater experiment has been utilized in the design of these heaters. In both the boiler section and the preheater, heat will be generated in tungsten wire elements surrounding the flow tube. Heat will be transferred from the heating elements to the Nb-1% Zr tube by thermal radiation only. In the boiler section, temperatures will be measured at known radial locations in the thick wall, enabling both the heat flux and the inside wall temperature to be determined.

Checkout of the 150-kW power supply has been completed. This supply will be used in conjunction with the boiler section of the Nb-1% Zr loop.

¹⁴Heineman, J. B., et al., Electromagnetic Flowmeter for Void Fraction Measurements in Two-Phase Metal Flow, Rev. Sci. Inst. 34, 399-401 (1963).

¹⁵Petrick, M., and Lee, K., Performance Characteristics of a Liquid Metal MHD Generator, ANL-6870.

The thermal radiation heater has operated for 400 hr. Approximately 250 hr of nonboiling and 150 hr of boiling operation have been obtained. The nonboiling data have yielded Nusselt numbers Nu somewhat higher than those predicted by the empirical correlation of Lubarsky and Kaufman. Data from the 150 hr of boiling operation at low pressure (less than 10 psia) are being analyzed. Both the heated section and the coil condenser behaved satisfactorily during the boiling operation.

(ii) Electron Bombardment Heating Experiment. Assembly of the electron-bombardment pool boiler is complete. Several problems concerning the readout equipment remain, but are being resolved. A technique for filling the system with clean sodium is being developed.

3. General Heat Transfer

a. Heat Transfer in Double-pipe Heat Exchangers

(i) Liquid Metal Cocurrent Turbulent Flow. Following a thorough cleaning, the mercury heat transfer loop (see Progress Report for August 1964, ANL-6936, p. 61) was filled with mercury. The mercury was then circulated and heated to 200°F. Except for slight leakage from the valves in the storage tank, and the collection of a small amount of water in the expansion chamber, initial operation was successful. Venting of the expansion chamber and heating of the mercury to 240°F appeared to eliminate water from the system permanently.

The magnets for the EM flowmeters were installed, and preliminary investigations of flowmeter operation began. The output signals were close to those expected, but drifted somewhat. Later, inspection of the electrodes revealed fairly rapid corrosion by the mercury. The electrodes were replaced by two sets of polished nickel pins, one set being copper plated. After circulation of the mercury for about 8 hr and heating of the mercury to 200°F, the output with the polished nickel pins remained constant for all temperatures of operation.

The loop has been dismantled for modifications to the flowmeters and the sight glass. In addition, the storage tank was removed and cleaned. New valves have been placed on the outlet of the storage tank to eliminate the leakage of mercury.

After re-assembly of the loop, the EM flowmeters will be calibrated by the use of calibrated orifices. The stainless steel-sheathed copper-constantan thermocouples have been calibrated with the switchbox and potentiometer to be used by the use of a temperature-controlled water bath and a resistance thermometer.

Two nickel test sections are near completion and should be ready for fitting into the loop within a month.

4. ANL-AMU Program

Other heat engineering experiments, performed as part of a joint program between the Laboratory and Associated Midwest Universities (AMU), are described below:

a. Propagation of Void Waves in an Air-Water System. More preliminary experiments were necessary before any test data could be obtained for the investigation of the behavior of void waves in an air-water system (see Progress Report for October 1964, ANL-6965, pp. 70-1).

When using an electrical resistivity probe for measuring voids, it is necessary that the probe be oriented parallel to the flow. If the probe is not oriented properly, two possible errors may be introduced. One is that the probe tip will not be located at the expected position. The other error arises if bubbles are deflected by the slanted probe. This effect has been checked with probes oriented at angles of 0° , 5° , and 10° with the axis of the channel; no significant error was introduced.

It is the aim of this research project to compare the experimental results with theoretical predictions. In order to accomplish this, a theoretical model must be used, but it must first be established that the air-water system used behaves according to this model. Sufficient data were taken to verify that the Marchaterre-Hoglund correlation holds in this system.

Two test runs were made to make a complete analysis and comparison with theory, and the data were analyzed on the IBM 704. No conclusion could be reached in this comparison on the basis of only two runs.

Four more runs will be made to determine if the analysis procedure is satisfactory.

G. Chemical Separations

1. Fluidization and Volatility Separation Processes

a. Recovery of Uranium from Low-enrichment Ceramic Fuels

(i) Laboratory Work. Laboratory work in support of the pilot-plant investigation of the fluid-bed fluoride volatility process is being continued. The fluorination of solid mixtures approximating those that result from the decladding of stainless steel-clad UO_2 fuel elements by HF-O_2 mixtures is being studied (see Progress Report for September 1964, ANL-6944, pp. 69-70). The purpose of the experiments is to determine the effect of the decladding products on plutonium retention by the bed after fluorination. The products of the decladding step are assumed to contain a mixture of UO_2F_2 , PuF_4 , fission product fluorides, and iron oxides. A mixture of these compounds was reacted with fluorine gas in a fluid-bed reactor containing sintered alumina as an inert bed material. The initial fluorination was a one-hour treatment with 5 to 20 v/o fluorine in nitrogen at 450°C . This was followed by recycle-fluorination with 100% fluorine at three temperature levels: 4 hr at 450°C , 5 hr at 500°C , and 10 hr at 550°C .

Two tests were performed in which solid mixtures simulating declad fuel were fluorinated. The feed materials for these tests contained nominally: 1 g plutonium tetrafluoride, 250 g uranyl fluoride, 2 g fission product fluorides, 40 g ferric oxide, and 450 g alumina. Residual concentrations in the alumina beds after fluorination were 0.041 w/o uranium and 0.0087 w/o plutonium in the first test, and 0.012 w/o uranium and 0.010 w/o plutonium in the second test. In an experiment to demonstrate the re-use of alumina bed material, the final alumina bed from the second test was used as the starting bed for the fluorination of an additional batch of the same feed material. The final bed from this test contained 0.033 w/o uranium and 0.014 w/o plutonium, which represented a uranium recovery of 99.9% and a plutonium recovery of 96.3%. Previous work has demonstrated that, although the residual plutonium concentration on the alumina increases from the first to the second addition-fluorination cycle, high plutonium recovery can be achieved upon successive re-use of the alumina, since the plutonium concentration on the alumina remains relatively constant during subsequent cycles (see Progress Report for June 1964, ANL-6912, pp. 76-77). It is believed that a residual plutonium concentration on the alumina bed equivalent to less than 1% of the plutonium charged to the reactor can be achieved by seven addition-fluorination cycles using feed material containing stainless steel decladding products.

(ii) Alpha Decomposition of Plutonium Hexafluoride. The effect of alpha-induced decomposition of plutonium hexafluoride has been investigated as a part of a fundamental study of the radiation behavior of plutonium hexafluoride. The results of short-duration PuF_6 decomposition tests

(0.5 to 16.0 days) indicated that the alpha decomposition of PuF_6 to PuF_4 and fluoroine proceeds at a high initial rate (see Progress Report for June 1964, ANL-6912, pp. 77-79). Examination of the PuF_6 decomposition vessel, a nickel sphere containing a No. 1479 Hoke valve, revealed that PuF_6 apparently attacked the phosphor-bronze bellows in the valves, which were exposed to PuF_6 during filling and emptying of the spheres. Analyses of the vessel from a 2-day test, for example, indicated that a total of 6.36 mg PuF_6 decomposed, 1.98 mg being attributed to decomposition by chemical attack on the bellows.

On the basis of these observations, all PuF_6 alpha-decomposition rates will be corrected for valve corrosion. The largest correction will be in the short-term results for which the total quantity of PuF_6 decomposed is small. The corrections, however, do not alter the relationship between decomposition rate and time.

(iii) Engineering-scale Alpha Facility. An engineering-scale alpha facility (see Progress Report for October 1964, ANL-6965, p. 76) is being installed to permit demonstration of the major steps of the fluid-bed fluoride volatility process for the recovery of uranium and plutonium from ceramic oxide fuels. Runs which are planned with fluorination equipment involve the use of HF-oxygen mixtures for reacting with and pulverizing unclad UO_2 pellets (see ANL-6965, p. 75).

In preparation for these tests, a brief study was made in glass equipment of the formation and movement of gas bubbles and the behavior of the fluidizing medium (alumina) in the voids of a fuel-support bed and a fuel-pellet bed. Good gas distribution below the fuel pellet bed is necessary to achieve uniform mixing of alumina in the pellet bed. The fluidized-bed system consisted of a $2\frac{3}{4}$ -in.-dia glass column in which unclad UO_2 pellets (1/2-in.-dia right cylinders) were immersed in alumina. Nickel balls (1/8 to 1/4 in. in diameter) were used as a pellet-bed support and as the gas distributor. The nitrogen fluidizing gas was introduced at the bottom of the glass column. The tests showed the following:

(1) Mixing of solids within the voids of the pellet bed is associated with bubble formation and movement; an increase in the intensity of solids mixing was observed with the growth of the bubbles as they moved up the column into regions of lower pressure.

(2) Gas distribution below the pellet bed is improved by the presence of alumina in the voids of the nickel balls used for the pellet-bed support.

(3) More uniform distribution of the alumina in the support bed and the pellet bed is achieved if the alumina is charged first to an empty reactor. On the basis of these tests, a pellet-bed support consisting of a 9-in. depth (minimum) of 1/8- to 1/4-in.-dia nickel balls has been recommended.

(iv) Decladding and Fluorination of Uranium Dioxide Fuels.

Development studies of the decladding and fluorination of uranium dioxide fuels in a fluid-bed reactor have continued. A current run explored the feasibility of recovering uranium from a UO_2 -stainless steel cermet fuel which was clad with stainless steel. The decladding step employed a previously demonstrated technique (see Progress Report for October 1964, ANL-6965, p. 75) which involves the chemical destruction of the stainless steel cladding by high-temperature reaction with oxygen and hydrogen fluoride. In this step, the uranium dioxide is converted to fine particles of uranyl fluoride and a small quantity of U_3O_8 and UF_4 . The uranium is recovered as uranium hexafluoride by subsequent direct fluorination of the uranium compounds.

The test was carried out in a $1\frac{1}{2}$ -in.-dia fluid-bed reactor. The fuel charge consisted of a 4-plate subassembly which was $11\frac{1}{16}$ in. by 0.5 in. by $8\frac{3}{8}$ in. long and weighed 90 g. Each plate was composed of 18 w/o UO_2 -stainless steel (Type 304) and clad in stainless steel. The fluid bed contained 480 g of sintered alumina grain (-48 +100 mesh).

The decladding step was carried out at 550°C for 4 hr with a reacting gas mixture of 40 v/o HF, 40 v/o O_2 , and 20 v/o N_2 . The subassembly was completely disintegrated at the end of the destructive oxidation. After the decladding step, the entire bed was reacted with elemental fluorine for 11 hr by a two-temperature fluorination procedure. The fluorination procedure involved gradually increasing the fluorine concentration from 2 to 90 v/o (remainder nitrogen) over a 6-hr period with the reactor bed fluidized and at a temperature of 250°C . The fluorination was continued with 90 v/o fluorine and the temperature of the fluidized reactor was slowly raised from 250°C to 550°C over a 3-hr period. The fluorination was then completed by increasing the fluorine concentration to 95 v/o and operating under static bed conditions for an additional 2 hr at 550°C .

High uranium recovery (>99%) was indicated by the low quantities of uranium retained by the alumina at the end of the fluorination step. The residual uranium concentration in the alumina amounted to 0.005 w/o, which corresponds to ~0.2% of the uranium charge. The quality of fluidization throughout both the pulverization and fluorination reactions was good, and the fluid bed after fluorination was free-flowing. Further work is planned toward establishing optimum operating conditions for the recovery of uranium from UO_2 -stainless steel cermet fuels.

b. Recovery of Uranium from Highly Enriched Uranium-Alloy Fuels by Chlorination and Fluorination

(i) High-activity-level Facility. A bench-scale facility has been constructed for the study of the fluid-bed chlorination-fluorination process with highly irradiated uranium-Zircaloy or uranium-aluminum alloy fuel materials (see Progress report for May 1964, ANL-6904, p. 89).

The tests involving processing of irradiated fuel are intended to define clearly the disposition of fission products and the total decontamination achieved in the process. The facility has been designed for complete remote operation and maintenance of all equipment components. The facility consists of a $1\frac{1}{2}$ -in.-dia fluid-bed reactor and a packed-bed filter with associated equipment for the containment of volatile chlorides and the uranium hexafluoride produced in the process.

Prior to installing the facility in the Senior Cave of the Chemical Engineering Division, shakedown runs with unirradiated alloys of uranium in either Zircaloy or aluminum were carried out. The fuel charges were reacted first with hydrogen chloride and then with elemental fluorine. Operation of the equipment was considered satisfactory, although several minor modifications were made prior to the final cold runs. These tests demonstrated that high uranium recoveries could be achieved in this facility and that essentially all the uranium charged could be accounted for.

Following these runs, the facility was installed in the Senior Cave. Tests with irradiated materials are now underway. The first two experiments will be with a 4 w/o uranium-Zircaloy alloy which has been irradiated to about 50% burnup and cooled for about 5 yr.

2. General Chemistry and Chemical Engineering

a. Preparation of Uranium Monocarbide. The fluid-bed preparation of uranium monocarbide by hydriding uranium has been continued. Uranium metal is hydrided at 250°C for about 4 hr to form particles suitable for fluidization and then the particles are fluidized with a propane-hydrogen mixture for 2 to 5 hr at 500-700°C. A velocity of 0.25 ft/sec for the fluidizing gas and hydrogen concentrations of 10, 20, 70, or 80 v/o in the fluidizing gas mixture have been utilized in seven recent runs. The results are encouraging since the UC product from a run with a 30 v/o C_3H_8 -70 v/o H_2 mixture contained 5.3 w/o carbon, and the UC product from a run with a 20 v/o C_3H_8 -80 v/o H_2 mixture contained 3.2 w/o carbon. It appears that stoichiometric UC (containing 4.8 w/o carbon) can probably be obtained by control of the temperature, the reaction time, and the hydrogen concentration in the gas.

b. Determination of the Critical Constants of Alkali Metals. The critical constants of alkali metals have been estimated but not measured. The critical constants of a metal can be used for calculating or estimating many thermodynamic and physical properties of the metal. Thermodynamic properties of alkali metals are of particular interest because these metals are used as heat-exchange media.

Work to determine the critical constants of alkali metals has started. The initial measurements are being made on cesium. Densities of the vapor and liquid phases of cesium (containing radioactive Cs^{134}) are

being measured from room temperature up to its critical point by measurements of the gamma radiation emanating through the collimator holes which extend from the vapor and liquid regions of the alkali metal held within a small capsule (see Figure 16). As the critical point is approached, the densities, and therefore the gamma activities emanating from the vapor and liquid regions approach each other. A preliminary value for the critical temperature of cesium is about 1700°C, but additional runs will be required to obtain a more reliable value and to resolve anomalies.

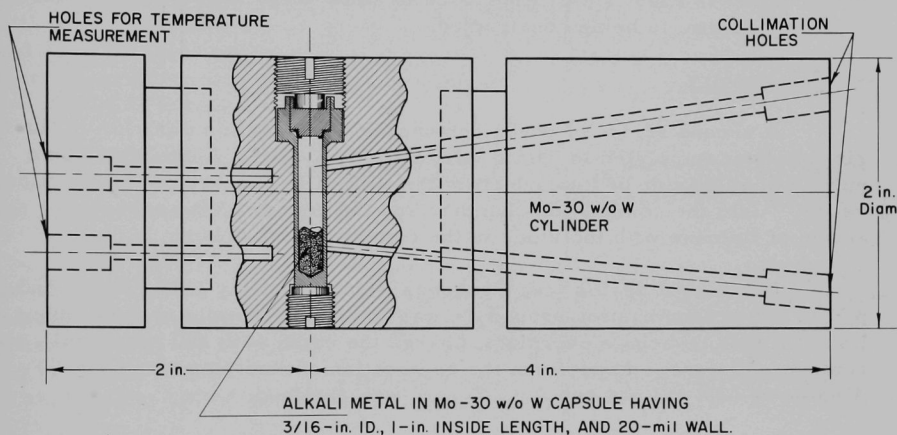


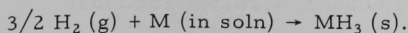
Figure 16. Apparatus for Determining Critical Constants

3. Chemical-Metallurgical Process Studies

a. Chemistry of Liquid Metals.

(i) Thermodynamics of Rare Earth-Cadmium Systems. The thermodynamics of rare earth-cadmium intermetallic systems are being studied by the effusion method. To compute the thermodynamic properties of all the compounds in a given system from vapor pressure data, it is necessary to know the decomposition pressures in all two-phase regions. Preliminary data have been obtained for the decomposition pressures in the two-phase regions SmCd-Sm, GdCd-Gd, and TbCd-Tb. Low decomposition pressures (10^{-2} to 10^{-3} Torr) were found in these systems.

(ii) Thermodynamics of Hydride Formation from Dilute Solutions of Plutonium and Uranium in Liquid Cadmium. An investigation of the thermodynamics of systems which consist of hydrogen, a solvent metal such as cadmium or zinc, and a solute metal (a rare earth or actinide) has begun. The reaction to be studied is



This reaction would be useful for reducing the concentration of solute in a solution or for determining thermodynamic properties by relating equilibrium pressures to solute concentrations.

Calculations have been made of the equilibrium uranium and plutonium concentrations in liquid cadmium in the presence of hydrogen at high pressure. It was calculated that at 400°C and a hydrogen pressure of about 100 atm, the equilibrium concentration of uranium is 20 ppm and that of plutonium is about 1.4%. Apparatus to study these reactions at pressures of about 100 atm is being constructed.

4. Calorimetry

A second series of seven combustions of tantalum diboride in fluorine has been completed to obtain information on ΔE_{blank} , the sum of the energy of expansion of fluorine from the tank of the two-chamber reaction vessel¹⁶ into the combustion chamber and the energy of the subsequent reaction of fluorine with moisture in the combustion chamber.

In the first series (see Progress Report for July 1964, ANL-6923, p. 73), the precombustion procedure was to place a sample in the combustion chamber, evacuate overnight, charge the bomb with 200 mm of BF_3 to remove moisture, and perform the combustion without removing the BF_3 . A value of 12.6 cal per run for ΔE_{blank} was obtained.

In the second series, the bomb was washed with water to remove TaF_5 following a run; the bomb was then dried, prefluorinated with 1200 mm F_2 at 110°C to remove adsorbed moisture, evacuated, and opened in a dry box for insertion of a new sample. In this series, ΔE_{blank} was 0.4 to 5.0 cal per run. Preliminary calculations of the data from the second series indicate that values of the energy of combustion will agree with the results for the first series of runs when the appropriate ΔE_{blank} correction values are used.

Eight calorimetric combustions of lanthanum and eight of nickel in fluorine have been carried out. The results of the combustions are being evaluated.

Five calorimetric combustions of red phosphorus in fluorine have been completed. The studies of the combustion of phosphorus are being made to obtain data necessary for the determination of the enthalpy of formation of uranium monophosphide. The preliminary value for the enthalpy of formation of PF_5 is $-376.6 \text{ kcal mole}^{-1}$. This may be compared with a value of $-377.2 \pm 0.8 \text{ kcal mole}^{-1}$ for the enthalpy of formation of PF_5 obtained by Gross *et al.*,¹⁷ who burned white phosphorus in fluoride.

¹⁶Nuttall, R. L., Wise, S., and Hubbard, W. N., Rev. Sci. Instr. 32, 1402 (1961).

¹⁷Gross, P., *et al.*, Fulmar Research Institute Report R146/4/23 (Nov 1960), Unpublished.

H. Plutonium Recycle Program

1. Physics Calculations

The THERMOS code is still in the process of being modified (see Progress Report for October 1964, ANL-6965, pp. 82-83). The code, when used with the CDC 3600 computer, permits 50 speed points, the use of either cylindrical or slab geometry, and 25 isotopes edited in the spectrum as determined by the problem. Further modifications are underway which will result in pointwise and various integral results for values of Σ_f , $\nu\Sigma_f$, and Σ_{tr} . These modifications will convert THERMOS to a general-purpose thermal-group cross-section-generating code which will be used to replace the SOFOCATE code.

THERMOS will be used to support the EBWR experimental program in comparing the measured and calculated isotopic changes that occur as the system is irradiated.

The Nelkin scattering kernel code, GAKER, has been recompiled so that the user is relieved of the responsibility of generating the temperature-dependent parameters used in the calculation. Since the Nelkin kernel is generally believed to provide the best available representation for scattering in water, GAKER will normally be used with THERMOS calculations to analyze the EBWR performance.

IV. ADVANCED SYSTEMS RESEARCH AND DEVELOPMENT

A. Argonne Advanced Research Reactor (AARR)

1. Fuel and Core Design

Fabrication of the irradiation test samples under Phase II of the verification studies for the fuel-fabrication process with Martin Company and Battelle Memorial Institute has been completed. Samples for irradiation in the ETR G-12 will be shipped to Idaho after the necessary examinations have been made at ANL.

The fuel-element brazing program with Pyromet Company has resulted in improvements in the work reported earlier. Extended post-braze cooling has virtually eliminated all distortion in the assembly, thus confirming the choice of the close dimensional tolerances originally selected as nominal working tolerances. Modifications in jiggling and in the application of braze compound has improved the quality of the brazed joints.

2. Heat Transfer

The experimental AARR steady-state heat transfer program was initiated in June 1964 to determine the maximum power conditions for the AARR fuel assembly and to measure voids in the flow channels.

Electrically heated nickel test sections, composed of a single rectangular flow channel, are being used. The single-channel test section will be investigated experimentally by measuring pressure drop, void, and flow characteristics of a single channel only. Experiments will also be conducted in which the test section will have a parallel bypass flow about nine times that of the single-channel test flow rate. These tests constitute the parallel-channel tests and are intended to simulate AARR operating conditions.

The single- and parallel-channel tests require two separate loops, but use the same power supply. The loops have been built and have been subjected to a shakedown period in which the test section, loop equipment, instrumentation, and operating procedures have been studied.

The preliminary testing began during this period with a 22-in. long, uniform, axial heat flux in the test section with a flow channel, 0.040-in. thick, 1.25-in. wide, and a heated length of 18 in. The loops have operated satisfactorily, and improvements in instrument reliability and operational technique have resulted.

The two main areas of concern have been with the location and adjustment of the burnout detector and with the channel spacing. The

shakedown period involved periodic measurements of the channel space after power conditions had been applied to the test section. It was noted that the nominal channel spacing of 0.040 in. had decreased near the exit to below 0.025 in. The preliminary single-channel test program was continued to check the burnout detector in spite of this problem. Constant flow rate, inlet temperature, and exit pressure were applied, and the power raised in small steps. Burnout of the test section occurred because of difficulties with the burnout detector.

The single-channel test conditions achieved at burnout which occurred $3/8$ in. from the exit in spite of the decrease in channel space were:

Exit pressure, psig	600
Inlet velocity, ft/sec	51.2
Inlet water temperature, °F	147
Exit water temperature, °F	153
Average heat flux, B/hr-ft ²	4.06×10^6
Total power, kW	372

A preliminary estimate of the critical heat flux based on the Zenkevich-Subbotin correlation gave 4.18×10^6 B/hr-ft². A preliminary estimate of flow instability indicated 362 kW would cause failure.

The difficulty with the burnout detector will be corrected and the channel space decrease, believed caused by the method of attaching the thermocouple, will be corrected.

3. Critical Experiment

Experimentation continued with the fuel loading (see Progress Report for October 1964, ANL-6965, p. 85) consisting of 315 fuel foils of 93% enriched uranium weighing approximately 54.7 g each. The metal-to-water ratio is 1:1 in the fuel zone. Dimensions of the internal thermal column (ITC), fuel region, and 90 v/o-10 w/o beryllium-Plexiglas radial reflector may be seen in Figures 17, 18, and 19.

Foil activation traverses shown in Figure 17 indicated an ITC peak approximately eleven times the maximum, or seventeen times the mid-plane (two-dimensional) average activation in the coolant channels. The radial traverses were taken at the level of a layer of Plexiglas in the beryllium-Plexiglas radial reflector. This layer was 3.2 cm below the midplane and 1.14 cm thick, being sandwiched between 10.16-cm-thick beryllium layers. Foils were located in coolant channels in the fuel zone.

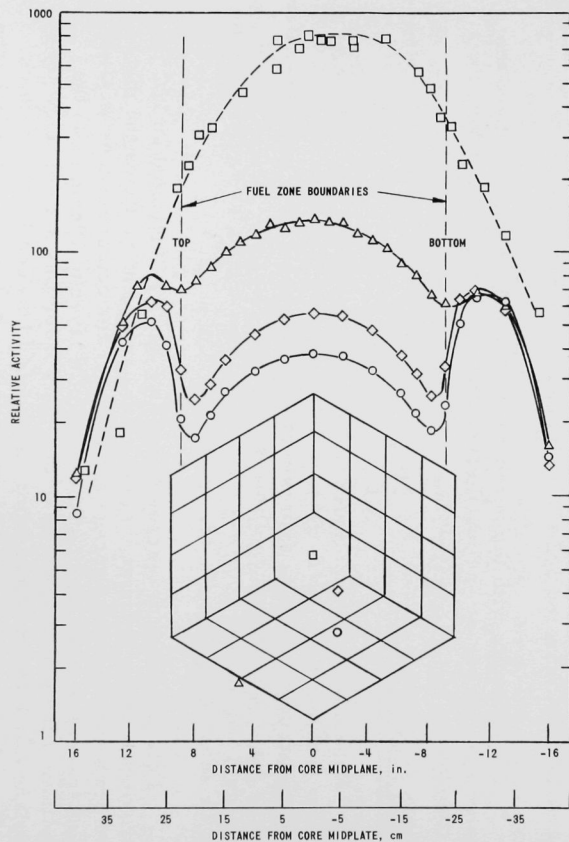
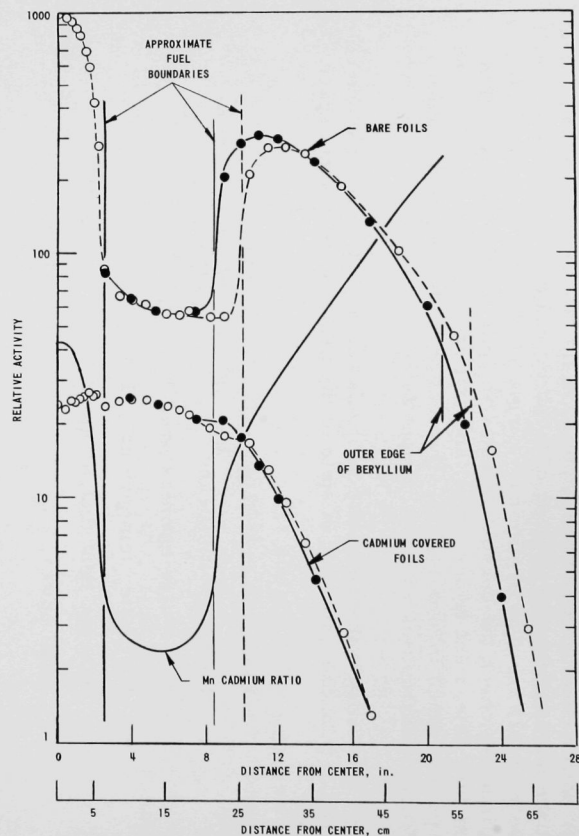


Figure 17. U-Al Vertical Activation Traverses

Figure 18. Mn Radial Activation Traverses
(for location of foils see Figure 19)

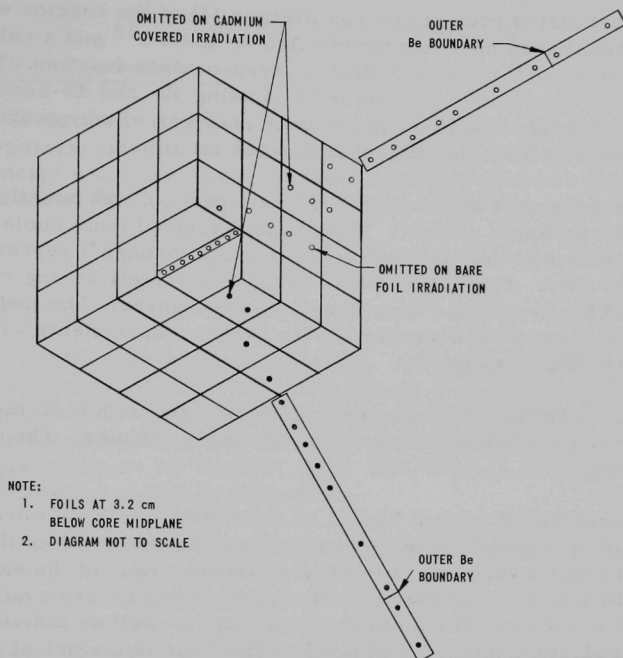


Figure 19. Foil Placement for Mn Radial Activation Mapping

Foil traverses in the vertical direction are shown in Figure 17, which also shows the locations involved. The axial (ITC) location was the most active, and the peripheral (safety blade) location was about one-sixth as active.

Cadmium ratios were taken with gold, copper, dysprosium, indium, manganese, and 93% enriched uranium foils with 0.05-cm-thick cadmium covers. These foils were irradiated near the location of minimum cadmium ratio shown in Figure 18 with the results given in Table XIX.

Table XIX. AARR Fuel Zone Cadmium Ratios

Material	Dimensions (cm)		Cadmium Ratio
	Diameter	Thickness	
Au	0.818	0.003	1.25 ± 0.03
Cu	0.818	0.005	2.2 ± 0.1
3.7 w/o Dy-Al	0.818	0.013	11.3 ± 1.0
In	0.818	0.003	1.32 ± 0.04
90 w/o Mn-Cu	0.818	0.006	2.5 ± 0.2
17.5 w/o U-Al	0.818	0.005	$3.5 \pm 0.3^*$

*Fission

The estimated prompt neutron lifetime (ℓ) of the reactor was 38.8×10^{-6} sec, based on a measured value of Rossi α^{18} and a calculated value ($\beta = 7.26 \times 10^{-3}$) of the effective delayed-neutron fraction. The measured values of $\alpha = \beta/\ell$ were 187 ± 8 and 187 ± 5 using 40- and 80- μ sec channel widths, respectively, in a 400-channel time analyzer which recorded output of one fission chamber after the other started the timer.

A measurement of the void coefficient gave -0.16% reactivity per percent void fraction of coolant. Water was displaced from coolant channels by Teflon strips which were distributed through a representative portion of the core. The Teflon was withdrawn remotely during reactor operation and the resulting rising period was measured. The method was shown to give reasonable accuracy during earlier experiments with the AHFR Critical Experiment.¹⁹

Danger coefficient measurements were made with fuel, moderator, control materials, and burnable poisons, in small samples. The data are being analyzed.

Calibrations of control blades by subcritical methods were inter-compared for the immediate purpose of estimating the worth of the control elements, but with a long-range interest in the accuracy of the various methods. Since a large number (12) of control elements are available, it is important to measure their effect as a group, as well as individually. The only satisfactory method evaluated at this time is the use of a computer code R-102 (Inverse Kinetics). This procedure gives consistent results within about 2% of the total worth, and the other methods vary by 25% or more. The code appears to be compatible with the available equipment and the experiment but has not yet been evaluated for use with multiple or grouped control elements. The worth of a single control blade has been measured at $1.77\% \pm 0.03\%$.

Gamma heating by use of manganese-activated CaF_2 phosphor is being measured to permit estimates of reflector cooling requirements and beam tube design. Although LiF is commonly used for this purpose, the neutron activation of Li^6 in the critical experiment was considered prohibitive. Reactor traverses have been made and samples are awaiting measurement.

¹⁸Karam, R. A., Measurement of Rossi-Alpha in Reflected Reactors, Trans. Am. Nuclear Soc. 7, No. 2, 283 (Nov 1964).

¹⁹DeVilliers, J. W. L. (Ed.), Critical Experiments for the Preliminary Design of the Argonne High Flux Reactor, ANL-6357, p. 41 (June 1961).

B. Magnetohydrodynamics (MHD)

1. MHD Power Generation - Jet Pump Studies

Information pertinent to a liquid metal design concept utilizing mercury-potassium alloy as the working fluid has been collected. This design concept will be directed toward the employment of a jet pump circuit in a liquid metal topping cycle for a central station reactor.

C. Regenerative Emf Cells

1. Bimetallic Cells

a. Sodium-Bismuth Cell Studies. Investigation of the solubility of Na_3Bi in the ternary eutectic 53.2 m/o NaI-31.6 m/o NaCl-15.2 m/o NaF has continued. This eutectic is being considered for possible use as the electrolyte for the sodium-bismuth cell. Preliminary solubility results (see Progress Report for October 1964, ANL-6965, p. 90) were thought to be high because of sampling difficulties.

In the present experiments samples were taken after filtering the electrolyte through a tantalum frit to eliminate any solid particles of Na_3Bi which might be present as a result of temperature cycling of the melt. By means of this technique, the scatter of the experimental points was reduced. The average sodium-to-bismuth ratio in the eutectic was 2.97 ± 0.03 as determined from bismuth and sodium analyses of 16 filtered samples. The solubility of Na_3Bi in the ternary eutectic ranged from 1.2 m/o at 552°C to 8.5 m/o at 839°C . The solubility of Na_3Bi at the proposed temperature of cell operation ($\sim 550^\circ\text{C}$) is not regarded as being prohibitively large. Additional experiments are planned to determine the solubility of nonstoichiometric sodium-bismuth intermetallic species in the ternary eutectic.

b. Vapor-Liquid Equilibrium Studies in the Sodium-Bismuth System. An ebulliometer has been constructed for the purpose of measuring total vapor pressures over Na-Bi alloys at various compositions and temperatures. This is part of an experimental program to obtain vapor-liquid equilibria data for the high-temperature portion of the regenerative cell cycle. In the ebulliometric apparatus, a sample of the molten alloy of interest is heated to the boiling point, and a mixture of liquid and vapor is transferred by means of a Cottrell pump through an orifice into the chamber where the vapor-liquid equilibrium is established at a particular experimental pressure. The equilibrium temperature is measured by a thermocouple set in a well in such a position that the liquid-vapor mixture contacts

it immediately upon entering the chamber. The pressure in the system is maintained by a Cartesian manostat.

The performance of the apparatus was tested by measuring the vapor pressure of pure sodium. No bumping was observed during heating of the sodium, and the apparatus operated satisfactorily. Experimental results extrapolated to 760 mm gave a normal boiling point of 1153.7°K for pure sodium. This value is in good agreement with the generally accepted literature values. Now in progress is an experiment to determine the vapor pressure of an alloy of Na-10 a/o Bi.

c. Engineering Material Study. Dynamic corrosion studies of liquid bismuth on low carbon steel are being continued. A thermal convection loop containing bismuth was put into operation with a hot-leg temperature of 850°C and a cold-leg temperature of 450°C. (The preparatory de-scaling procedure used for the loop was described in the Progress Report for October 1964, ANL-6965, p. 90.)

After 430 hr of operation, a leak developed in the hot leg. The loop was sectioned and the sections examined microscopically. The attack of the low carbon steel by bismuth was greatest at the entrance to the hot leg of the loop, where the temperature gradient was largest. Extensive mass transfer was noted: loose aggregates of metallic crystals were found in the general area of the entrance to the cold-leg section. Although low carbon steel is still being considered for a container material for the cell itself, it is evident that other high-temperature materials, particularly refractory metals, must be investigated as possible materials of construction for the regenerator. Molybdenum-30 w/o tungsten is being considered as the first refractory metal alloy to be tested.

D. Thermionic Conversion

1. Comparison of Dc and Rf Power Output

In recent experiments, light bulbs were used to indicate the rf-power output by comparing its brightness with a test bulb heated by dc power. In previous experiments the power was determined by observing the rms voltage across an inductance-free resistance. Since some of the rf output comes in short pulses, the use of the rms meter and resistance to measure output could be inaccurate. The results with the bulbs indicate that the rf-power output is higher than previously obtained.²⁰

Results obtained with the cesium cell are given in Table XX. The ratio of rf/dc power output rises above 20% and, as expected, the rf-power maxima occur when the load on the dc output approaches zero and is highest for a 2-mm emitter-collector separation distance. The rf-power output is also influenced by the emitter temperature and cesium pressure.

²⁰

AMU-ANL Conference on Direct Energy Conversion, Nov 4-5, 1963, ANL-6802, pp. 132-141.

Table XX. Power Output from the Cesium Diode

Emitter Temperature, °K	Cs Pressure, mm Hg x 10 ³	Cs Atom Density, (atoms/cm ³) x 10 ⁻¹³	Emitter-Collector Distance, mm	dc Power, mW	rf Power, mW	rf/dc Power Ratio, %
2082	3.6	6.3	2	50	6	12
2206	3.6	6.3	2	200	35	17.5
2240	3.6	6.3	1	300	10	3.3
2279	1.5	3.2	2	460	115	25
2270	1.5	3.2	1	500	23	4.6
2394	2.5	5.5	2	1000	190	19
2354	2.5	5.5	1	930	?	?
2284	8	20	2	310	44	14
2268	8	20	1	500	25	5
2380	8	20	2	900	95	10.5

2. Rf-voltage Pulses

It was previously observed²⁰ through the use of an oscilloscope that the peak-to-peak voltage of the short pulses exceeded the 5-7-V level. Recent investigations showed these peak-to-peak voltages exceeded 17 V. The results are shown in Table XXI.

Table XXI. Peak-to-Peak and Amplitude Voltages of Short Pulses from the Cesium Diode at a Cesium Pressure of 3.6×10^{-3} mm Hg

Temperature of Emitter, °K	Emitter-Collector Distance, mm	Voltage on Collector, V					
		0(dc)		1(dc)		2(dc)	
		P-P-V	AMPL-V	P-P-V	AMPL-V	P-P-V	AMPL-V
2082	2	7.5	-	5	-	4	-
2206	2	17.5	15	12	10	-	-
2240	1	11.0	8	10	7	-	-

V. NUCLEAR SAFETY

A. Thermal Reactor Safety Studies1. Metal-Water Reactions

a. High-temperature, High-pressure Furnace. In order to evaluate the effect of pressure on the reactions of steam with various materials of interest, a high-temperature, high-pressure furnace has been constructed (see Figure 20) and is now in operation. The furnace is capable of operating at pressures up to 1000 psi. The internal, steam-filled zone is wholly surrounded by an alumina tube which can be heated to 1700°C or higher by external molybdenum resistance wires. The external zone is argon-filled, and the pressures in the two zones are automatically matched to avoid stresses on the alumina tube. At the start of an experiment the sample is elevated from a moderate temperature zone (~800°C), where the rate of reaction with steam is negligible, into the high-temperature zone. Upon completion of the experiment, the sample is lowered to its initial position in the moderate temperature zone.

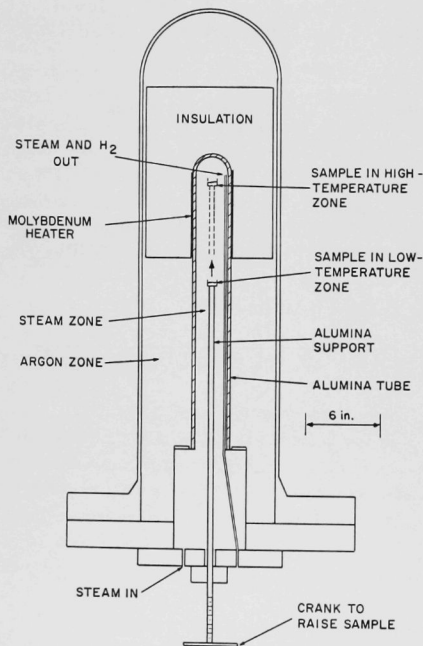


Figure 20. High-pressure Furnace for Studies of Molten Metal-Steam Reactions

The hydrogen generated by reaction of the sample with steam is removed continuously from the top of the steam zone, along with some unreacted steam. The rate of reaction is determined by measuring the rate of hydrogen evolution; the extent of reaction is determined by measuring the total amount of hydrogen evolved.

In the first experiment conducted in this furnace, a 200-mg sample of 15-mil zirconium wire was reacted with steam at a pressure slightly above atmospheric and at a temperature of 1450°C. The weight gain of the sample indicated stoichiometric conversion to ZrO_2 . A volume of hydrogen corresponding to 99.2% metal-steam reaction was collected over a period of 90 min. It is believed that the rate of hydrogen collection was probably limited by the low steam flow rate.

The second experiment was designed to simulate the

environment of a loss-of-coolant accident. The sample consisted of a number of high-density UO_2 pellets clad with Type 304 stainless steel. The

27-mil cladding was closed at both ends to form a can about $3/8$ in. in diameter by 8 in. long. The sample was raised at the rate of 1 in./min over a total stroke of 8 in. to the highest position possible in the furnace. The upper end of the sample reached a maximum temperature of 1500°C ; the lower end, a maximum of 890°C . The steam pressure in the furnace was slightly above atmospheric. The fuel pin was kept in position for 180 min. The amount of hydrogen evolved corresponded to a reaction of about 62% of the stainless steel, most of the reaction occurring during the first 90 min.

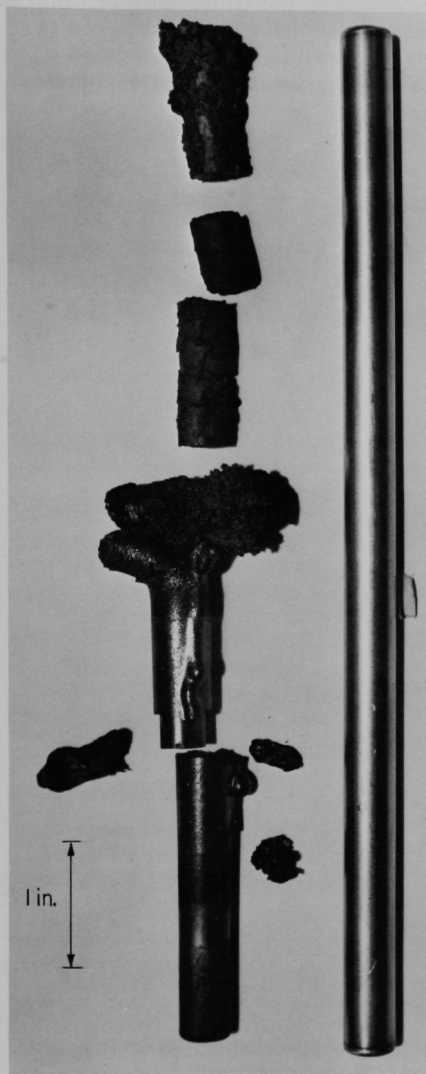


Figure 21. Type 304 Stainless Steel-clad UO_2 , Simulated Fuel Rod after Exposure to Steam (1500°C and 15 psig) in High-pressure Furnace

In Figure 21 the sample fuel rod after removal from the furnace is compared with an unreacted fuel rod. The appearance of the reacted sample shows that relatively little reaction occurred at the lower temperature, and that extensive stainless steel reaction and foaming occurred in the region of the cladding where the temperature was between about 1400 and 1500°C . The spongy mass at the top of the fuel rod is probably the remains of the relatively thick ($1/4$ in.) top end cap. Several of the upper UO_2 pellets were very nearly bared of cladding. Visual examination of these UO_2 pellets indicated extensive cracking and deterioration. Further examination of the UO_2 pellets will be made by chemical and X-ray diffraction analyses.

b. Scale-up Experiments in TREAT. A program has been initiated to study metal-water reactions under conditions simulating

a power excursion incident in a typical bundle of reactor fuel elements. In all preceding experiments, only single fuel pins were used. The present series of experiments will utilize approximately 100 times as much fuel as previous studies. The types of fuel elements which will be subjected to TREAT transients include uranium rods and stainless steel-clad and Zircaloy-clad UO_2 fuel rods. A schematic diagram of the scale-up autoclave for these experiments is shown in Figure 22.

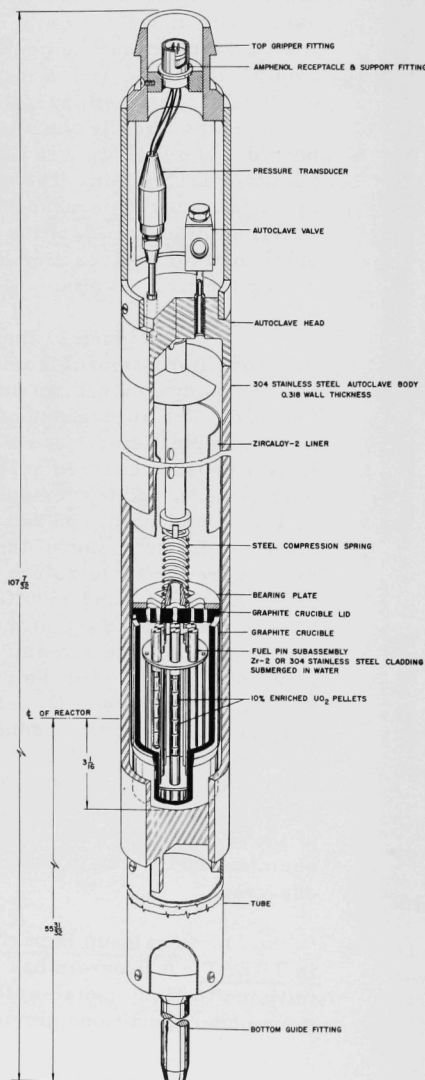


Figure 22
Scale-up TREAT Metal-
Water Autoclave

The first two experiments, with 20% enriched uranium fuel rods, have been completed. Table XXII summarizes conditions of the experiments and results available. In CEN-196-S, complete meltdown of the subassembly occurred and resulted in 10.7% metal-water reaction. The autoclave from CEN-197-S has not yet been disassembled; however, a greater degree of fragmentation of the fuel is expected from the more energetic transient. An interesting and possibly significant feature of the second experiment was the fact that the reactor power-time record indicated that a change in reactivity of the TREAT reactor had occurred. This perturbation is believed to have been caused by the change in the geometry of the test subassembly during meltdown.

Table XXII. TREAT Metal-Water Scale-up
Experiments with Uranium

<p>Conditions: 1. Subassembly consisted of 9 uranium rods in a square cluster on 5/8-in. centers with 3 rows of 3 elements per row. Each fuel pin was 0.2-in. in diameter by 5 $\frac{5}{8}$ in. long and was 20% enriched with U²³⁵. The total weight of the 9 element bundle was 490 g.</p> <p>2. Fuel subassembly submerged in distilled water initially at ambient reactor temperature, ~25°C.</p> <p>3. 20 psia helium atmosphere above the water.</p>		
<u>Reactor Characteristics</u>	<u>TREAT-CEN Transient No.</u>	
	<u>196-S</u>	<u>197-S</u>
Integrated Power, MW-sec	91	222
Peak Power, MW	255	361
Reactor Period, msec	157	140
<u>Results</u>		
Peak Pressure Rise, psi	65	570
Max Rate of Pressure Rise, psi/sec	50	2150
Estimated Energy Input, cal/g U	-	-
% of Uranium Reacted with Water	10.7	-
Appearance of Cluster after Transient	Melted into two large irregularly shaped masses plus some fragments and particles.	

c. Short-period Transient Irradiations. Preparations have been completed for the metal-water experiments which will be conducted during the Kiwi-TNT test, a planned single, short-period (0.5 msec) excursion during which it is expected that the Kiwi reactor will be destroyed. The destructive test is to be conducted as a part of the Los Alamos Rover program in the early part of January 1965 at the Nuclear Rocket Development Station at Jackass Flats, Nevada. Twenty-four autoclaves have been loaded, leak-checked, and sent to the Nevada test site. Each autoclave (enclosed in a secondary capsule which will serve as a blast shield) contains a fuel specimen submerged in water beneath a helium atmosphere. Six specimens of four different types of fuels will be used: (i) Zircaloy-2-clad, UO_2 -core pins; (ii) Type 304 stainless steel-clad, UO_2 -core pins; (iii) uranium-5 w/o zirconium-1.5 w/o niobium alloy pins; (iv) uranium-aluminum plates of the SPERT type. The autoclaves will be mounted in positions external to the reactor at various distances from the core so that the fuel specimens will be exposed to a range of neutron energies during the destructive transient.

2. Metal Oxidation-Ignition Studies

a. Ignition Studies of Irradiated Uranium. Studies of the oxidation of irradiated uranium were resumed briefly in order to clarify results of previous experiments in which no definite ignition in air was observed for irradiated specimens (see Progress Report for September 1964, ANL-6944, p. 85). In the present experiments thermocouples were imbedded in holes drilled in two irradiated specimens and one thermocycled, unirradiated specimen to obtain better thermocouple contacts than were obtained in the earlier experiments. Temperature-time traces obtained by the burning-curve method showed greater self-heating and spontaneous thermocycling (i.e., a greater oxidation rate) at about 400°C for the irradiated specimens than for the control sample. However, no clear-cut evidence of ignition was observed for either type sample in these experiments. No further experimental work on this problem is being planned.

B. Fast Reactor Safety Studies

1. Transient Tests with Uranium Sulfide

Transient high-temperature experiments have been performed to study the behavior of uranium sulfide fuel specimens under meltdown conditions. The fuel, compacted to 96% of theoretical density, contained approximately 2.5% UO_2 and 3.5% UOS. It was prepared in short pellets, of 0.381-cm diameter, and stacked to a height of about 19 cm. Two samples, each in a W-26% Re metal tube of nominal 0.07-cm wall thickness, were run in TREAT under irradiation conditions summarized in Table XXIII.

Table XXIII. Conditions of Irradiation of Uranium Sulphide

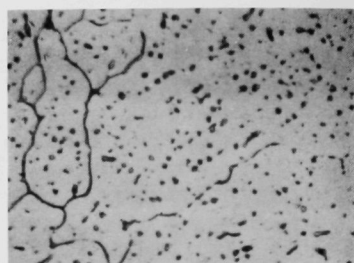
Sample	Test	TREAT Energy Release, MW-sec	Maximum Cladding Surface Temperature, °C	Estimated Maximum Central Fuel Temperature,* °C
1	1	95	1115	1850-2100
1	2	130	1310	2300-2462
1	3	195	1965	melted
2	4	242	2160	melted
2	5	243	2180	melted

*Melting point of uranium sulfide is 2462°C.²¹

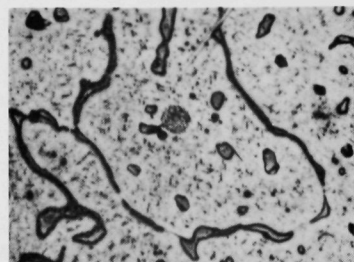
After testing, both US samples were examined and had a "cast" type appearance. The fuel had cracked away from the cladding, apparently in cooling, forming an irregular separation of the order of 0.01 mm. No cladding failures were observed. Visual evidence from motion pictures taken during the experimental runs indicated that fuel material flowed inside the cladding during experiments 3, 4, and 5. No significant variation in fuel structure was found between Sample No. 1 (one transient above the US melting point) and Sample No. 2 (two cycles above US melting point). However, both specimens displayed a variation in structure along the sample radius (see Figure 23). The fuel at the extreme edge (see Figure 23a) was almost entirely composed of large amounts of UOS (light grey) and possibly some UO_2 (dark grey) in a matrix composed of US grains. At a distance from the edge of about one-quarter of the cylinder radius (see Figure 23b), the UOS had migrated from the grain boundaries into the US grain in a direction normal to the edge. At a distance from the edge of one-half to three-quarters of the cylinder radius (see Figure 23c), less UOS was located at the grain boundaries and more dispersed within the matrix. At the center of the cylinder (see Figure 23d), the UOS was distributed as a fine dispersion within the US grains.

Some evidence of reaction between the fuel and cladding was observed in several areas. Intergranular cracks appeared in the cladding, but it was not certain whether the alien phase located at the metal grain boundaries was due to a reaction with the fuel, or was a result of penetration of fuel into the cracks in the cladding.

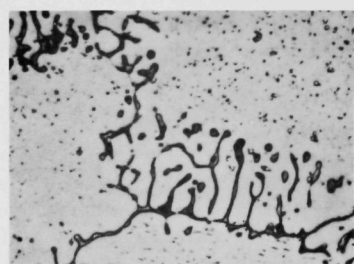
²¹Cater, E. David, The Vaporization, Thermodynamics, and Phase Behavior of Uranium Monosulfide, ANL-6140 (March 1960).



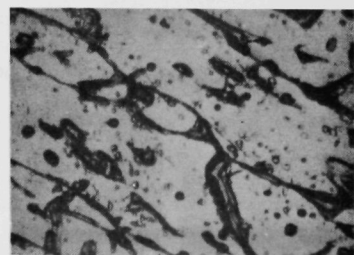
a



b



c



d



 $2 \times 10^{-3} \text{ cm}$

Figure 23. Structure of US Samples after Irradiation

Calculations of the transient sample temperature were made with the ARGUS code in order to establish relationships between the measured cladding surface temperatures and the experimentally unknown fuel temperatures, and to check for possible changes in thermal behavior. The thermal conductivity of US was obtained by extrapolation of measurements covering approximately one-third of the temperature range of interest (see Progress Report for May 1963, ANL-6739, p. 33). The specific heat for the US was 0.0466 cal/g-°C, a value obtained by analyzing experimental temperature data from earlier TREAT experiments on US. (An experimental out-of-pile measurement of 0.045 cal/g-°C has been reported at room temperature in Progress Report for August 1964, ANL-6936, p. 51.) Values for the fuel-cladding interface conductance were obtained by making detailed comparisons of experimental and calculated delays between reactor power and cladding surface temperature, initial rates of cladding surface temperature rise, and cladding surface temperature curve shapes. Results of this compound analysis are given in Table XXIV.

Table XXIV. Results of Temperature Analyses

Sample	Test	TREAT Energy Release, MW-sec	Maximum Cladding Surface Temperatures, * °C	Estimated Interface Conductance, W/cm ² -°C
1	1	95	1090, 1140	0.1-0.2
1	2	130	1270, 1350	0.15-0.25
1	3	195	1910, 2020	0.3-0.7
2	4	242	1940, 2160	0.3-0.75
2	5	243	1900, 2180	0.3-0.75

*Two thermocouples.

It may be noted that the three highest energy transients showed an appreciably larger span in maximum measured cladding temperatures. This may be purely "instrumental" or it may be associated with the spread of interface conductance (which could have resulted from extensive movement of molten fuel along the inside of the cladding). The low value of conductance for test 1 is consistent with results of previous experiments; the tendency to increasingly higher values with higher energy transients is consistent with fuel movement resulting from the low US-UOS eutectic melting temperature and from gross melting.

2. Analysis of Coolant Expulsion from Heated Channels

A check of theoretical techniques for the analysis of transient pressure generation and coolant expulsion from heated channels is being made. A set of simple transient expulsion tests was performed using water at atmospheric pressure and comparatively low heating rates.²² The heating surface consisted of an EBR-II fuel tube, 0.442 cm in diameter, having an active length of 7.62 cm. Water was contained between the heater tube and a 1-cm-OD by 0.8-cm-ID Pyrex tube, 60 cm long. The fuel tube extended beyond the heated length in order to define the flow channel for the coolant during expulsion.

The coolant expulsion was calculated on the basis of the following assumptions. It was assumed that the rate of rise of the steam pressure can be calculated from the rate of temperature rise of the tubing, and that the pressure acts on a cross-sectional area equal to the coolant annulus. Delays existing between the onset of heating and the beginning of expulsion, and the details of expulsion beyond a distance equal to the heated length, are beyond the scope of the analytical model employed. Two power settings were used: 50.4 W and 207 W in the heated section, corresponding to tubing temperature rises of approximately 25°C/sec and 102.8°C/sec, respectively. Table XXV shows results of a comparison of calculated and experimental coolant expulsion velocities at an expulsion distance of 7.62 cm.

Table XXV. Coolant Velocities at End of Heated Section

Run	Power Output to Cladding, W	Mass of Water, g	Bulk Water Temperature, °C	Calculated Velocity, cm/sec	Experimental Velocity, cm/sec
1	50.4	7.02	-*	185	-**
2	207	7.02	83	260	130
9	207	7.02	85	260	210
3	50.4	11.7	85	80	89
4	50.4	11.7	83	80	80
5	207	11.7	71	250	224
6	207	11.7	69	250	224
7	207	11.7	64	250	230
8	207	11.7	63	250	230

*Not recorded.

**No clear single surge of coolant was observed. Coolant did not completely leave heated section.

For all runs except 1 and 2 there appears to be reasonable consistency between experiment and calculation. One possible explanation for the discrepancies of Runs 1 and 2 is that significant amounts of air remained dissolved in the water after two trial heating runs made immediately before run No. 1.

²²A summary of results of a check in which the techniques were used to correlate transient voiding experimental data from in-pile tests, in water, with reactor periods ranging from 1 to 10 ms may be found in Progress Report for October 1964, ANL-6965, pp. 94-96.

3. Sodium Expulsion Studies

A small-scale experiment has been planned to investigate the expulsion of sodium from a reactor channel during a power excursion. The first tests will use water as the fluid rather than sodium, due to ease in handling. Instrumentation and power supply problems will be greatly reduced.

The feasibility of using automotive storage batteries as an energy source in the pulse heating of a test element was experimentally investigated. Two 12-V batteries were connected in series with a 6-in. length of a 3/4-in.-OD by 0.005-in.-wall 316 SS tube and a manual switch. The current was measured through a 1500-Amp shunt, and the voltage drop across the SS tube was measured by direct connection to a voltmeter. The temperature of the tube was also measured. The signals were all recorded on an oscillograph with a chart speed of 10 ft/second using galvanometers with frequency responses of 3300 cps.

After closing the battery switch, the current through the test section rose to 396 Amp in 1 ms, slowly dropping to 380 Amp during the next 30 ms and holding at this value throughout the run. The voltage drop across the section was $15(\pm 1)$ V. The test section burned out after 1.43 sec after reaching a temperature of approximately 3500°F.

It appears that storage batteries can be used in the current expulsion tests, provided that the circuit breaker will open the circuit before burnout. The operating characteristics of the circuit breaker are now being experimentally determined.

C. TREAT

1. Large TREAT Loop

Two sets of the compound bellows system are now in ANL shops for rebuilding. Other bellows which were returned to the vendor are in the process of refabrication.

Pit cover drawings are being revised.

The pipe hangers which have been received from the vendor were found to be faulty and were returned for correction.

The cold-trap cooling system has been assembled and crated for shipment to Idaho. This shipment completes the list of cooling system parts required from ANL.

The gas system of the large TREAT loop includes a pressure switch which controls the maximum blanket-gas pressure by actuating a normally

closed solenoid valve if the pre-set pressure is exceeded. A second pressure switch has been added to the gas system to actuate alarms if the blanket-gas pressure is outside the control range. Three pressure gauges have also been added to indicate the blanket-gas pressure: a) in the dump vessel, b) in the storage vessel, and c) at the liquid-nitrogen-cooled charcoal trap. Prints of the complete gas system and the revised bills of material are now being checked.

Several of the gas-system components, including the pressure regulator, pressure switch, and rupture discs, have been received. The four 75 psi, 300°F rupture discs for the dump and storage vessel gas piping were stacked together for shipment without the use of any spacing material. During shipment, the tab on the vacuum support of each rupture disc dented and wrinkled the top support of the rupture disc upon which it rested. Three of these four rupture discs thus appear to be unsatisfactory for use. The manufacturer has been apprised of their condition.

VI. PUBLICATIONS

PapersTHERMOCHEMISTRY OF DILUTE AQUEOUS SULFURIC ACID
COMPARISON OF THEORY AND EXPERIMENT AT 25°C

T. F. Young, Y. C. Wu, and W. L. Groenier

Abstracts of Papers, 19th Calorimetry Conference,
October 13-16, 1964THE HEATS OF FORMATION OF THE DIBORIDES OF ZIRCONIUM,
HAFNIUM, AND TANTALUM BY FLUORINE BOMB CALORIMETRY

G. K. Johnson, E. Greenberg, J. L. Margrave, and W. N. Hubbard

Abstracts of Papers, 19th Calorimetry Conference,
October 13-16, 1964THE HEATS OF FORMATION OF C_3O_2 , Se_4N_4 AND OF THE VARIOUS
CRYSTALLINE FORMS OF TiO_2 BY COMBUSTION CALORIMETRY

B. D. Kybett, C. K. Barker, G. K. Johnson, and J. L. Margrave

Abstracts of Papers, 19th Calorimetry Conference,
October 13-16, 1964FLUORINE COMBUSTION TECHNIQUE FOR METALS FORMING
NONVOLATILE (IONIC) FLUORIDES

E. Rudzitis, H. M. Feder, and W. N. Hubbard

Abstracts of Papers, 19th Calorimetry Conference,
October 13-16, 1964THE DECOMPOSITION OF PLUTONIUM HEXAFLUORIDE BY GAMMA
RADIATION

M. J. Steindler, D. V. Steidl, and J. Fischer

J. Inorg. Nucl. Chem. 26, 1869-1878 (1964)EFFECTS OF SOLID THERMAL PROPERTIES ON HEAT TRANS-
FER TO GAS FLUIDIZED BEDS

E. N. Ziegler, L. B. Koppel, and W. T. Brazelton

Ind. Eng. Chem. Fundamentals 3(4), 324-328 (November 1964)STUDIES OF LITHIUM HYDRIDE SYSTEMS. I. SOLID-LIQUID
EQUILIBRIUM IN THE LITHIUM CHLORIDE-LITHIUM HYDRIDE
SYSTEM

C. E. Johnson, S. E. Wood, and C. E. Crouthamel

Inorg. Chem. 3, 1487-1491 (November 1964)

DOSIMETRY FOR RADIATION DAMAGE STUDIES

A. D. Rossin

IEEE Trans. NS-11(5), 130-136 (November 1964)

STUDIES IN THE SYSTEM URANIUM CARBIDE-URANIUM SULPHIDE

P. D. Shalek and G. D. White

Carbides in Nuclear Energy. Proc. Symp. held at Harwell,
November 5-7, 1963, ed. L. E. Russell et al. McMillan,
London, 1964. Vol. 1, pp. 266-272

IRRADIATION OF PuC AND UC-PuC

L. A. Neimark, J. H. Kittel, and C. C. Crothers

Carbides in Nuclear Energy. Proc. Symp. held at Harwell,
November 5-7, 1963, ed. L. E. Russell et al. McMillan,
London, 1964. pp. 864-878

NEUTRON RADIOGRAPHY AS AN INSPECTION TECHNIQUE

Harold Berger

Proc. 4th Intern. Conf. on Nondestructive Testing, London,
September 9-13, 1963. Butterworths, London, 1964. pp. 113-117

SYNTHESIS OF URANIUM MONOPHOSPHIDE BY THE PHOSPHINE REACTION

Yehuda Baskin and P. D. Shalek

J. Inorg. Nucl. Chem. 26, 1679-1684 (1964)

FAST CANCELLATION OF GAMMA RADIATION BACKGROUND PULSES IN HORNYAK BUTTONS WITH AN ACTIVE CIRCUIT

K. G. Porges, Alexander DeVolpi, and P. W. Polinski

Rev. Sci. Instr. 35, 1602 (November 1964) Note

THE SOLUTION OF BOUNDARY VALUE PROBLEMS WITH ASYMMETRIC BOUNDARY CONDITIONS BY MEANS OF FINITE FOURIER TRANSFORM

Gabriel Cinelli

IEEE Convention Record, Part II, New York, March 23-26, 1964.
IEEE, New York, 1964. pp. 235-244

STATISTICAL THEORY OF NUCLEAR COLLISION CROSS SECTIONS. II. DISTRIBUTIONS OF THE POLES AND RESIDUES OF THE COLLISION MATRIX

P. A. Moldauer

Phys. Rev. 136, B947-B952 (November 23, 1964)

AVERAGE COMPOUND NUCLEUS CROSS SECTIONS

P. A. Moldauer

Rev. Mod. Phys. 36, 1079-1084 (October 1964)

PHYSICS MEASUREMENTS ON A 600 LITER FAST NEUTRON
CARBIDE CORE

G. K. Rusch, E. R. Bohme, L. R. Dates, S. A. Grifoni, W. Y. Kato,
G. W. Main, H. H. Meister, Masao Nozawa, and R. L. Stover
236

PHYSICS MEASUREMENTS IN TUNGSTEN-BASED ALUMINUM
REFLECTED FAST REACTORS

R. C. Doerner, W. G. Knapp, and K. K. Almenas
236

CALCULATIONS OF ZPR-III FAST ASSEMBLIES USING A TWENTY-
SIX GROUP CROSS SECTION SET

David Meneghetti and J. R. White
237

TWENTY-SIX GROUP CROSS SECTIONS

D. M. O'Shea, H. H. Hummel, W. B. Loewenstein, and David Okrent
242

MEASUREMENT OF β_{eff} AND POWER CALIBRATION IN FAST
REACTORS

R. A. Karam
248

STRUCTURAL FEEDBACK EFFECTS IN EBR-I, MARK IV

R. R. Smith, R. O. Haroldsen, and F. D. McGinnis
248

FAST-REACTOR REACTIVITY COEFFICIENTS; THE EFFECT OF
EXCESS REACTIVITY

W. B. Loewenstein
249

SODIUM-VOID COEFFICIENT MEASUREMENTS IN A LARGE CAR-
BIDE FAST ASSEMBLY

S. A. Grifoni, Masao Nozawa, and W. Y. Kato
250

DOPPLER-EFFECT MEASUREMENTS IN PLUTONIUM-FUELED
FAST ASSEMBLIES

G. J. Fischer, D. A. Meneley, and E. F. Groh
252

SOME ELASTIC NEUTRON ANGULAR DISTRIBUTIONS

A. B. Smith and P. T. Guenther

267

DOPPLER BROADENING OF RESONANCES BY SAMPLE MOTION

C. E. Till

273

MEASUREMENT OF ROSSI-ALPHA IN REFLECTED REACTORS

R. A. Karam

283

PROPERTIES OF ALUMINUM REFLECTORS OF FAST CRITICAL ASSEMBLIES

K. K. Almenas, W. G. Knapp, and R. C. Doerner

304

THE BREEDING RATIO OF EBR-I, MARK IV

R. R. Smith, R. O. Haroldsen, R. E. Horne, and R. G. Matlock

305

THEORY AND METHODS OF CORRECTION FOR RESOLUTION LOSSES OF COUNTING EQUIPMENT

K. E. Plumlee

341

IN-CORE EXPERIMENTS WITH A LITHIUM-6 "SANDWICH" FAST NEUTRON SPECTROMETER

R. J. Huber and J. K. Long

368

FAST NEUTRON SPECTROSCOPY BY 4π RECOIL PROPORTIONAL COUNTING

E. F. Bennett

369

EVALUATION OF A THERMIONIC DIODE FOR SPACE POWER USING A LIQUID METAL ELECTRON COLLECTOR

A. J. Ulrich

377

A PILOT PLANT FOR FLUID-BED FLUORIDE VOLATILITY PROCESSING OF URANIUM DIOXIDE-PLUTONIUM DIOXIDE REACTOR FUELS

G. J. Vogel, E. L. Carls, N. M. Levitz, and W. J. Mecham

396

DEVELOPMENT OF A METAL FUEL ALLOY FOR THE SEFOR FAST
CRITICAL EXPERIMENT FOR ZPPR

L. R. Kelman, H. V. Rhude, and Howard Savage
401

PROPERTIES OF URANIUM-PLUTONIUM-FIZZIUM ALLOYS

R. J. Dunworth, L. R. Kelman, Howard Savage, E. R. Gilbert, and
H. V. Rhude
405

COMPATIBILITY OF U-Pu-FIZZIUM FUEL ALLOYS WITH VANA-
DIUM AND VANADIUM-TITANIUM CLADDINGS

C. M. Walter and J. A. Lahti
406

FABRICATION OF DRIVER FUEL ELEMENTS CONTAINING RARE
EARTH BURNABLE POISONS

C. H. Bean, F. D. McCuaig, and J. H. Handwerk
410

FABRICATION OF VANADIUM-20 WT % TITANIUM (TV-20) TUBING
FOR NUCLEAR FUEL CLADDING

W. R. Burt, W. C. Kramer, and R. M. Mayfield
430

TRANSIENT IN-PILE OXIDATION EXPERIMENTS ON METALLIC
FUELS

Harry Lawroski
447

STUDIES ON THE MELTDOWN IN WATER OF OXIDE CORE,
ZIRCALOY-2 CLAD FUEL IN TREAT

R. C. Liimatainen, Louis Baker, R. O. Ivins, F. J. Testa,
J. F. Boland, and Harry Lawroski
448

MANIPULATOR SYSTEMS DEVELOPMENT AT ANL

R. C. Goertz
467

Also, Proc. 12th Conf. on Remote Systems Technology,
San Francisco, November 30-December 3, 1964. Am. Nucl.
Soc., Hinsdale, 1964. pp. 117-136

AN INERT ATMOSPHERE GLOVEBOXED EXTRUSION PRESS

George Burton and A. B. Shuck
475

Also, Proc. 12th Conf. on Remote Systems Technology,
San Francisco, November 30-December 3, 1964. Am. Nucl.
Soc., Hinsdale, 1964. pp. 217-227

THE ANL ALPHA-GAMMA METALLURGY HOT CELL -- ITS DESIGN PHILOSOPHY AND COMPONENTS

R. C. Goertz, K. R. Ferguson, J. F. Lindberg, D. P. Mingesz,
R. A. Blesch, C. W. Potts, J. H. Grimson, G. A. Forster,
F. L. Brown, and J. L. Armstrong
483

Also, Proc. 12th Conf. on Remote Systems Technology,
San Francisco, November 30-December 3, 1964. Am. Nucl.
Soc., Hinsdale, 1964. pp. 285-306

STARTUP OF THE ANL ALPHA-GAMMA METALLURGY HOT CELL

F. L. Brown and B. J. Koprowski
484

Also, Proc. 12th Conf. on Remote Systems Technology,
San Francisco, November 30-December 3, 1964. Am. Nucl.
Soc., Hinsdale, 1964. pp. 307-313

A SYSTEM FOR A NITROGEN ATMOSPHERE IN AN ALPHA-GAMMA HOT CELL

B. J. Koprowski, W. H. Livernash, and F. L. Brown
484

Also, Proc. 12th Conf. on Remote Systems Technology,
San Francisco, November 30-December 3, 1964. Am. Nucl.
Soc., Hinsdale, 1964. pp. 315-322

BORAX-V NUCLEAR SUPERHEAT OPERATING EXPERIENCE

J. D. Cerchione, W. R. Wallin, and R. E. Rice
489

PRELIMINARY CONSIDERATION ON THE SAFETY ANALYSIS OF FARET

P. J. Persiani, Watanabe, Akira, Wolff, Ulrich, S. A. Grifoni, and
R. A. Warman
501

FURTHER DEVELOPMENT IN DYNAMIC ANALYSIS OF COOLANT CIRCULATION IN BOILING WATER NUCLEAR REACTORS

C. K. Sanathanan
509

SPECULATIONS ON FUTURE RAMIFICATIONS OF NUCLEAR ENERGY

B. I. Spinrad
527

EVALUATION OF BREEDERS FROM A CONSERVATION STANDPOINT

P. F. Gast
530

A REPAIRABLE NUCLEAR SPACE POWER PLANT

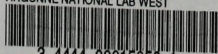
M. J. Janicke and J. C. Carter

533

ANL Reports

- ANL-6889 THE GRAETZ PROBLEM IN COCURRENT-FLOW,
DOUBLE-PIPE; HEAT EXCHANGERS
Ralph P. Stein
- ANL-6897 A STUDY OF THE $1/E$ SLOWING-DOWN NEUTRON
SPECTRUM USING 4π -RECOIL PROPORTIONAL
COUNTERS
Edgar F. Bennett
- ANL-6907 THE EFFECT OF PARTICLE SIZE ON THE PROPER-
TIES OF GAS-FLUIDIZED BEDS
K. S. Sutherland
- ANL-6918 HALIDE SLAGGING OF URANIUM-PLUTONIUM ALLOYS
G. A. Bennett, L. Burris, Jr., and R. C. Vogel

ARGONNE NATIONAL LAB WEST



3 4444 00015058 1